# Synthesis, characterisation and potential employment of Pt-modified $TiO_2$ photocatalysts towards laser induced $H_2$ production

**Anzel Falch**

Dissertation submitted in partial fulfilment of the requirements for the degree Master of Science in Chemistry at the Potchefstroom Campus of the North-West University

Promoter: Dr. R.J. Kriek

November 2011

Potchefstroom

Innovation through diversity ™

NORTH-WEST UNIVERSITY
YUNIBESITI YA BOKONE-BOPHIRIMA
NOORDWES-UNIVERSITEIT
POTCHEFSTROOM CAMPUS

# ACKNOWLEDGEMENTS

*So do not fear, for I am with you; do not be dismayed, for I am your God. I will strengthen you and help you; I will uphold you with my righteous right hand.*

***Isaiah 41:10***


I am much obliged to acknowledge and thank the following people:

NORTH-WEST UNIVERSITY
YUNIBESITI YA BOKONE-BOPHIRIMA
NOORDWES-UNIVERSITEIT
POTCHEFSTROOM CAMPUS

Dr. R.J. Kriek | Prof. C.A. Strydom | Dr. T. Arfin

Dr. L. Tiedt | Ms. B. Venter

| | |
|---|---|
| PerkinElmer For the Better | CSIR our future through science |
| Mr. R. Volsteed | Mr. M. Fazakas<br>Mr. H. van Wyk and Mr. T. du Plooy |

Mr. E.L.J Kleynhans

Me. Z. Falch (Graphics)

My parents Lourens and Ester Falch

# CONTENTS


**LIST OF FIGURES** **v**

**LIST OF TABLES** **viii**

**ABSTRACT** **1**

**OPSOMMING** **2**

**CHAPTER 1: BACKGROUND AND AIMS** **3**

1.1 Background 3

1.2 Aim of study 6

**CHAPTER 2: LITERATURE STUDY** **7**

2.1 Introduction 7

2.2 Economic interest regarding fossil fuels 8

2.2 Environmental impact of fossil fuels 11

2.3 Hydrogen as an alternative energy carrier 11

2.4 Band gap 14

*Band gap determined by absorption spectroscopy* *15*

*Band gap determined by Kubelka and Munk* *16*

*Kubelka-Munk expression for powder samples* *16*

2.5 Photocatalysis 17

2.6 Photocatalysts 19

2.7 Titanium dioxide 21

2.8 Review and recent developments using $TiO_2$ 24

2.9 Chemical additives to enhance hydrogen production 25

*Addition of electron donors* *25*

*Organic compounds as electron donors* *25*

*Addition of carbonate salt or iodide anion* *26*

2.10 Enhancement of $H_2$ production by photocatalyst modification techniques 28

*Noble metal loading* *28*

*Metal ion doping* *29*

*Sensitisation* *31*

2.11 Lasers as an energy source employed for photocatalysis and general principles 32

*Wave properties of light* *32*

*Nd:YAG Laser* *34*

**CHAPTER 3: EXPERIMENTAL 36**

3.1 Materials 36

3.2 Preparation of Pt-$TiO_2$ catalysts 36

3.3 Unsupported $TiO_2$ sample 37

3.4 Characterisation of the Pt-$TiO_2$ catalysts 38

*X-ray Diffraction (XRD)* *38*

*Transmission Electron Microscopy (TEM)* *39*

*Diffuse Reflectance Spectroscopy (DRS)* *39*

*Inductive Coupled Plasma (ICP)* *40*

*Scanning Electron Microscopy (SEM) and Energy Dispersive X-ray spectroscopy (EDX)* *40*

3.5 Hydrogen production and measurements 40

*Reaction vessel* *40*

*Experimental setup* *42*

*Gas chromatography* *46*

**CHAPTER 4: RESULTS AND DISCUSSION 47**

4.1 Characterisation of the various photocatalysts 47

*Optical characterisation using diffuse reflectance spectroscopy* *47*

*Determination of crystal size by XRD* *49*

*Microstructure and morphology of Pt modified catalysts* *51*

*SEM and EDX* *52*

4.2 Photocatalytic $H_2$ production 54

*Selection of laser energy (40mJ)* *54*

*The change in physical properties of $TiO_2$ following exposure to laser irradiation* *55*

*Effect of Pt on the photocatalytic activity of $TiO_2$* *57*

*Photocatalytic production of $H_2$* *58*

**CHAPTER 5: CONCLUSION** **65**

5.1 Project evaluation 65

5.2 Recommendations 66

5.3 Final conclusion 67

**Appendix** **68**

a) Band gaps 68

b) Photonic efficiency 74

**BIBLIOGRAPHY** **75**

# LIST OF FIGURES


Figure 1.1: Excitation of $TiO_2$. Electrons absorb photons and progress to the conduction band, consequently generating positive holes 4

Figure 2.1: Direct conversion devices for solar energy utilisation (Clark *et al.*, 1982) 8

Figure 2.2: Trends of proven world crude oil reserves and consumption from 1980 to 2007. Data collected from Energy Information Administration (EIA) and British Petroleum (BP) (Shafiee & Topal, 2008) 9

Figure 2.3: Trends of proven world coal reserves and consumption from 1987 to 2005. Data collected from Energy Information Administration (EIA) and British Petroleum (BP) (Shafiee & Topal, 2008) 9

Figure 2.4: Trends of proven world natural gas reserves and consumption from 1980 to 2007. Data collected from Energy Information Administration (EIA) and British Petroleum (BP) (Shafiee & Topal, 2008) 10

Figure 2.5: Consumption of fossil fuels worldwide from 1965 to 2030. Data collected from Energy Information Administration (EIA) and British Petroleum (BP) (Shafiee & Topal, 2008) 10

Figure 2.6: A graph of absorbance versus wavelength 15

Figure 2.7: A graph that illustrates how the band gap is obtained from the intersection between the linear fit and the photon energy axis 17

Figure 2.8: Photocatalytic splitting of water to produce hydrogen and oxygen 18

Figure 2.9: Possible reactions which can take place when $TiO_2$ is irradiated by a light source composed of certain wavelengths 19

Figure 2.10: Molecular structure of titanium (IV) dioxide (IMS, 2011) 21

Figure 2.11: Standard potentials for various reduction half reactions compared with the band gap of $TiO_2$ (Atkins & De Paula, 2006) 24

Figure 2.12: The photocatalytic formation of hydrogen from ethanol on Pt-$TiO_2$ (Yang *et al.*, 2006b) 25

Figure 2.13: An illustration of how dissociative adsorption occurs on the Pt-$TiO_2$ surface. The presence of Pt stabilizes the excited electrons in the conduction band 26

Figure 2.14: Movement of the Fermi level in extrinsic semiconductors after doping 29

Figure 2.15: a) Interstitial and b) substitutional doping of $TiO_2$ 30

Figure 2.16: The basis on which a dye works as sensitiser (Ni *et al.*, 2007) 32

Figure 2.17: Propagation of an electromagnetic wave 33

Figure 2.18: Temporal coherence 33

Figure 2.19: Spatial coherence 34

Figure 3.1: Borosilicate glass cylinder containing a 0.7 $W/m^2$ UV light 36

Figure 3.2: Schematic diagram of the photocatalytic reaction system used for loading 0.5–2wt% Pt-$TiO_2$: a) Peristaltic pump, b) Suspended Pt-$TiO_2$ solution and magnetic stirrer, c) UV light reactor 37

Figure 3.3: Photos of the different Pt loadings. a) pre-treated $TiO_2$, b) 0.5wt% Pt-$TiO_2$, c) 1wt% Pt-$TiO_2$, d) 1.5wt% Pt-$TiO_2$, e) 2wt% Pt-$TiO_2$ 38

Figure 3.4: Integrating sphere used for DRS measurements 39

Figure 3.5: Specially designed reaction vessel used in the laser studies a) side view b) top view 41

Figure 3.6: a) Individual components of a specially designed reaction vessel b) Plastic rings used to keep the gas dispenser in place c) A side-front view to show the round indent of the gas dispenser 41

Figure 3.7: Gas sampling attachment used for $H_2$ sampling 42

Figure 3.8: Diameter of laser beam 43

Figure 3.9: Experimental setup for studying laser induced photocatalytic water splitting 45

Figure 4.1: Diffuse reflectance spectra of $TiO_2$ and the various Pt-$TiO_2$ photocatalyst 47

Figure 4.2: XRD of $TiO_2$ and Pt loaded $TiO_2$ photocatalysts 50

Figure 4.3: TEM results for the a) 0.5wt%, b) 1.0wt%, c) 1.5wt% and d) 2.0wt% Pt loadings with a scale of 250 nm 52

Figure 4.4: SEM images a) untreated $TiO_2$, b) pre-treated $TiO_2$, c) 0.5wt% Pt-$TiO_2$, d) 1.0wt% Pt-$TiO_2$, e) 1.5wt% Pt-$TiO_2$ and f) 2.0wt% Pt-$TiO_2$ 53

Figure 4.5: a) Pre-treated $TiO_2$, b) Pt-$TiO_2$ photocatalyst c) blue-grey colour of the various photocatalysts after laser irradiation 55

Figure 4.6: Speculated reaction mechanism for water splitting over Pt-$TiO_2$ (Sayama & Arakawa, 1997) 58

Figure 4.7: Schematic representation of the proposed steps for the photocatalytic molecular hydrogen production from an aqueous methanol solution over Pt-$TiO_2$ 60

Figure 4.8: Time course of the photocatalytic $H_2$ evolution over different photocatalysts. Conditions: 1g/L photocatalyst, water (50ml): methanol (50ml, 0.0125M), laser energy (40mJ), temperature 25°C (arrows indicating an increase) 64

Figure 4.9: Amount of $H_2$ produced over different photocatalysts. 64

# LIST OF TABLES


Table 2.1: Properties of the three main polymorphs of $TiO_2$ (Carp *et al.*, 2004) 22

Table 2.2: Frequently used dyes (Jana, 2000) 31

Table 2.3: Operating wavelengths of a Nd:YAG laser 34

Table 3.1: Amounts of $H_2PtCl_6.6H_2O$ used for the individual loadings 37

Table 3.2: Parameters used for DRS 39

Table 3.3: Experimental parameters 44

Table 3.4: Gas chromatography settings used for gas analyses 46

Table 4.1: Band gap values for the various photocatalysts 48

Table 4.2: D and $W_A$ values obtained by XRD for the various photocatalysts 51

Table 4.3: Composition of the photocatalysts as determined by EDX 54

Table 4.4: Effect of laser light on the rutile:anatase ratio of the various Pt-$TiO_2$ photocatalysts 56

# ABSTRACT

The photocatalytic production of $H_2$ from water as well as from a 1:1 methanol:water solution employing pre-treated $TiO_2$ and various Pt-$TiO_2$ photocatalysts was studied by using an Nd:YAG laser as irradiation source. The photocatalysts (0.5-, 1-, 1.5- and 2 wt% Pt-$TiO_2$) were prepared by utilizing a photocatalytic reduction method after which characterisation by various analytical techniques, i.e. XRD, TEM, ICP, SEM, and EDX, were conducted. XRD clearly indicated that platinum was not present in the crystal structure of $TiO_2$, but was rather loaded onto the surface of $TiO_2$. TEM analysis confirmed the presence of Pt on the surface with a particle/cluster size between 11 nm and 22 nm. SEM showed that repeatable results in respect of surface appearance were obtained. ICP and EDX indicated that the loading method was successful with only a slight deviation between the actual amount loaded and the calculated amount loaded. The impact of the loaded Pt on the band gaps of the different photocatalysts was investigated by diffuse reflectance spectroscopy (DRS) and calculated by employing the Kubelka-Munk method. The band gap values shifted sequentially from 3.236eV to 3.100 eV as the loading increased, moving closer to the absorbance region for visible light. The amount of hydrogen produced from the individual photocatalysts dispersed in both pure water and aqueous methanol solutions, was measured manually with a gas chromatograph. As soon as irradiation was initiated, a distinct colour change from shades of grey to dark blue-grey was observed for all the photocatalysts. XRD confirmed that it was due to the anatase phase transforming to produce more rutile phase. No $H_2$ was detected for the various photocatalysts suspended in water, i.e. in the absence of methanol. The amount of hydrogen produced from the various Pt photocatalysts suspended in the aqueous methanol solution was found to be the highest for the 0.5wt%- and 1.5wt% Pt-$TiO_2$ photocatalysts and the lowest for the 2wt% Pt-$TiO_2$. This could be due to loading Pt above the optimum amount to such an extent, preventing sufficient light from reaching the $TiO_2$ surface. Pt particles can also touch and overlap which will decrease Pt contact with $TiO_2$ thus decreasing effective charge transfer.



**Keywords:** Band gap, $H_2$ production, laser, platinum, titanium dioxide ($TiO_2$)

# OPSOMMING

Die fotokatalitiese produksie van $H_2$ uit water sowel as uit ‘n 1:1 metanol:water oplossing in die teenwoordigheid van vooraf-behandelde $TiO_2$ en verskeie Pt-$TiO_2$ fotokatalisatore is bestudeer deur die gebruik van ‘n Nd:YAG laser as die bestralingsbron. Die fotokatalisatore (0.5-, 1-, 1.5- and 2 wt% Pt-$TiO_2$) is berei deur ‘n fotokatalitiese reduksiemetode waarna karakterisering gedoen is deur verskeie analitiese tegnieke, soos XRD, TEM, ICP, SEM, en EDX. XRD het aangedui dat Pt nie teenwoordig was in die kristalstruktuur van $TiO_2$, maar eerder gelaai was op die oppervlak van die $TiO_2$. TEM-analise het die teenwoordigheid van Pt op die oppervlak met ‘n spesifieke partikel/trosgrootte tussen 11 nm en 22 nm bevestig. SEM het getoon dat herhalende resultate in terme van oppervlakvoorkoms bereik is. ICP en EDX het aangetoon dat die laaimetode suksesvol was, met net ‘n klein afwyking tussen die werklike hoeveelheid gelaai en die berekende hoeveelheid gelaai. Die impak van die gelaaide Pt op die bandgapings van die verskillende fotokatalisatore is ondersoek deur diffuse reflekterende spektroskopie (DRS) en bereken deur die gebruik van die Kubelka-Munk metode. Die bandgaping waardes het sekwensieel geskuif van 3.236eV to 3.100 eV soos wat die hoeveelheid Pt toegeneem het, en nader beweeg aan die absorbsie-omgewing vir sigbare lig. Monsters van die hoeveelheid $H_2$ wat deur die individuele fotokatalisatore geproduseer is, gesuspendeer in suiwer water en ‘n waterige metanol-oplossing, is met die hand geneem en met ‘n gaschromatograaf geanaliseer. So gou as wat bestraling begin het, het sigbare kleurveranderinge voorgekom en veranderinge van grys skakerings tot donker blougrys kon gesien word vir al die fotokatalisatore. XRD het bevestig dat dit die resultaat was van die anatase-fase wat getransformeer is om meer rutiel-fase te produseer. Geen $H_2$ kon opgemerk word vir die verskillende fotokatalisatore gesuspendeer in water nie, dit is, in die afwesigheid van metanol. Die hoeveelheid waterstof wat geproduseer is uit die verskillende fotokatalisatore gesuspendeer in die waterige metanol-oplossing is gevind om die hoogste te wees vir die 0.5wt%- en 1.5wt% Pt-$TiO_2$ fotokatalisatore en die laagste vir die 2wt% Pt-$TiO_2$. Dit kan toegeskryf word aan Pt wat bo die optimale hoeveelheid gelaai word wat voorkom dat genoeg lig die $TiO_2$ oppervlak kan bereik. Pt deeltjies kan ook aanmekaar raak en oormekaar laai, wat die Pt kontak met $TiO_2$ verminder, en dus ook effektiewe elektronoordrag verminder.

**Sleutelwoord:** Bandgaping, $H_2$ produksie, laser, platinum, titanium dioksied ($TiO_2$)

# CHAPTER 1: BACKGROUND AND AIMS

## 1.1 Background

Most of the world`s energy demand is met by fossil fuels today. Technologies related to fossil fuel extraction, transportation, refining and in particular their combustion, have harmful impacts on the environment and economy. Views concerning world fossil fuel reserves and predictions of exactly when supplies of fossil fuels will be exhausted differ (Shafiee & Topal, 2008). Recently, growing environmental concern and an increasing energy demand have many companies and researchers working hard on the development of technologies and processes which can efficiently exploit the potential of hydrogen as a clean energy carrier. At present only about 5% of commercial hydrogen is produced by making use of renewable energy sources while about 95% of hydrogen is mainly derived from fossil fuels (Ni *et al.*, 2004).

Much attention has been attracted to the photo-assisted stoichiometric production of $H_2$ and $O_2$ from water splitting and the potential utilisation of solar energy, a renewable energy source. On the other hand, efficient conversion of solar energy has been a challenging problem and numerous studies have been undertaken in this direction (Galin'ska & Walendziewski, 2005). Significant progress has, however, been made in the use of integrated chemical systems based on semiconductor particulates in gaseous and liquid phase photoredox processes (Bamwenda *et al.*, 1995).

One of the most extensively studied and promising photocatalysts for $H_2$ production by means of water splitting is $TiO_2$. It has been widely used in many photocatalytic reaction systems due to its high activity and high stability (Kandiel *et al.*, 2011). When $TiO_2$ is excited by photons with energy greater and/or equal to its band gap of 3.26eV (Carp *et al.*, 2004) charge separation occurs (reaction 1.1).

$$TiO_2 \overset{hv}{\rightarrow} e^-_{TiO_2} + h^+_{TiO_2} \qquad 1.1$$

Energy is transferred from absorbed photons to electrons and is subsequently excited from the valence band (VB) to the conduction band (CB); consequently generating positive holes (Figure 1.1).

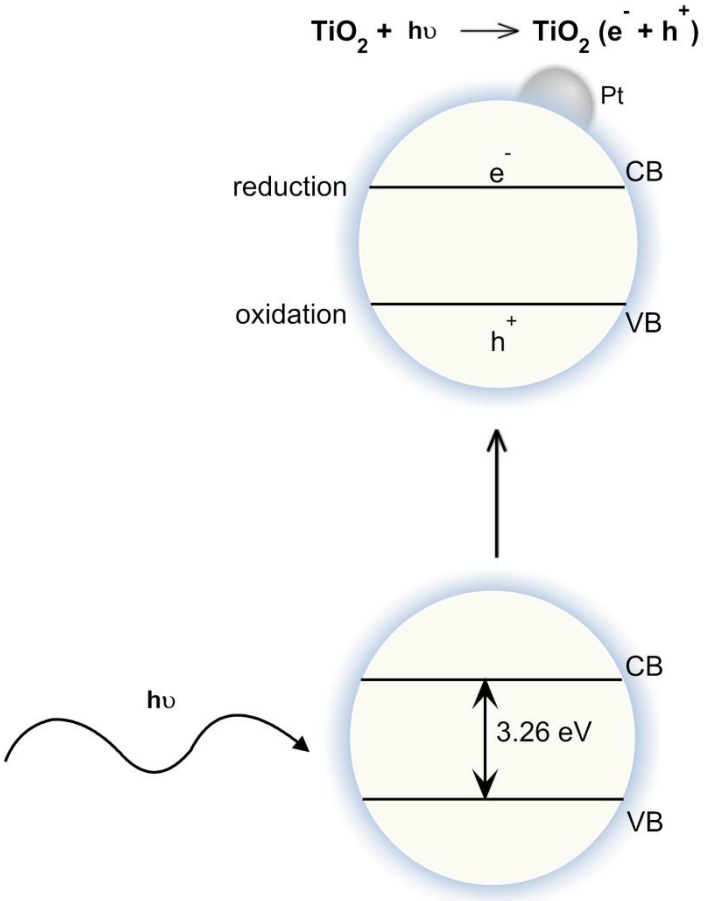



**Figure 1.1: Excitation of $TiO_2$. Electrons absorb photons and progress to the conduction band, consequently generating positive holes**

The excited electrons ($e^-$) and positive holes ($h^+$) can mainly undergo recombination and/or partake in oxidation and reduction reactions respectively. For a semiconductor to be considered as a potential photocatalyst for the production of $H_2$ by water splitting (reaction 1.2), the potential of the VB should be more positive than the water oxidation level ($E^{\Theta}/V = 1.23$) and the CB should be more negative than the hydrogen production level ($E^{\Theta}/V = 0$).

$$2H_2O \xrightarrow[TiO_2]{} 2H_2 + O_2 \qquad 1.2$$

Theoretically, all types of semiconductors that satisfy this requirement can be used for hydrogen production, but other physical and chemical properties such as photocorrosion of the semiconductor play a role when selecting a suitable

photocatalyst for water splitting. $TiO_2$ consists of exceptional resistance to photocorrosion; it is abundant and interacts with water and light simultaneously. The photocatalytic properties of $TiO_2$ can also be altered significantly by various methods affecting the electronic structure and defect chemistry (Nowotny *et al.*, 2006; Nowotny *et al.*, 2005). The most studied modification is the alteration of the $TiO_2$ band gap with loaded (Figure 1.1) or doped Pt metal. The Pt acts as an electron accepting species by creating sinks for the electrons thus inhibiting electron-hole recombination. Many studies conducted on the enhancement of $TiO_2$ by means of loading Pt onto the surface report an enhancement in the photocatalytic activity of the reaction investigated (Li & Li, 2002).

A means of enhancing $H_2$ production is by the use of sacrificial agents. Methanol is frequently used as a sacrificial agent to act as an electron donor for photocatalytic $H_2$ production. According to literature methanol is the most reactive alcohol acting as a sacrificial agent for $H_2$ production (Yang *et al.*, 2006b; Cortright *et al.*, 2002; Sakata & Kawai, 1981). Methanol, however, can also be a direct source of $H_2$ (Yang *et al.*, 2006a; Yang *et al.*, 2006b) when coupled with $TiO_2$ photocatalysis.

In general, most of the research studies reported on photocatalysis are based on the use of conventional lamps in the UV and visible region as energy source. Very little work has been conducted on photocatalysis where a laser acts as the energy source (Gondal *et al.*, 2004a; Gondal *et al.*, 2004b; Hameed & Gondal, 2004; Hameed *et al.*, 2004b; Gondal *et al.*, 2002). Laser light exhibits special properties like monochromaticity, high intensity, low beam divergence, directionality and it is coherent. From literature found regarding the employment of lasers as energy source for $H_2$ production, only $WO_3$, NiO, $Fe_2O_3$ and $TiO_2$ (rutile) were studied in the presence of $Fe^{3+}$, $Ag^{+}$ and $Li^{+}$ (Gondal *et al.*, 2004a; Hameed & Gondal, 2004). It is therefore of great interest to investigate the employment of lasers as excitation source to study the activity of other photocatalysts for the potential production of $H_2$. This work can then be compared with studies done using conventional lamps and potentially applying this knowledge to future work employing sunlight as the irradiation source (Gondal *et al.*, 2004a). The production of hydrogen through the use of lasers as irradiation source could be much faster (minutes) than conventional lamps (hours and days), but the cost of $H_2$ production would be much higher.

## 1.2 Aim of study

It is essential to find an alternative, environmentally friendly, economically viable and sustainable energy source to replace fossil fuels.

In working towards this global goal, this study has as main aims the following:

The (i) synthesis of various Pt-$TiO_2$ photocatalysts by means of a photocatalytic reduction process, (ii) determination of the band gaps of these Pt-$TiO_2$ photocatalysts, and (iii) evaluation of these photocatalysts for laser induced photocatalytic production of $H_2$ under mild conditions from an aqueous methanol solution

To ensure that these aims are met, this study also has as specific aims the following:

- The compilation of a thorough literature survey in which sufficient knowledge regarding the state of fossil fuel reserves, hydrogen as an alternative energy carrier, the role of efficient photocatalysts and lasers as energy source in potential photocatalytic $H_2$ production, is summarised. The literature study was also conducted to serve as a literature review bases for further studies conducted in this field at the North-West University,

- Designing and manufacturing a specialised reaction vessel to employ in laser induced $H_2$ production studies.

- The setting up of a suitable nanosecond laser pulse system for $H_2$ production studies.

- Comparing the results obtained in this study with available results found in literature.

- Since this is the first investigation of this nature, it might not deliver a final and clear result, but it can make recommendations pertaining to future research.

# CHAPTER 2: LITERATURE STUDY

## 2.1 Introduction

Energy is the basis of the economy and modern life. The majority of energy consumed today is obtained from the chemical energy stored in fossil fuels, with coal as the main supplier in the nineteenth century and crude oil and natural gas in the twentieth century (Varin *et al.*, 2009). Other sources of energy are mineral fuels, nuclear and hydroelectric sources. Fossil fuels are considered to be non-renewable sources because they cannot be replenished once they are exhausted. Views concerning world fossil fuel reserves and predictions of exactly when supplies of fossil fuels will be exhausted differ. Consequently, in terms of pollution production and environmental impact, energy production can be considered a harmful industry since the industrial revolution in the $18^{th}$ century (Serrano *et al.*, 2009). Our dependence on fossil fuels has unfortunately led to a number of other problems (such as global warming), which include undeniable climate changes due to growing amounts of greenhouse gasses in the atmosphere and a decrease in urban air quality to name only a few.

During the 1970s the concept of hydrogen as a clean, efficient and viable remedy for addressing energy problems gained momentum (Varin *et al.*, 2009) and offers a potential solution to satisfy energy and environmental requirements globally. Hydrogen as an alternative energy carrier, incorporating solar energy as a prominent method to produce hydrogen has become a major point of interest over the past few decades (Clark *et al.*, 1982). Systems/devices where solar energy is utilised for energy conversion is illustrated in Figure 2.1, which indicates that solar energy can play a vital role towards the replacement of fossil fuels. The refinement of methods and technologies where solar light is incorporated for hydrogen production is still underway, however, many other studies of hydrogen production (Murphy, 2007; Gondal *et al.*, 2004b; Hameed *et al.*, 2004b; Gondal *et al.*, 2002; Hashimoto *et al.*, 2001; Clark *et al.*, 1982) have been conducted and are still being improved to obtain an economically viable and environmentally favourable method.

The necessity to find another reliable, sustainable and environmentally friendly energy source to substitute fossil fuels is becoming a major priority and research conducted up to this point on hydrogen seems to be very promising.

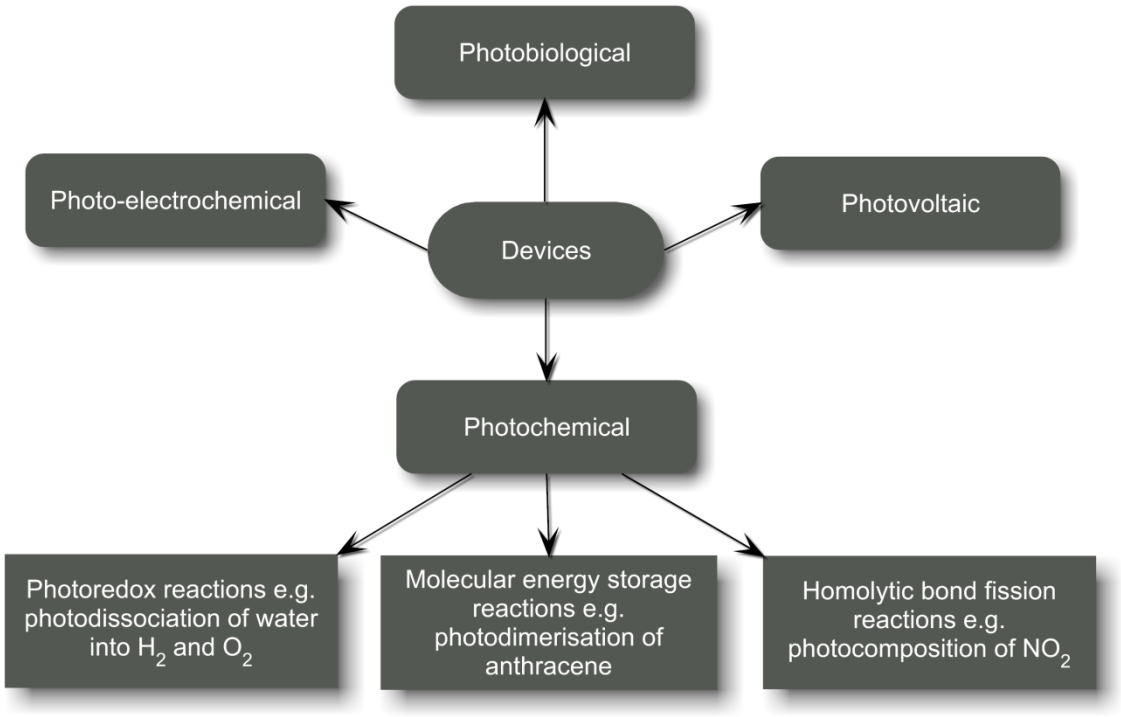



**Figure 2.1: Direct conversion devices for solar energy utilisation (Clark *et al.*, 1982)**

## 2.2 Economic interest regarding fossil fuels

Fossil fuels play a crucial role in the world energy market. The World Energy Outlook (WEO) 2007 (Shafiee & Topal, 2008) forecasts that energy generated from fossil fuels will remain the major source and is still expected to meet about 84% of the energy demand in 2030. In Figures 2.2-2.4, a correlation between oil, coal and natural gas consumption with their reserves is illustrated independently. An interesting observation concerning fossil fuels is that although there has been a rise in consumption of oil and gas, the quantities of known reserves are also rising with time. This is due to discoveries of other new reserves (not the case for coal), but even so, fossil fuels reserves are still deteriorating and will eventually be exhausted.

In Figure 2.5 the trend of fossil fuel consumption worldwide from 1965 to 2030 is illustrated and an increase over the next 20 years is forecast. The consumption of fossil fuels has increased over the last 50 years and the same trend is expected for the foreseeable future, simultaneously verifying the depletion of fossil fuels worldwide.

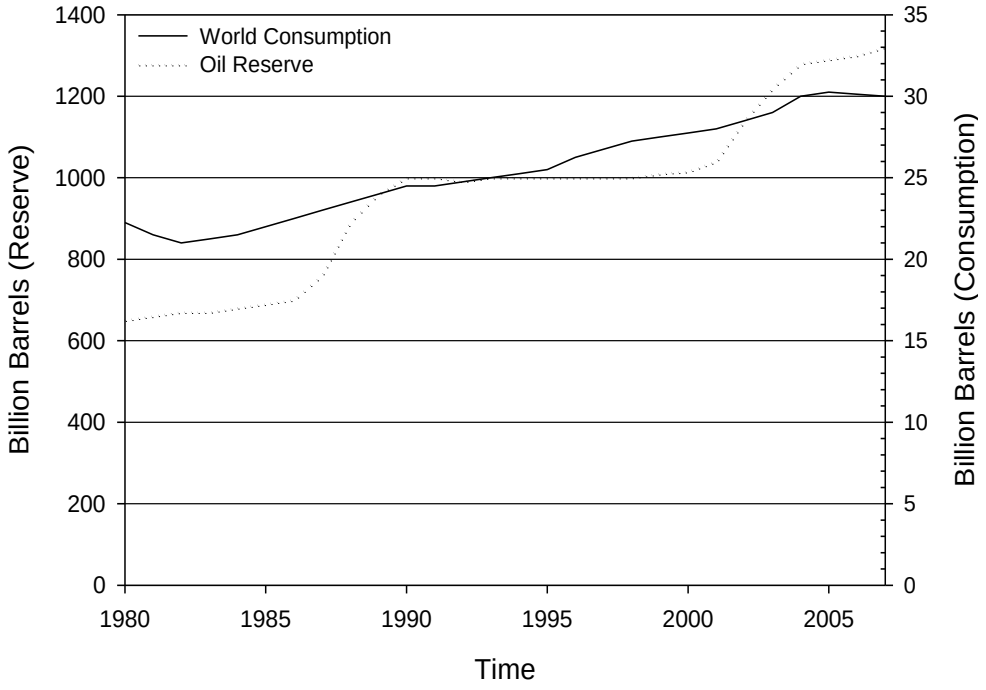



**Figure 2.2:** **Trends of proven world crude oil reserves and consumption from 1980 to 2007. Data collected from Energy Information Administration (EIA) and British Petroleum (BP) (Shafiee & Topal, 2008)**

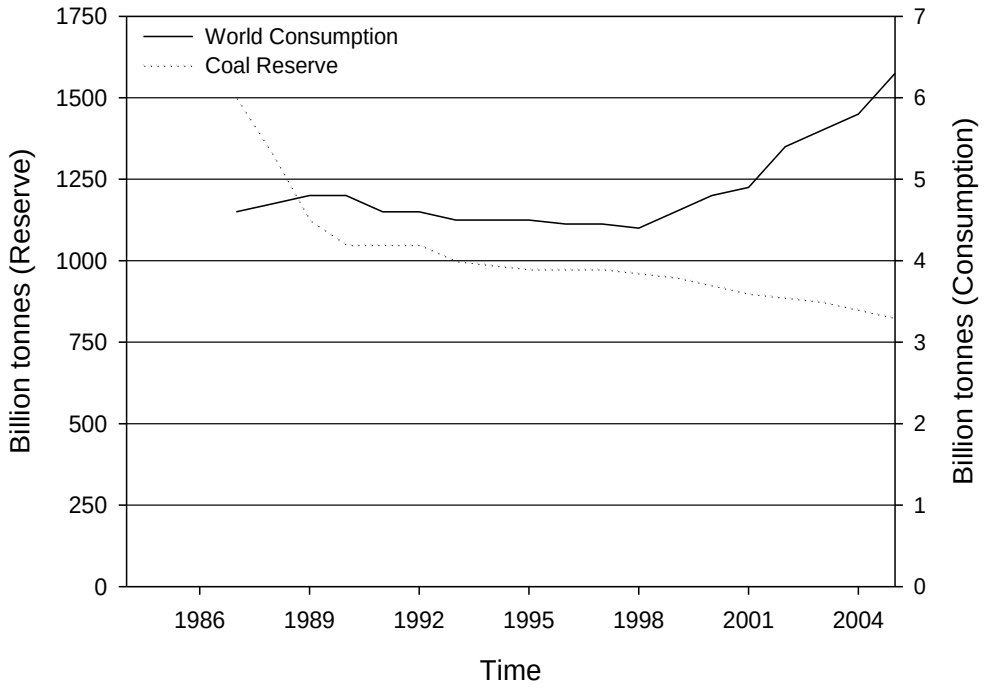



**Figure 2.3:** **Trends of proven world coal reserves and consumption from 1987 to 2005. Data collected from Energy Information Administration (EIA) and British Petroleum (BP) (Shafiee & Topal, 2008)**

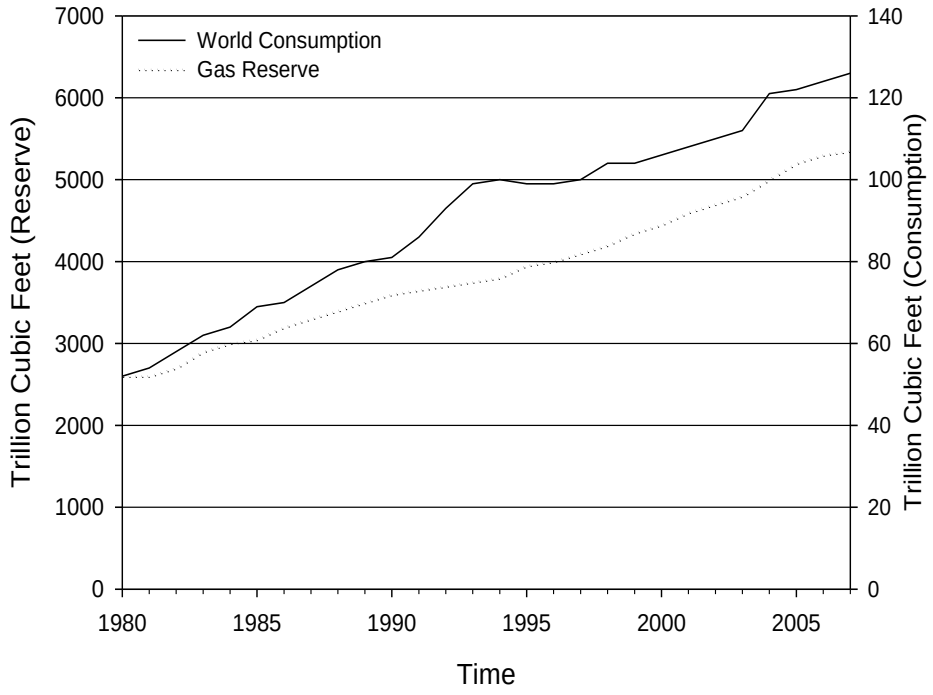



**Figure 2.4: Trends of proven world natural gas reserves and consumption from 1980 to 2007. Data collected from Energy Information Administration (EIA) and British Petroleum (BP) (Shafiee & Topal, 2008)**

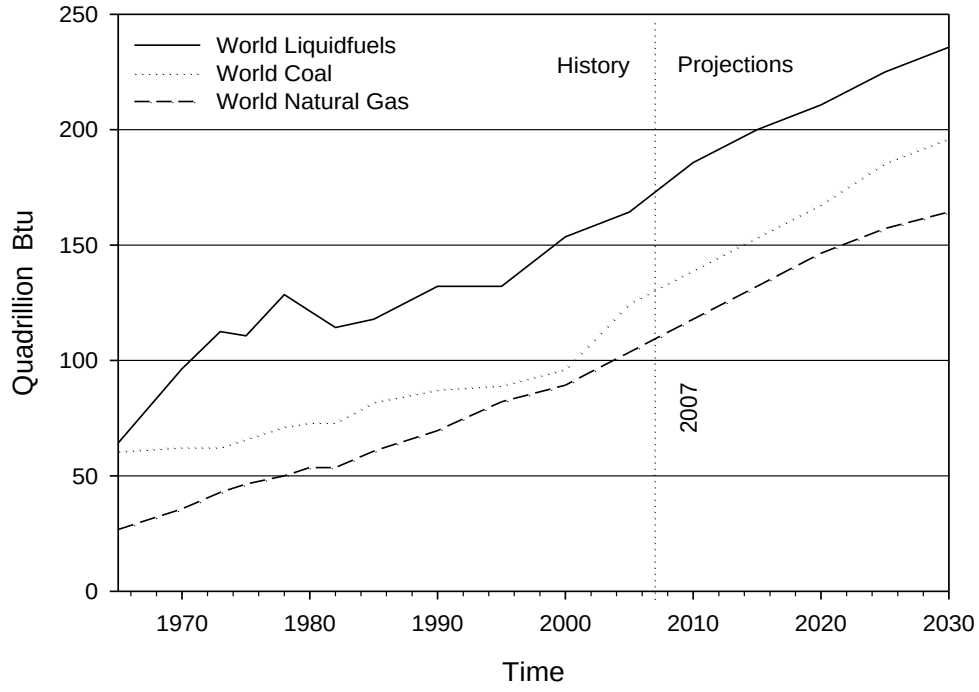



**Figure 2.5: Consumption of fossil fuels worldwide from 1965 to 2030. Data collected from Energy Information Administration (EIA) and British Petroleum (BP) (Shafiee & Topal, 2008)**

## 2.2 Environmental impact of fossil fuels

Energy resources are essential to satisfy human needs and improve the quality of life, but consumption of these energy sources may unfortunately lead to negative environmental impacts. The sources of fossil fuels are rapidly depleting and the ways of extraction, transportation, processing and the greatest influence, their combustion, have significant effects on the environment. Spills and/or leakages do occur during the transportation and storage of oil and gas, causing severe water and air pollution. Air pollution is mainly produced from the combustion of fossil fuels with the introduction of various gases ($CO_x$, $SO_X$, $NO_X$, and CH), toxic organic compounds and traces of soot, ash and tar etc. into the atmosphere, causing damage to human health, crop, and structures as well as reduced visibility to name only a few (Barbir *et al.*, 1990). These compounds just named are known as primary pollutants and once they are introduced into the atmosphere, secondary pollutants may form. These secondary pollutants in turn may react with sunlight forming ozone and aerosols or react with water for instant rain, causing various acids, which in turn cause soil pollution (Record *et al.*, 1982). Fossil fuels react in a chain reaction of negative impacts and emphasises the subsequent development of clean and sustainable energy sources.

## 2.3 Hydrogen as an alternative energy carrier

Due to the depleting state and diminishing availability of fossil fuels, developing alternative sources for energy production is a necessity. Factors such as climate and environmental impact, reliability, efficiency of use, health and economic interest play important roles in efforts to change the present energy system to a sustainable one. Many possibilities are considered and are currently being investigated.

Hydrogen is one of the considerations as a renewable and sustainable alternative energy solution, for it has the potential to replace fossil fuels (Thomas *et al.*, 1998) and also offers many advantages (Midili & Dincer, 2008). It is a non-toxic clean energy carrier and produces non-toxic exhaust emissions. A stable environment is ensured with regards to the transportation of hydrogen because it can be safely done by making use of pipelines. Hydrogen also offers long-term energy use, for it can be produced by means of various production techniques from non-fossil fuel based sources and stored for long periods of time, compared to electricity. Application wise it can be

advantageously used as a chemical feedstock in the petrochemical, food, ferrous and non-ferrous metal, microelectronics, chemical and polymer synthesis and metallurgical process industries. This in turn ensures social and economic sustainability. Thus, a new pathway emerges for an energy system that is more environmentally friendly and leads to a reduction in the dependence on fossil fuels as energy source.

In this century hydrogen has mainly been produced from fossil-based sources, including coal, natural gas, hydrocarbons etc. by applying different techniques such as reforming, gasification 2.1, pyrolysis etc. (U.S. Department of energy, 2011; Midili & Dincer, 2008). The majority of global hydrogen is produced by the reformation of methane or natural gas by steam (reaction 2.2). The cost of this method is very low and the efficiency of this method is 70-80%. The negative aspect of this process is that $CO_2$ is produced simultaneously with $H_2$ (Serrano *et al.*, 2009) in a second step reaction 2.3 of hydrogen production.

Coal gasification reaction (unbalanced)

$$CH_{0.8} + O_2 + H_2O \rightarrow CO + CO_2 + H_2 + other\ species \qquad 2.1$$

Gas reformation

$$CH_4 + H_2O \rightarrow CO + 3H_2 \qquad 191.7\ kJ\ mol^{-1} \qquad 2.2$$

$$CO + H_2O \rightarrow CO_2 + H_2 \qquad -40.4\ kJ\ mol^{-1} \qquad 2.3$$

In order to reduce the utilization of fossil-based fuels and methods that are not environmentally friendly, the development of new catalytic processes must be considered and put into practice. The most ideal catalytic process known to humanity is artificial photosynthesis illustrated in reaction 2.4 where plants allow photon energy to be converted into chemical energy which is stored in the bonds of glucose (Anastas, 2009).

$$H_2O + CO_2 \rightarrow {}^{1}/_{6}\,(C_6H_{12}O_6) + O_2 \qquad \Delta G = 502\ kJmol^{-1} \qquad 2.4$$

One of the most promising artificial photosynthetic reactions to produce hydrogen is by the photocatalytic splitting of water to produce hydrogen and oxygen gas under solar light irradiation (Anastas, 2009). This dissociation of water may be achieved by a one-electron (reaction 2.5), a two-electron reaction 2.6 or a four-electron process reaction 2.7 respectively (Anon, 1991).

| | | |
|---|---|---|
| $H_2O \rightarrow H^{\cdot} + OH^{\cdot}$ | 248 nm; 5 eV | 2.5 |
| $2H_2O \rightarrow H_2O_2 + H_2$ | 712 nm; 1.74 eV | 2.6 |
| $H_2O \overset{h\nu}{\rightarrow} H_2 + {}^1/_2\, O_2$ | 1000nm; 1.23 eV | 2.7 |

The simplified dissociation of water occurs as follows (Naito & Arashi, 1995):

| | |
|---|---|
| $H_2O \rightarrow HO + O$ | 2.8 |
| $HO \rightarrow H + O$ | 2.9 |
| $2H \rightarrow H_2$ | 2.10 |
| $2O \rightarrow O_2$ | 2.11 |

Sunlight is composed of a broad range of wavelengths, but few of the wavelengths are smaller or equal to 248 nm, therefore reaction 2.5 is not favourable do be driven by sunlight. From literature it is proven that reaction 2.7 is the most efficient for the decomposition of water using solar energy (Bolton, 1987; Bolton *et al.*, 1985). The production of hydrogen by employing solar energy for photocatalytic water splitting is, however, low, mainly due to the following reasons (Ni *et al.*, 2007):

1. When electrons are excited from the valence band to the conduction band in the photocatalyst, the holes in the valence band can recombine with the excited electrons releasing energy in the form of unproductive heat or photons;

2. Energy is required to decompose water into hydrogen and oxygen, thus the backward reaction (formation of water) is more favourable;

3. UV light occupies 3-4% of the total solar spectrum that reaches the earth with visible light occupying about half (50%) (Rayalu *et al.*, 2007; Yang *et al.*, 2006a) and it should be emphasised that water is transparent to visible light (Ashokkumar, 1998), therefore a photocatalyst which is visibly light-responsive should ideally be used.

As a result, a lot of research has been conducted on systems capable of decomposing water or its component reduction and oxidation reactions, i.e.

$$2H^+ + 2e^- \rightarrow H_2 \qquad 2.12$$

$$2H_2O \rightarrow O_2 + 4H^+ + 4e^- \qquad 2.13$$

Water does not absorb sunlight and undergo spontaneous decomposition. In order to utilise solar energy for the decomposition of water and the production of hydrogen, a light absorbing specie which may be a metal complex, organic dye, semiconductor or a chloroplast must be added to the system (Anon, 1991). Success in the direct stoichiometric splitting of pure water was achieved by Abe *et al*. (2001) using a Z-scheme system (mimicking the photosynthesis of green plants, where water is oxidised into $O_2$ and the received electrons are utilized to fix $CO_2$ into carbohydrates) consisting of Pt-loaded TaON ($H_2$ production), Pt-loaded $WO_3$ ($O_2$ production) and an $IO_3^-/I^-$ redox mediator.

## 2.4 Band gap

To determine whether a semiconductor is capable of a required reaction is it necessary to know the band gap of the semiconductor. One of the most important parameters which is used to characterise the optical properties of a semiconductor is its band gap energy, $E_g$. The band gap is defined as the energy difference between the valence bands (VB) and conduction bands (CB), a range of energies to which no orbital corresponds (Atkins, 1998). Many different methods for the determination of the band gap of semiconductors exist, all of which are based on different assumptions and theories. Three different methods for the determination of the band gap for semiconductors will briefly be discussed.

***Band gap determined by absorption spectroscopy***

The band gap can directly be determined by detecting the optical absorbance of a semiconductor by using absorbance (transmission) spectroscopy. A graph as follows is obtained (Figure 2.6).

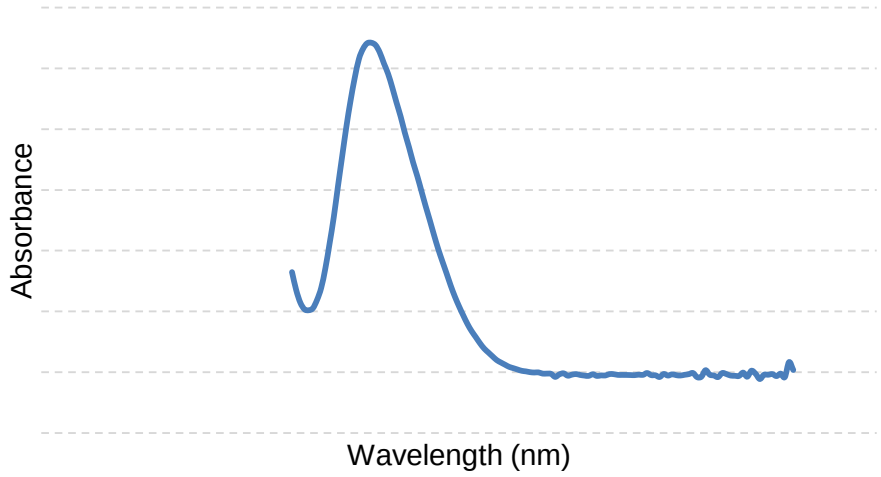



**Figure 2.6: A graph of absorbance versus wavelength**

The band gap can be calculated with the following equation (Atkins, 1998):

$$E(J) = c \times h/\lambda$$

Where,

$\boldsymbol{c}$: speed of light, $2.99793\times10^{8}$ $m.s^{-1}$

$\boldsymbol{h}$: Planck's constant, $6.62608\times10^{-34}$ J.s

$\boldsymbol{\lambda}$: wavelength (nm) (centre of the peak)

**1eV** = $1.60218\times10^{-19}$ J

*(By definition, one eV is equal to the amount of kinetic energy gained by a single unbound electron when it accelerates through an electric potential difference of one volt.)*

Unfortunately, due to the large scattering component and inaccurate transition edges, this technique is not applicable for semiconductor powder samples (Gal *et al.*, 1999).

A more accurate approach is to generate the first derivative of absorbance with respect to photon energy and finding the maxima in the derivative spectra at the lower energy sides (Mecerril *et al.*, 2004).

***Band gap determined by Kubelka and Munk***

Diffuse reflectance spectroscopy (DRS) is the most applicable optical method to study powder samples. It is non-destructive radiation of materials based on the interaction between light and matter. Radiation is reflected in all directions and occurs in samples where the particles are oriented in different directions, e.g. powders. DRS is widely used in industrial applications and in the study of solid-solid reactions, surface phenomenon, absorbed species, etc. (Gal *et al.*, 1999). By applying the Kubelka-Munk treatment (Originated in an article "An Article on Optics of Paints Layers" written by Paul Kubelka and Franz Munk, August 1931 and modified by various scientist over preceding years) to diffuse reflectance spectra of semiconductor powder samples it is possible to extract their $E_g$ unambiguously (Escobedo Morales *et al.*, 2006).The powder sample should consist of 1-3mm thickness to ensure that all the incident light is absorbed or scattered before reaching the surface of the sample holder and thus having no influence on the value of reflectance (R) (Murphy, 2007).

***Kubelka-Munk expression for powder samples***

$$[F(R_\infty)hv]^2 = C_2(hv - E_g)$$

Where,

$F(R_\infty) \equiv \frac{(1-R_\infty)^2}{2R_\infty}$: the Kubelka-Munk function with $R_\infty = R_{sample} / R_{standard}$

$hv$: photon energy

$C_2$: proportionality constant

By plotting $[F(R_\infty)hv]^2$ against $hv$(eV), the band gap can be obtained from the intersection between the linear fit and the photon energy axis. A graph as follows is obtained (Figure 2.7).

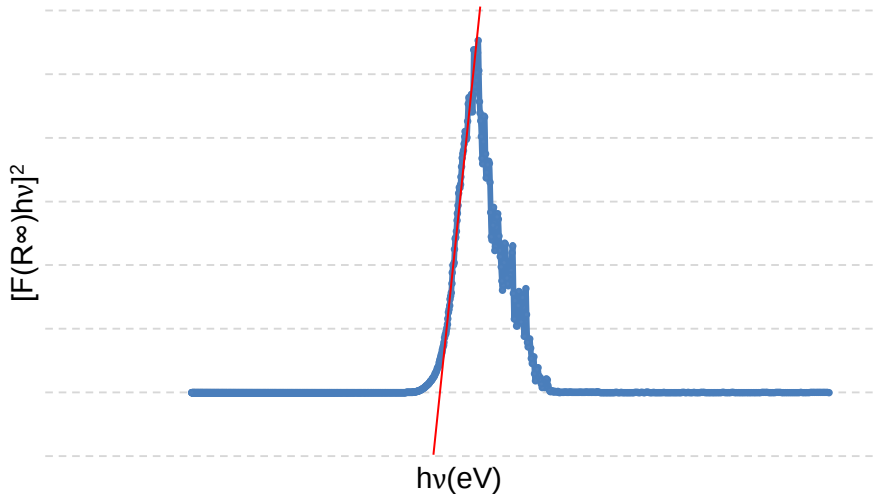



**Figure 2.7: A graph that illustrates how the band gap is obtained from the intersection between the linear fit and the photon energy axis**

DRS is a more convenient characterisation technique to use than UV-Vis absorption spectroscopy, since the powder does not have to be dissolved in a liquid medium and also because DRS takes into consideration the effect of light scattering (Escobedo Morales *et al.*, 2006).

## 2.5 Photocatalysis

Photocatalysis implies that for a chemical reaction or an acceleration of a reaction to occur, a light source (energy source) and a photocatalyst need to be present. Most of the studies conducted in this field have been carried out with broadband UV lamps (Ohno *et al.*, 1998; Maruthamuthu *et al.*, 1989). To achieve the splitting of water (Figure 2.8 & Figure 2.9), adsorbed water reacts with the valence band holes to produce hydroxyl radicals ($OH^{\bullet}$) (by donation of electrons) as well as $O_2$ (oxidation). $H_2$ is produced by the other portion of dissociated water, i.e. $H^+$ by means of capturing the electrons (reduction) present in the conduction band (Hameed & Gondal, 2004). In order to achieve photocatalysis and to prevent recombination of the electron ($e^-$) with

the positive hole ($h^+$), either in bulk or on the surface of the semiconductor, the excited electron should have a noticeable lifetime in the conduction band and must be able to reach the surface of the material in order to undergo reaction with the required medium. There are three ways for the excited electron to return to the ground state: (i) recombination with the positive hole, (ii) the excited electron can participate in a reduction reaction if an electron can be obtained from another reductant and (iii) the excited electron reduces an oxidant present and the positive hole can be used for oxidation (Kriek, 1994:5-8).

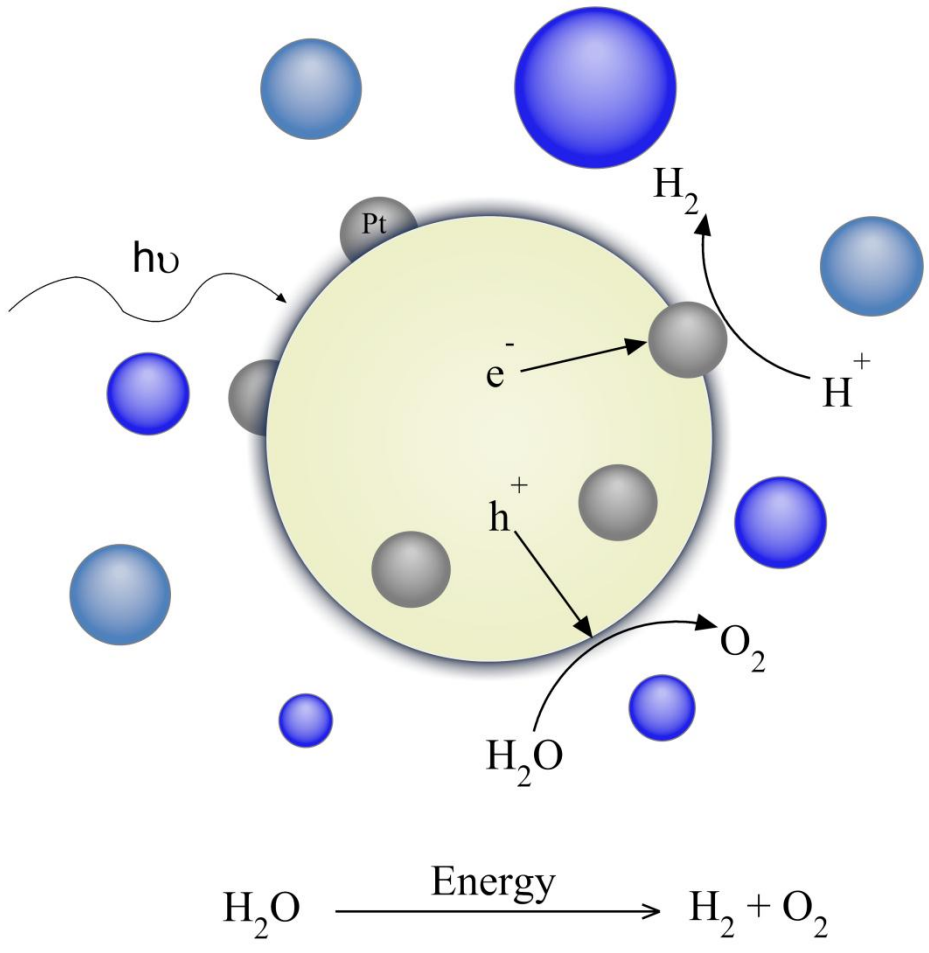



**Figure 2.8: Photocatalytic splitting of water to produce hydrogen and oxygen**

Many ways of enhancing the photocatalytic activity of photocatalysts by means of reducing the recombination rate, which have been studied by the scientific community, will be discussed in the following sections.

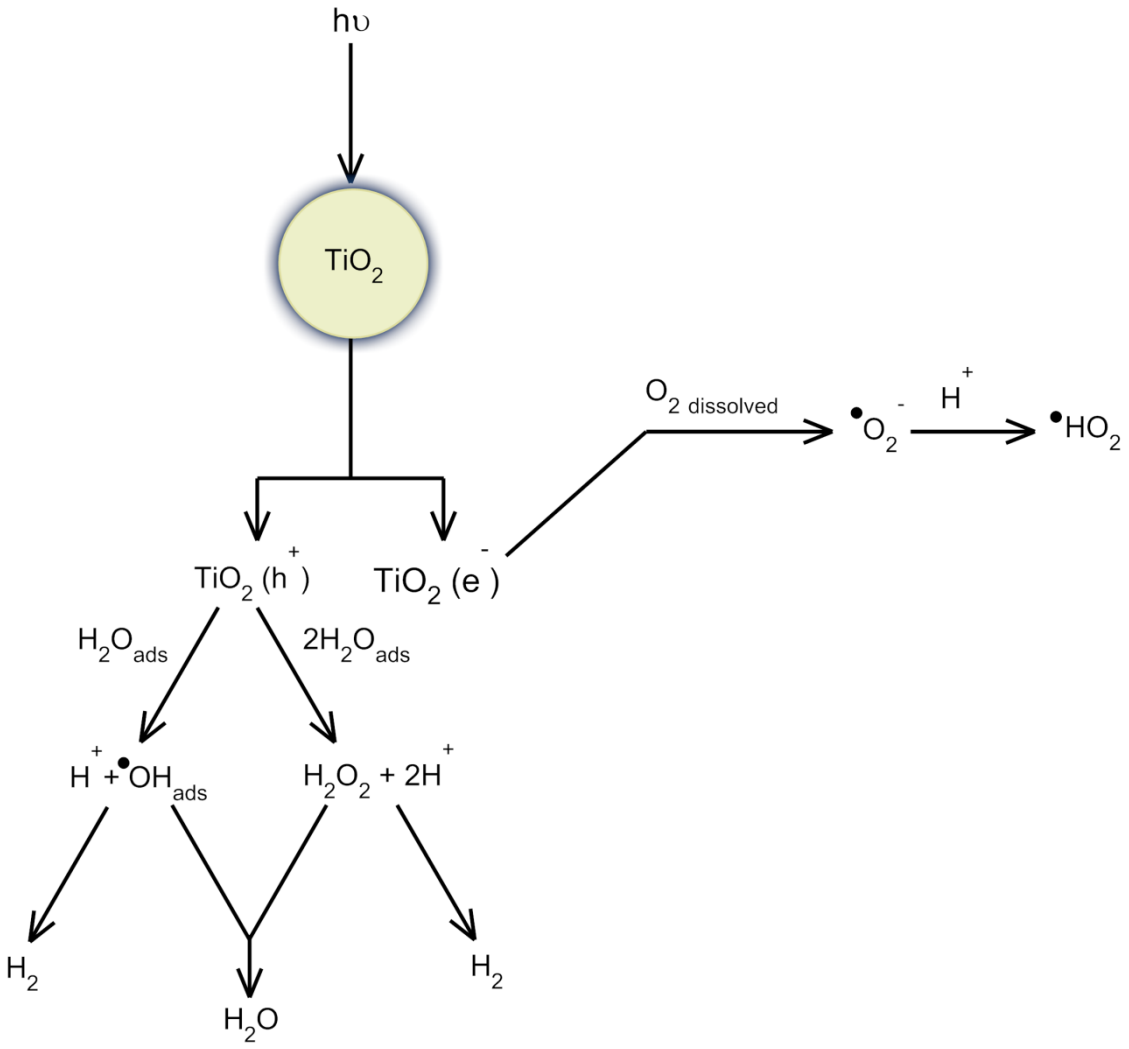



**Figure 2.9: Possible reactions which can take place when $TiO_2$ is irradiated by a light source composed of certain wavelengths**

## 2.6 Photocatalysts

*Semiconductors*

The potential to apply semiconductor materials in the conversion of solar energy to electrical energy was realised by the scientific community when Fujishima and Honda (Fujishima & Honda, 1972) reported the use of semiconductor electrodes. Semiconductor materials have been used to date as electrodes, colloids, thin films and in powder form. The powder form is of interest in this study for more reactive surface is available, a concept which emerged in 1979 through work done by Bard (Matsuoka *et al.*, 2007). Methods of hydrogen production include the electrochemical, biological,

photo-electrochemical and the photocatalytical. The capability of a semiconductor to decompose water into hydrogen and oxygen depends on the energy levels of the semiconductor's conduction and valence band for it determines the ability of the semiconductor to transfer electrons to the absorbed particle obtained by the absorbance of light ($h\upsilon \geq E_g$). Another characteristic of a photocatalyst is to adsorb two reactants simultaneously enabling oxidation and reduction of the reactants simultaneously. For the process of water splitting, an ideal semiconductor should consist of a conduction band level more negative than the hydrogen reduction level, $H^+/H_2$ (0V) and a valence band level more positive than the water oxidation level, $OH^-/O_2$ (1.23V). This enables efficient decomposition of water into hydrogen and oxygen by employing light energy (Ashokkumar, 1998). The electrons receive energy from the photons which enable them to shift from the VB to the CB if the energy gain is higher than the band gap energy. Thus a catalyst with a band gap of more than 1.23eV is necessary to effectively split water photocatalytically into hydrogen and oxygen, but the conduction band must lie beneath 0eV and the valence band above 1.23eV. Theoretically, a potential difference of more than 1.23eV is equivalent to the energy of a photon with a wavelength of about 1010nm, which clearly includes the visible light region, indicating that it is possible to split water utilising visible light.

If the valence band is partially filled with electrons, it is hard to make a distinction between the valence and conduction band and the material is then known as a conductor, thus no band gap will exist. An insulator is a material with a band gap larger than 5eV which makes it difficult to excite electrons to the conduction band, in other words, the electrons are restricted in there motion (Oudenhoven *et al.*, 2004). The material is known as a semiconductor if the valence band is completely filled with electrons and if the band gap lies between 0 and 5eV.

Among the various photocatalysts, $TiO_2$ is the most attractive to be used for water splitting. This is due to its low cost, abundant reserves, exceptional resistance to photocorrosion as well as corrosion in aqueous environments, stability over a period of many years (Nowotny *et al.*, 2006), and its ability to react with both water and light simultaneously. The properties of $TiO_2$ can also greatly be altered by various methods affecting the electronic structure and defect chemistry of the crystal lattice (Bak *et al.*, 2003).

## 2.7 Titanium dioxide

The discovery of titanium dioxide (Figure 2.10) was simultaneous to the discovery of titanium.

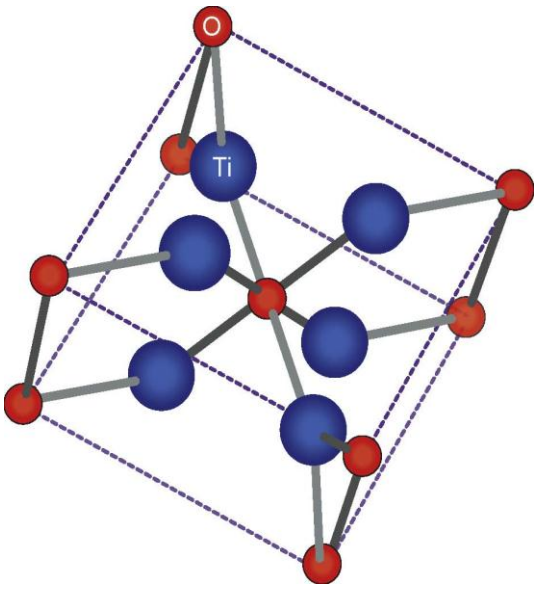
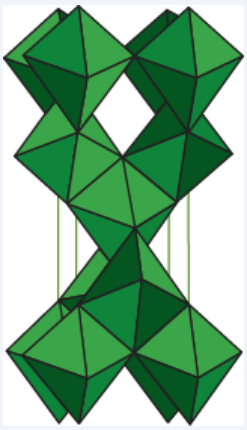
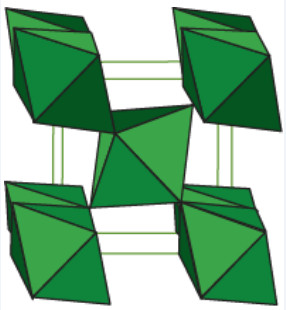
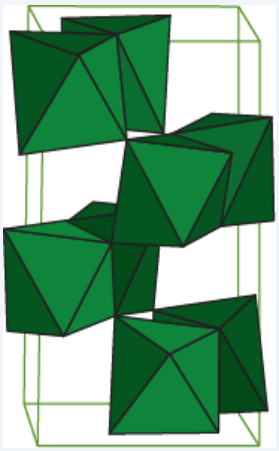



**Figure 2.10: Molecular structure of titanium (IV) dioxide (IMS, 2011)**

Titanium was first discovered by Reverend William Gregor in 1791 in England as an element present in the mineral ilmenite which exists in forms containing 44% to 70% of titanium dioxide (Carp *et al.*, 2004). Titanium is the world`s eighth most abundant metal and the ninth most abundant element in the earth's crust. The primary minerals in which titanium is present are rutile, ilmenite, leucoxene, anatase, brookite, perovskite, and sphene, but the main forms in which titanium dioxide is mainly present are rutile (96%), anatase (longer vertical axis than rutile) and brookite as can be seen in Table 2.1. Rutile is considered as the most stable phase at all temperatures and pressures up to 60kbar, but the small differences in Gibbs free energies at normal temperatures and pressures between the three phases would indicate that the metastable polymorphs are almost as stable as rutile. For the use of $TiO_2$ as photocatalyst, it is therefore advisable to work at room temperature as the transformation of anatase into rutile occurs at increased temperatures and/or pressures where rutile is basically nonexistent at room temperature.

**Table 2.1: Properties of the three main polymorphs of $TiO_2$ (Carp *et al.*, 2004)**

| | $TiO_2$ | | |
|---|---|---|---|
| **Types** | Anatase | Rutile | Brookite |
| **Band gap(eV)** **(Banerjee *et al.*, 2006)** | 3.2 | 3.02 | 2.96 |
| **Wavelength (nm)** | 387 | 410 | 419 |
| **Colour** | White-grey | Mainly reddish brown, but also yellowish, bluish or violet | Dark brown<br>Greenish black |
| **Discovery** | 1801 by R.J. Hauy | Major ore, 1803 by Werner in Spain | 1825 by A. Levy in Snowen |
| **Crystal structure** |  |  |  |
| | Octahedrals are connected at vertices (tetragonal) | Edges are connected (tetragonal) | Vertices and edges are connected (orthorhombic) |
| **Refractive index** | $n_g$ $n_p$<br>2.5688 2.6584 | $n_g$ $n_p$<br>2.9467 2.6506 | $n_g$ $n_p$<br>2.809 2.677 |

Rutile absorbs light with a wavelength of 410nm or lower and anatase light with a wavelength of 387nm or lower. Both of them absorb light in the ultraviolet region but rutile is somewhat closer to the visible region. This leads to the conclusion that rutile is more suitable for the use as a photocatalyst because of the wider range in which it can absorb light. However, it has been found that anatase exhibits higher photocatalytic activity compared to rutile. A reason for this phenomenon can be ascribed to the difference in their energy structure. In both of the $TiO_2$ types, the valence band lies low compared to the conduction band and sufficient oxidation by positive holes can occur. The conduction band is positioned near the oxidation-reduction potential for hydrogen, with anatase positioned closer to this potential than rutile leading to anatase having a stronger reducing power than that of rutile (Amemiya, 2004).

$TiO_2$ is also noteworthy for its wide range of applications. As can be seen from Table 2.1, $TiO_2$ consists of a high refractive index. Due to this property, it is most widely used as a white pigment, i.e. white food colourant, provides whiteness and opacity to products such as paints, coatings, plastics, papers, inks, toothpastes and is also found in many sunscreens because of its capability to absorb strong UV rays. Other applications include the decontamination and purifying of water and air, used in antifogging coatings for mirrors and glass (Fujishima *et al.*, 1999) and used in anticancer treatments for skin and stomach (Fujishma *et al.*, 2000).

*Electronic structure of $TiO_2$*

Titanium dioxide exists as $Ti^{4+}$ ($3d^0$) and oxygen atoms organised in a distorted octahedral formation. Elemental Ti and O have the following electron configurations (Banerjee *et al.*, 2006):

$$Ti: 1s^2 2s^2 2p^6 3s^2 3p^6 4s^2 3d^2$$

$$O: 1s^2 2s^2 2p^4$$

Hybridisation of the 2p orbitals of oxygen and the 3d orbitals of Ti primarily forms the valence band of $TiO_2$, while the conduction band is made up from the pure 3d orbital of Ti. Other 3d-transition metal oxides in this series have 3d-states in both the VB and CB. The fact that $TiO_2$ consist of dissimilar parity (difference in the nature of the CB and VB), unlike the other 3d-transition metal oxides, reduces the recombination of the

excited electron and positive holes formed during excitation. Different standard potentials for various reduction half reactions can be seen in Figure 2.11, which clearly indicates why titanium dioxide is the chosen semiconductor for the oxidation of water with subsequent production of hydrogen.

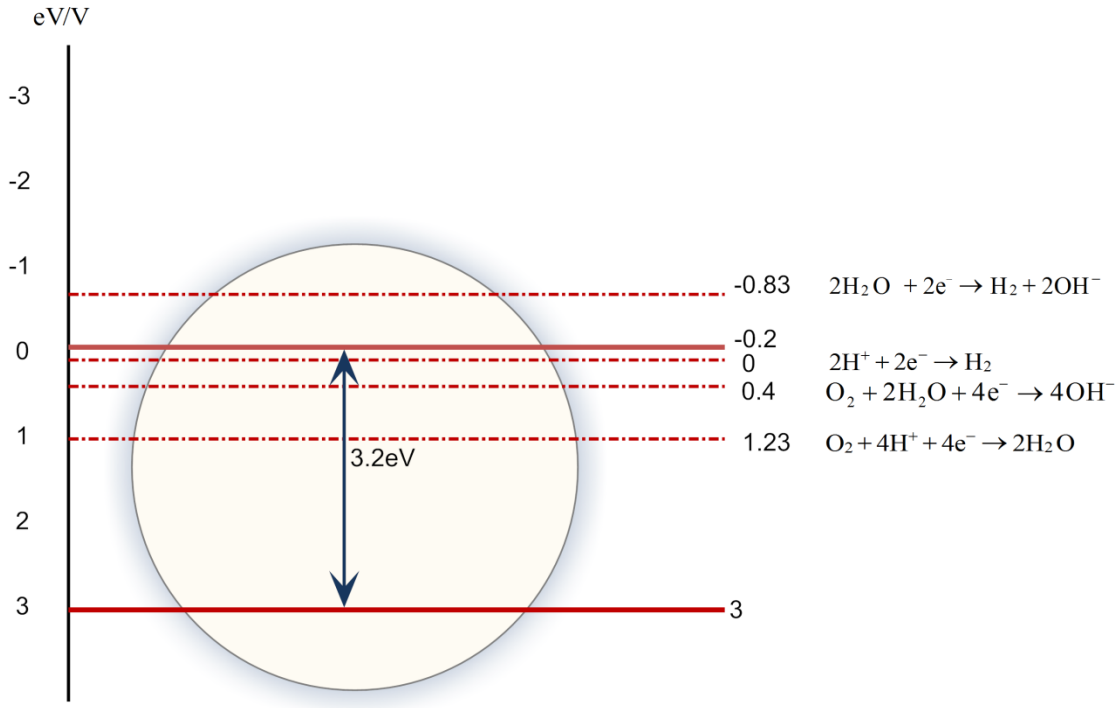



**Figure 2.11: Standard potentials for various reduction half reactions compared with the band gap of $TiO_2$ (Atkins & De Paula, 2006)**

## 2.8 Review and recent developments using $TiO_2$

Only 5% of commercial hydrogen is at present produced through the application of renewable energy, mainly through water electrolysis. The remaining 95% of hydrogen is produced from non-renewable fossil fuels as the costs associated with hydrogen production from fossil fuels are much lower. Hydrogen production through possible photocatalytic water splitting using $TiO_2$ and sunlight is a promising way for green and low-cost production of hydrogen.

## 2.9 Chemical additives to enhance hydrogen production

### *Addition of electron donors*

The first problem that occurs when an electron is excited from the VB to the CB is the rapid recombination of the photo-generated holes in the VB with the excited electrons in the CB which decreases the efficiency of water splitting. A solution to this problem is obtained by adding electron donors, also known as sacrificial agents or hole scavengers, that limits/prevents the recombination of the positive hole with the photo-generated electron by reacting irreversibly with the positive hole in the VB. The chosen electron donor should be added continuously or in excess for they are consumed during the photocatalytic reaction. Higher quantum efficiency is then obtained due to enhanced electron/hole separation.

### *Organic compounds as electron donors*

In a study conducted by Nada *et al.* (2005), EDTA, methanol, ethanol, $CN^-$ and lactic acid were studied with regards to enhancing hydrogen production. The following was obtained in decreasing order of facilitating $H_2$ production, EDTA > methanol > ethanol > lactic acid. Other inorganic ions that were used as sacrificial agents include $S^{2-}/SO_3^{2-}$ (Koca & Sahim, 2002), $Ce^{4+}/Ce^{3+}$ (Bamwenda & Arakawa, 2001) and $IO_3^-/I^-$ (Abe *et al.*, 2001). In a study conducted by Yang *et al.* (2006), it was found that alcohols can act as a direct source of hydrogen (Figure 2.12).

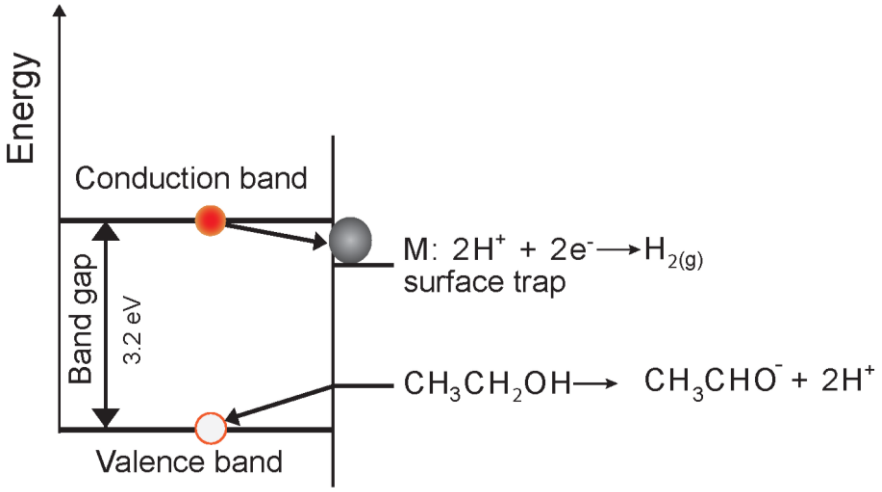



**Figure 2.12: The photocatalytic formation of hydrogen from ethanol on Pt-$TiO_2$ (Yang *et al.*, 2006b)**

On the surface of $TiO_2$ in the presence of noble metals, the alcohol forms ethoxide and hydroxyl groups between the metal particles and $TiO_2$ by dissociative adsorption as can be seen in Figure 2.13. The ethoxide species act as effective hole traps and the hydroxyls are reduced by the stabilised electrons from the metal particles. From a selection of alcohols methanol was found to be most effective and active for assisting in hydrogen production (Bamwenda *et al.*, 1995).

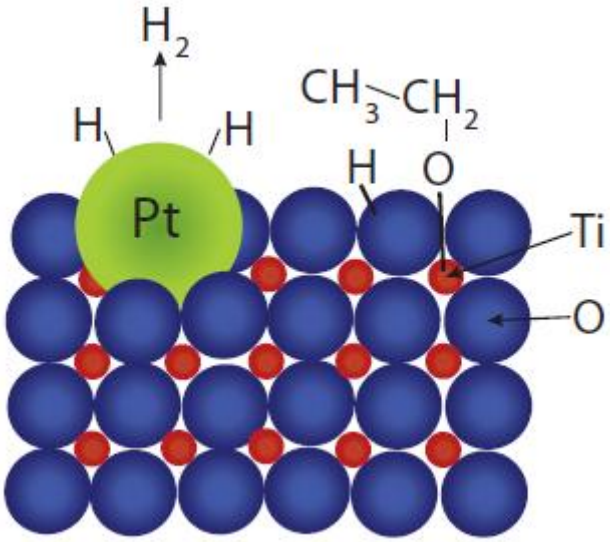



**Figure 2.13: An illustration of how dissociative adsorption occurs on the Pt-$TiO_2$ surface. The presence of Pt stabilizes the excited electrons in the conduction band**

### *Addition of carbonate salt or iodide anion*

When a photocatalyst is irradiated, hydrogen evolution is observed but not always oxygen. The reason for this observation can be ascribed to peroxo-species that can form on the catalyst during irradiation (Mills & Porter, 1982a) or the presence of $Ti^{3+}$ in the fresh catalyst (Kiwi, 1986). Extensive investigations of promoted semiconductors such as Pt-$TiO_2$ have been conducted and the problem just mentioned occurred in these studies. Addition of carbonate salts, especially $Na_2CO_3$, was found to significantly enhance the overall decomposition of water as the photo-generated holes were prevented from reacting with the excited electrons because they were consumed by several carbonate species. Species such as $HCO_3^-$, $CO_3^{\bullet-}$, $HCO_3^{\bullet}$ and $C_2O_6^{2-}$ were found to cover the surface of the Pt-$TiO_2$ catalyst through infrared studies and these carbonate species were formed as a result of the following reactions (Ni *et al.*, 2007):

$$CO_3^{2-} + H^+ \rightleftharpoons \mathrm{HCO_3^-} \quad (2.14)$$

$$\mathrm{HCO_3^-} + h^+ \rightleftharpoons HCO_3^{\cdot} \quad (2.15)$$

$$HCO_3^{\cdot} \rightleftharpoons H^+ + CO_3^{\cdot -} \quad (2.16)$$

$$2CO_3^{\cdot -} \rightarrow C_2O_6^{2-} \quad (2.17)$$

The backward reaction to form water was also minimized by the decomposition of peroxy-carbonates ($C_2O_6^{2-}$) into $O_2$ and $CO_2$, enhancing the desorption of $O_2$ from the photocatalyst.

$$C_2O_6^{2-} + 2h^+ \rightarrow O_2 + 2CO_2 \quad (2.18)$$

In turn the $CO_2$ was converted into $HCO_3^-$, again affecting $H_2$ production (Ni *et al.*, 2007). It was also found that the concentration of $Na_2CO_3$ added determined the evolution rates of $H_2$ and $O_2$ (Sayama & Arakawa, 1992), but the mechanism of how the $Na_2CO_3$ affects the reaction rate has not been fully clarified (Matsuoka *et al.*, 2007).

Another study (Abe *et al.*, 2003) concluded that the backward reaction, caused by the Pt loaded onto the $TiO_2$ surface, can effectively be suppressed by the addition of iodide. In the absence of iodide, only a small amount of $H_2$ but no $O_2$ was evolved. In the presence of a small amount of NaI in the photocatalyst suspension, a stoichiometric evolution ratio of $H_2$:$O_2$ = 2:1 was observed. In the presence of high concentrations of NaI, the evolution rate decreased to a stoichiometric ratio of $H_2$:$O_2$ = 0.15. This phenomenon was speculated to be due to the fact that the oxidation of $I^-$ was more favoured than the oxidation of water. The following reactions occur in acidic and basic solutions (Abe *et al.*, 2001):

$$2I^- + 2h^+ \rightarrow I_2 (or\ I_3) \quad \text{acidic solution} \quad (2.19)$$

$$I^- + 6OH^- + 6h^+ \rightarrow IO_3^- + 3H_2O \quad \text{basic solution} \quad (2.20)$$

Compared to the $Na_2CO_3$ system (pH~11, 2M), the iodide reaction can be carried out under milder conditions due to the small amounts of NaI required (pH~6-7) and

important to note for both the systems is that adding too much of the carbonate salt or iodide anion will reduce the efficiency of the systems as it will decrease light harvesting to the catalyst surface (Sayama & Arakawa, 1996).

## 2.10 Enhancement of $H_2$ production by photocatalyst modification techniques

### *Noble metal loading*

Many studies have been conducted on the enhancement of $TiO_2$ photocatalysts, some working more efficiently than others. Enhancement includes the deposition of, for example, Pt, Au, Pd, Rh, Ni, Cu and Ag onto the $TiO_2$ surface. As electrons are excited into the CB they are transferred to the noble metal particles present on the surface of $TiO_2$, which stabilises these electrons due to the fact that the Fermi levels are now shifted lower than those of $TiO_2$ (Ni *et al.*, 2007). Photo-generated holes remain in the VB of the $TiO_2$, thus enhancing electron/hole separation.

In order to determine whether a metal can be considered as a loading agent it should possess at least the following three properties:

a) it should be resistant to oxidation during the catalytic process,

b) as mentioned it should be an efficient electron trap to prevent electron-hole recombination and

c) it must be efficient for H-H recombination ($H_2$ production).

Electron transfer from $TiO_2$ to Pt particles was observed by Anpo and Takeuchi (Anpo & Takeuchi, 2002) after they investigated this electron transfer by employing Electron Spin Resonance (ESR). It was found that with the increase in irradiation time, the signals of $Ti^{3+}$ present in $TiO_2$ increased, but that the loading of Pt reduced the amount of $Ti^{3+}$. The effect of the Pt concentration loaded onto $TiO_2$ and also the method of loading was investigated by Ikuma and Bessho (Ikuma & Bessho, 2007) and they found that an increase in the concentration of Pt loaded increased the amount of $H_2$ evolved but only up to an optimal concentration. Three different loading methods were investigated, i.e. an $H_2$ reduction method, a photo-catalytic method and a formaldehyde method which was found to be the most efficient.

### *Metal ion doping*

When a semiconductor consists of the intrinsic property of conductivity in the pure state it is known as an intrinsic semiconductor. The Fermi level ($E_F$), is an energy level situated near the middle of the band gap. It is the probability where an electron can be present, either near the VB or near the CB (Miessler & Donald, 2004). In contrast to intrinsic semiconductors, extrinsic semiconductors' (Figure 2.14) conductivity is controlled by the process known as doping (Kotz *et al.*, 2006), where a chosen material is added to the crystalline structure of the photocatalyst.

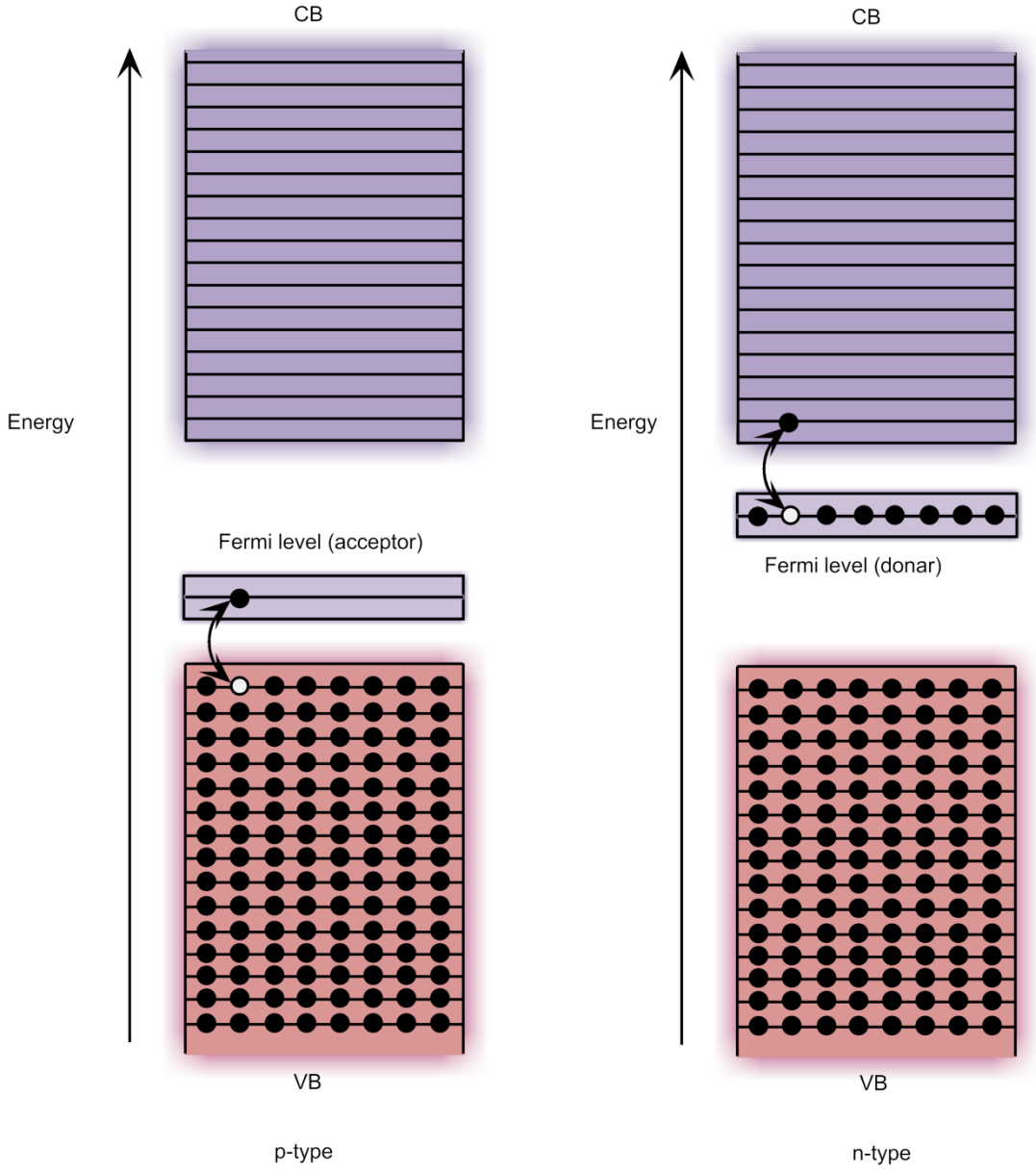



**Figure 2.14: Movement of the Fermi level in extrinsic semiconductors after doping**

If the dopant that is added consists of more valence electrons than the host material, the catalyst is named an n-type semiconductor and the Fermi level of that semiconductor moves closer to the conduction band. If the dopant consists of fewer valence electrons than the host material it is named a p-type semiconductor and the Fermi level moves closer to the valence band (Miessler & Donald, 2004; Jana, 2000).

The effectiveness of doping works on the basis of creating impurity energy levels into the $TiO_2$ lattice structure either by placing the dopant between the other atoms (interstitial) of the chosen lattice or by replacing atoms of the chosen crystalline structure (substitutional) as can be seen in Figure 2.15 (Miessler & Donald, 2004).

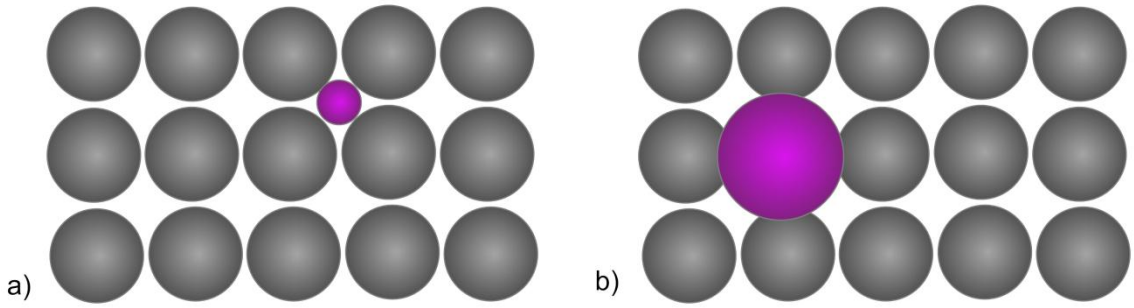



**Figure 2.15: a) Interstitial and b) substitutional doping of $TiO_2$**

Choi *et al.* (1994) studied the effect of enhancing photoreactivity by doping $TiO_2$ with 21 different metal ions and found that among the 21 studied, Fe, Mo, Ru, Os, Re, V and Rh ions increased the photoreactivity and expanded the photo-response of $TiO_2$ into the visible spectrum. A study conducted by Ohno *et al.* (Atkins *et al.*, 2006) proved that by doping $TiO_2$ powder with Ru in the presence of iron (III) ions shifted the photo-reactivity of the catalyst into the visible region and that effective oxygen evolution occurred. Another method which also modifies the $TiO_2$ lattice structure is metal ion-implantation where the semiconductor is injected with transitional metal ions such as V, Cr, Mn, Fe and Ni, by high energy bombardation. This modifies the electronic structure of the semiconductor and as a consequence shifts the photo-response into the visible region (Ni *et al.*, 2007). It is important to emphasise that the photocatalytic reactivity of the metal ion-implanted $TiO_2$ retained the same photocatalytic efficiency as the original unimplanted $TiO_2$ under UV light irradiation. As a consequence, these results clearly suggest that altering the crystal lattice of $TiO_2$ by means of implantation does not work

as electron-hole recombination centres but only modifies the electronic properties of the $TiO_2$ photo-catalyst (Anastas, 2009).

### *Sensitisation*

The word sensitisation refers to a process where something is made sensitive to certain physical or chemical stimuli and in previous studies dye sensitisation was used to utilise visible light for energy conversion in water splitting. Table 2.2 lists dyes that are frequently used for this purpose. The basis on which a dye works as sensitiser is as follows (Figure 2.16): when a dye is excited by visible light, an excited dye is formed and can inject electrons to the CB of the semiconductor which in turn can migrate to particles loaded onto the semiconductor and so initiate desired catalytic reactions. By adding sacrificial agents such as $IO^-_3/I^-$, as mentioned in section 2.9, the dyes can be regenerated and continuous addition is not necessary. Some dyes, for example, O/EDTA and T/EDTA, are able to absorb visible light in the absence of a semiconductor and produce hydrogen at very low rates by acting as a reducing agent (Bi & Tien, 1984).

**Table 2.2: Frequently used dyes (Jana, 2000)**

| **Dye** | **$\lambda_{max}$ (nm)** |
|---|---|
| Methylene blue (MB) | 665 |
| Acridine orange (AO) | 492 |
| Crystal violet | 578 |
| Malachite green | 625 |
| Methyl violet | 580 |

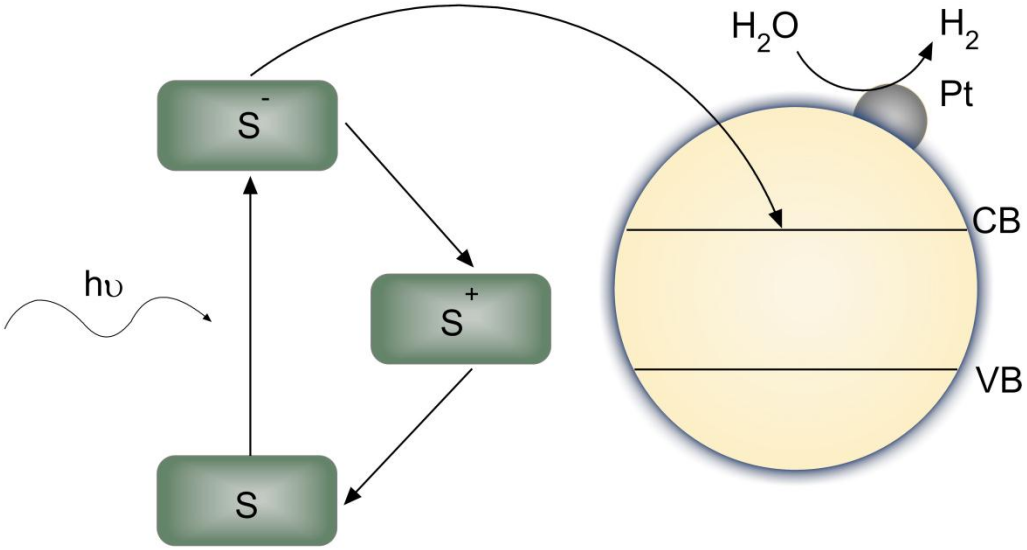



**Figure 2.16: The basis on which a dye works as sensitiser (Ni *et al.*, 2007)**

## 2.11 Lasers as an energy source employed for photocatalysis and general principles

The word laser is an acronym formed form *Light Amplification by Stimulated Emission of Radiation* and simultaneously describes how the light is produced. After the introduction of the term photon by Albert Einstein in 1905, Theodore Herold Maiman, an American physicist, was the first man to construct a laser in 1960 by the excitation of ruby atoms with a flash light (Bush *et al.*, 2007). The use of lasers increased dramatically due to their unique properties and applications. In the modern world today, lasers are present in various forms ranging from large industrial lasers used for cutting and welding, to smaller lasers used in the medical field, to harmless laser used in the entertainment industry, naming only a few (Anon, 2007).

### *Wave properties of light*

The true nature of light was first predicted by Maxwell`s equations in 1864 when he showed that light can be presented as a travelling electromagnetic wave (Silfvast, 2004). An electromagnetic wave consists of an electric (E) field and a magnetic (B) field which are perpendicular to each other as well as the direction of the propagation of the EM-wave (Halliday *et al.*, 2001). Figure 2.17 illustrates the propagation of an electromagnetic wave.

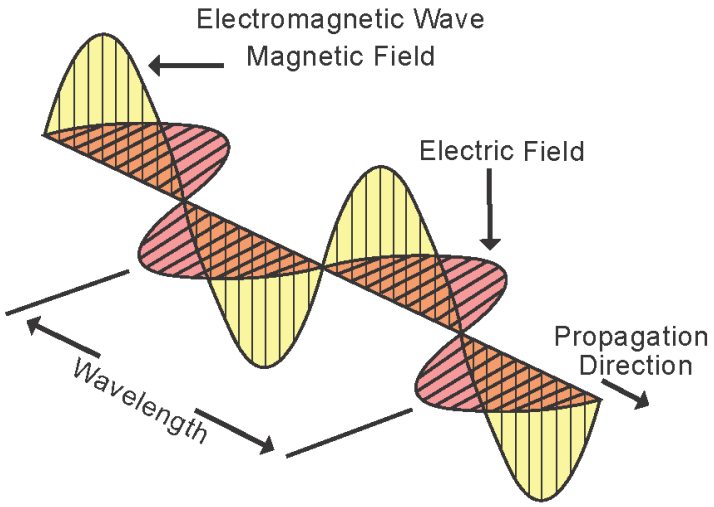



**Figure 2.17: Propagation of an electromagnetic wave**

Electromagnetic waves are characterised by their phase, frequency, direction and the vector property of the transverse field oscillation and can be polarised. From Figure 2.17 it is clear that light consists of planes in which the waves oscillate in a random orientated manner about the direction of propagation. Interference can occur for two sources of electromagnetic waves. Interference can be constructive or destructive depending on the relative phase between them. Only for a coherent light source will one plane of oscillation be dominant. There are two basic properties which describe coherent interference: temporal and spatial coherence. Temporal coherence describes the correlation between signals observed at different moments in time (Figure 2.18) where spatial coherence describes the relation between signals at different points in space (Figure 2.19).

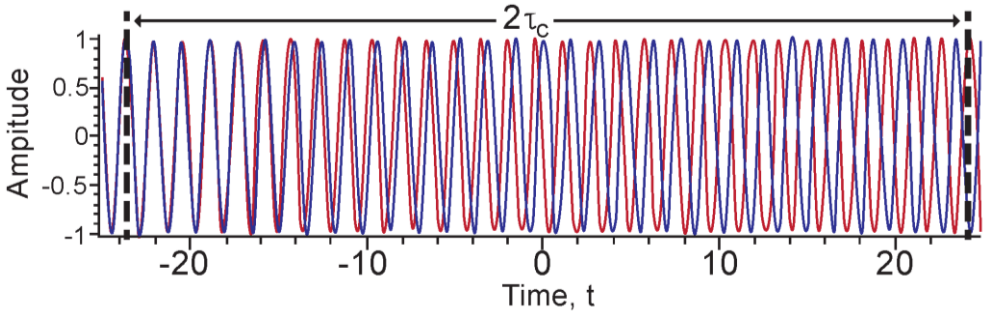



**Figure 2.18: Temporal coherence**

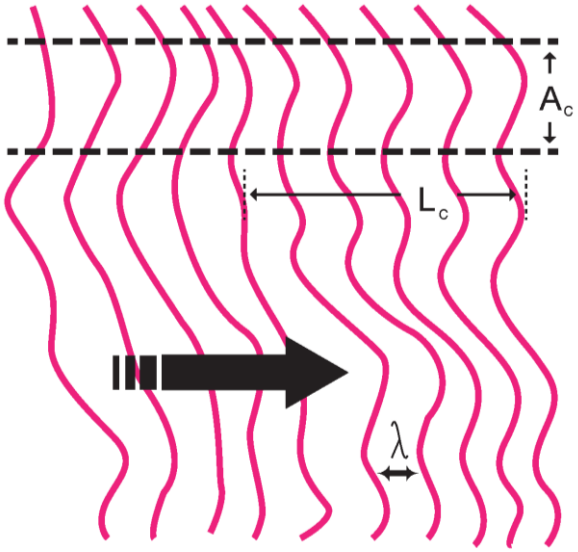



**Figure 2.19: Spatial coherence**

### *Nd:YAG Laser*

YAG is the acronym for yttrium aluminium garnet ($Y_3Al_5O_{12}$) and the term YAG laser is usually used for solid state lasers (Paschotta, 2008). In one form, YAG lasers can consist of $Nd^{3+}$ ions and is then known as an Nd-YAG laser. Other rare-earth-doped YAG crystals also exist which include ytterbium, erbium, thulium or holmium. An Nd-YAG laser can operate at different wavelengths which are listed in Table 2.3.

**Table 2.3: Operating wavelengths of a Nd:YAG laser**

| Wavelength (nm) | Description |
|---|---|
| 266, 355, 532 | Generated by frequency doubling, frequency tripling, and frequency quadrupling |
| 946 | Functions as a quasi-three level laser |
| 1064 | Most common wavelength |
| 1123, 1319, 1338, 1444 | Other wavelengths |

Most of the research studies reporting on photocatalysis are based on the use of conventional lamps in the UV and visible region. Very little work has been conducted on photocatalysis where a laser acts as the energy source (Gondal *et al.*, 2004a; Gondal *et al.*, 2004b; Hameed & Gondal, 2004; Hameed *et al.*, 2004b; Gondal *et al.*, 2002).

Duonghong *et al.* (1981), conducted laser photolysis experiments with $Ru(bpy)_3^{2+}$ /$MV^{2+}$ (methyl viologen) aqueous solution as sensitiser at 602 nm and 470 nm in the presence of $Pt/RuO_2$-$TiO_2$ bifunctional catalysts leading to hydrogen and oxygen production from water.

$Fe_2O_3$, $WO_3$, $TiO_2$ (rutile) and NiO catalysts were irradiated under a strong laser beam at 355 nm in the presence and absence of electron capturing agents such as $Fe^{3+}$, $Ag^+$ and $Li^+$ for the first time by Gondal *et al.* (2004a). Optimization was done for $WO_3$ and NiO and found to be optimum for 400mg $WO_3$ and 300mg NiO at 100mJ. $TiO_2$ (rutile) was only used for comparative reasons with regard to the amount of $H_2$ being produced. The production of hydrogen was observed for all the catalysts investigated in this study (Hameed & Gondal, 2004).

Another study conducted by Hameed *et al.* (2004a) investigated the pH changes under UV laser illumination for finger printing the action of oxygen and metal ions as electron capture agents, and the action of methanol as hole-capture agent.

Following on the above-mentioned literature survey there exists a gap for investigating the effect of laser light and laser energy on the photocatalytic production of $H_2$ employing other catalysts apart from those mentioned above, in different aqueous solutions.

# CHAPTER 3: EXPERIMENTAL

## 3.1 Materials

Commercially available Degussa P-25 $TiO_2$ powder with an anatase/rutile ratio of 86.3/13.7 was used throughout. Chloroplatinic acid ($H_2PtCl_6.6H_2O$), methanol (99.5%), hydrochloric acid (HCl, 32%) and ethanol (99.5%) were obtained from MERCK and SIGMA-ALDRICH and used without further purification.

## 3.2 Preparation of Pt-$TiO_2$ catalysts

A photocatalytic method was employed to prepare all photocatalysts. A stock solution containing 400ml water, 100ml HCl and 25g $H_2PtCl_6.6H_2O$ was prepared, using all the available salt, due to the hygroscopic nature of $H_2PtCl_6.6H_2O$. All photo-reaction experiments were carried out in a photocatalytic reactor system, which consisted of a borosilicate glass cylinder containing a 0.7 W/m$^2$ UV light. Rubber rings were used at both ends of the lamp to ensure that none of the solution leaks out when pumping it through the glass cylinder. The glass cylinder was covered with foil and black tape on the outside to ensure maximum exposure of the photocatalysts to the UV light (Figure 3.1). 1g of $TiO_2$ was placed in a 500ml water, $H_2PtCl_6.6H_2O$ (Table 3.1) and ethanol (3g) solution to produce a suspension through magnetic stirring. The suspension was pumped through the continuous flow-through UV light reactor with a flow rate of 400ml/min for 25min at 20°C as shown in Figure 3.2. The solution was subsequently filtered to yield Pt deposited $TiO_2$ powder (Figure 3.3) and placed in a vacuum oven at 80°C for 30min to dry and to evaporate all the ethanol. Samples of the filtrate were taken for ICP analysis.

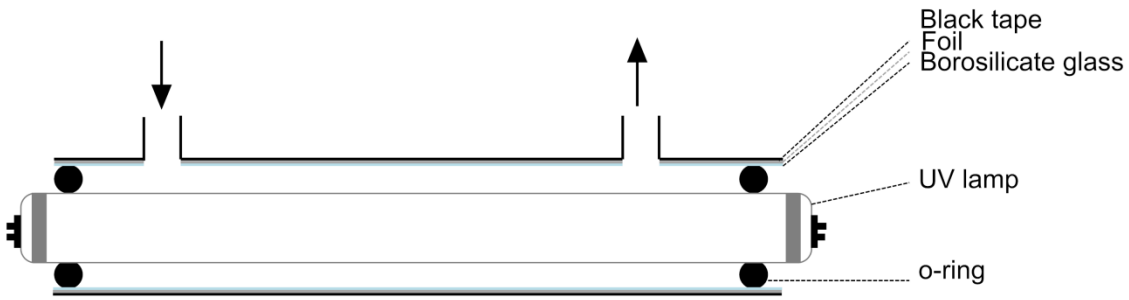



**Figure 3.1: Borosilicate glass cylinder containing a 0.7 W/m$^2$ UV light**

**Table 3.1: Amounts of $H_2PtCl_6.6H_2O$ used for the individual loadings**

| Run | wt% Pt | $H_2PtCl_6.6H_2O$, ml |
|---|---|---|
| 1 | 0.5 | 0.2659 |
| 2 | 1 | 0.5319 |
| 3 | 1.5 | 0.7978 |
| 4 | 2 | 1.0638 |

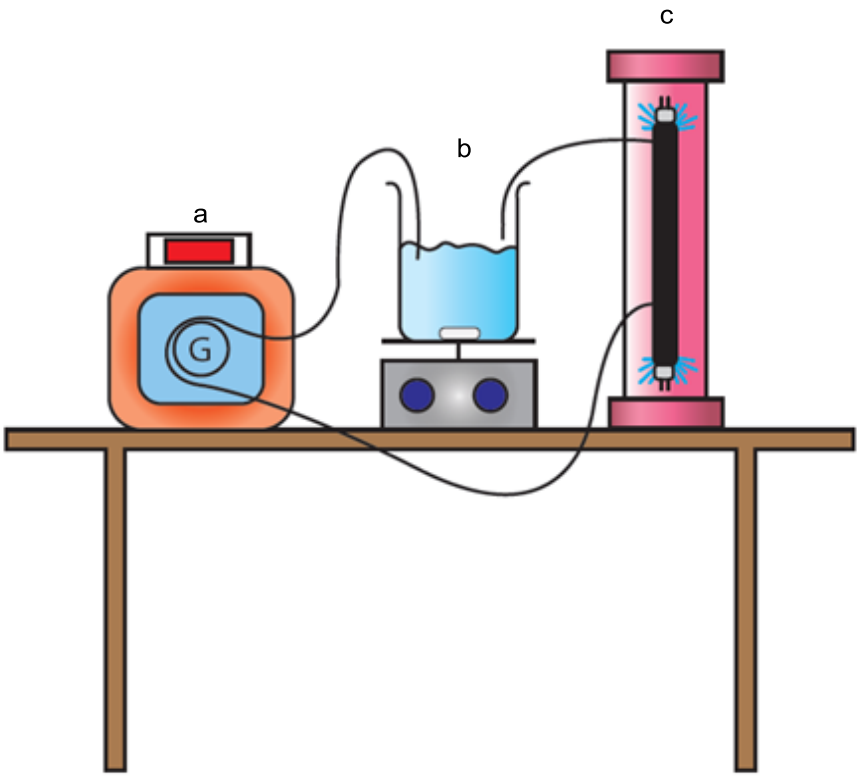



**Figure 3.2: Schematic diagram of the photocatalytic reaction system used for loading 0.5–2wt% Pt-$TiO_2$: a) Peristaltic pump, b) Suspended Pt-$TiO_2$ solution and magnetic stirrer, c) UV light reactor**

## 3.3 Unsupported $TiO_2$ sample

Unsupported $TiO_2$ (Figure 3.3a) was prepared by pre-treating it in identical fashion to the corresponding Pt-$TiO_2$ samples, but without incorporating the metal. The band gap of the pre-treated $TiO_2$ was compared with untreated $TiO_2$.

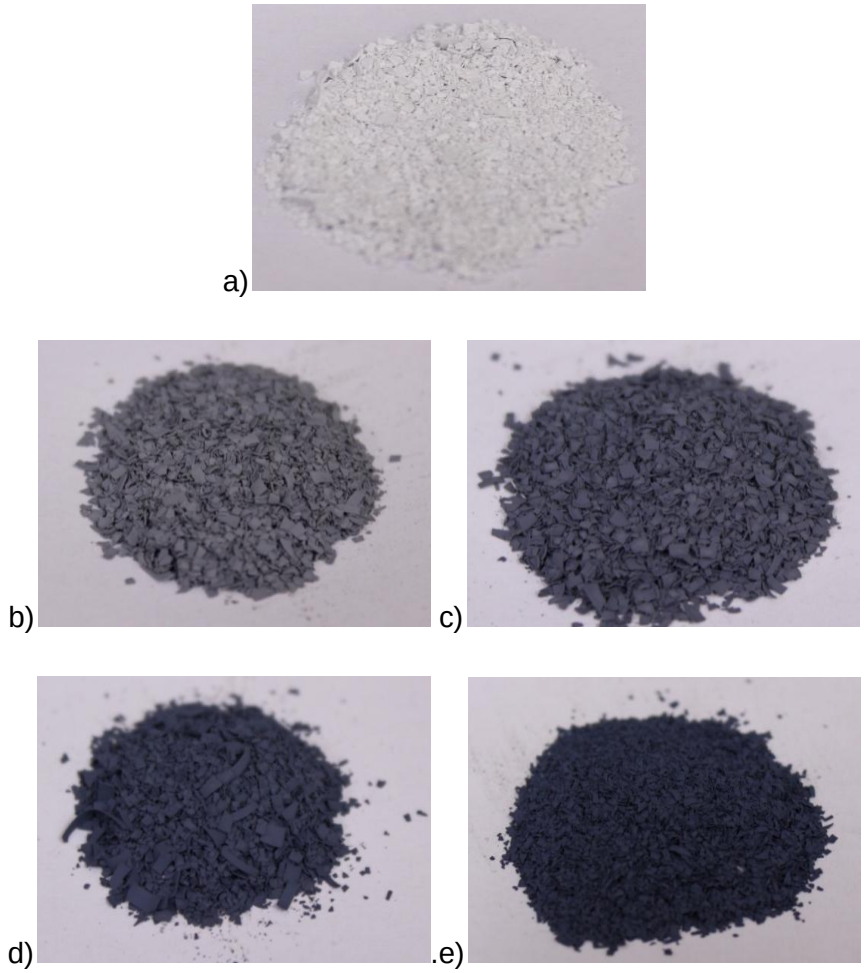



**Figure 3.3: Photos of the different Pt loadings. a) pre-treated $TiO_2$, b) 0.5wt% Pt-$TiO_2$, c) 1wt% Pt-$TiO_2$, d) 1.5wt% Pt-$TiO_2$, e) 2wt% Pt-$TiO_2$**

## 3.4 Characterisation of the Pt-$TiO_2$ catalysts

### *X-ray Diffraction (XRD)*

Structural characterisation was performed by X-ray powder diffraction measurements, carried out on a Philips X-ray diffractometer (PW 3040/60 X'Pert Pro) with Cu Kα radiation (λ=1.540598nm). An acceleration voltage of 40kV and an emission current of 45mA were employed. The measurements were performed between 15° and 79° (2θ) and point scanning of 0.02 (2θ) with 17s counting time at each step. The rutile and anatase contents were calculated from the intensity of the most intense diffraction peaks, with rutile (110) at 27.43˚ and anatase (101) at 25.29˚, according to the JCPDS database.

### *Transmission Electron Microscopy (TEM)*

Transmission electron microscopy analyses were conducted employing a Philips CM10 electron microscope (Philips Netherlands) working with a 100kV accelerating voltage. The samples were sonically dispersed in an ethanol solution for 2 min and a drop of the solution was deposited onto a copper grid covered by a porous carbon membrane for observation.

### *Diffuse Reflectance Spectroscopy (DRS)*

The UV-Vis reflectance spectra of the photocatalysts were recorded by making use of a diffuse reflectance spectrophotometer (Figure 3.4), a white Spectralon standard as reference and a Specord S600 (Analytika Jena) UV-VIS spectrophotometer. Settings used in the DRS measurements are tabulated in Table 3.2. The band gaps for the individual photocatalysts were calculated by employing the Kubelka-Munk equation. WinAspect, Excel and SigmaPlot were employed to process the data.

**Table 3.2: Parameters used for DRS**

| Parameters | |
|---|---|
| Lamp | Halogen lamp (HL) |
| Integration time (ms) | 780-822 |
| Accumulation | 5 |
| Dark current correction | YES |

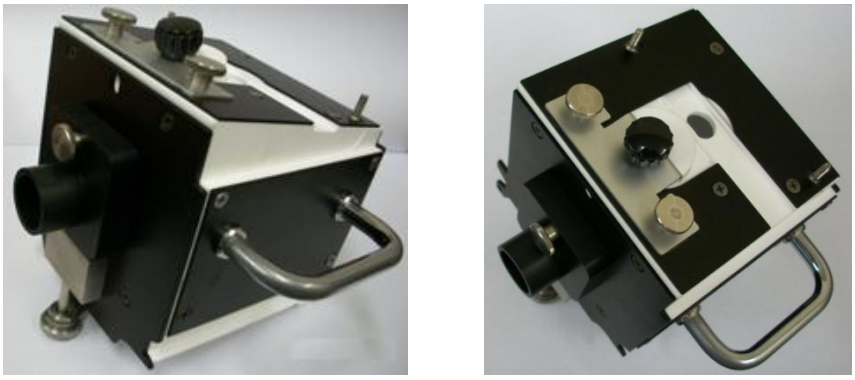


**Figure 3.4: Integrating sphere used for DRS measurements**

### *Inductive Coupled Plasma (ICP)*

The efficiency of the loading method was evaluated by inductive couple plasma analysis. ICP was conducted employing an iCAP 6000 Series (Thermo Scientific DUO) system incorporated with an Nd-YAG laser, 266nm range. Analyses were done in radial and axial view and processed utilizing iTEVA software.

### *Scanning Electron Microscopy (SEM) and Energy Dispersive X-ray spectroscopy (EDX)*

The surface morphology of the catalysts was analysed with a FEI QUANTA 200 ESEM with an integrated OXFORD X-SIGHT EDS system operating at a 15.00 kV voltage. The samples were deposited on a standard aluminium holder and coated with Pt for observation.

## 3.5 Hydrogen production and measurements

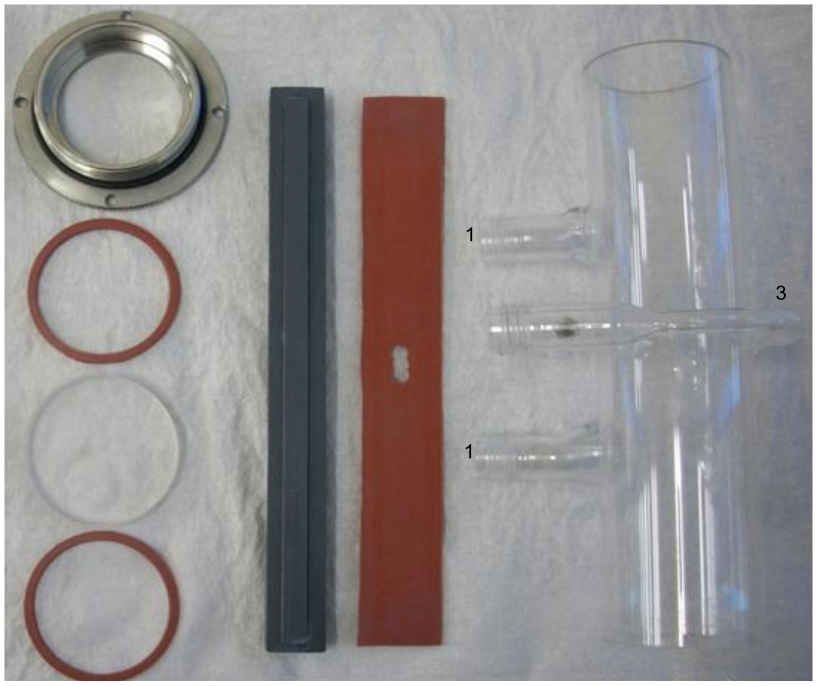
### *Reaction vessel*

Pictures of the reaction vessel used in the laser studies are presented in Figure 3.5. A special glass cell (40 mm diameter, 150 mm length and 3 mm thick), equipped with optical grade N-BK7 (40mm) windows for transmission of UV and visible laser beams, was fabricated. The reaction cell was built into an ultrasonic bath (Jeken PS-10A) to ensure that the catalysts stayed in suspension and also to enable change in temperature when required. The whole vessel can be taken apart for effective cleaning between measurements and can also be assembled very quickly (Figure 3.6).Three outlet/inlet openings were constructed on top of the glass cell (Figure 3.6a). The two openings (Figure 3.6a(1)) next to each other were connected to a gas sampling attachment (Figure 3.7) equipped with a rubber septum (Thermogreen™ LB-2 Septa) at the top (Figure 3.7 (2)) enabling gas sampling. A gas dispenser was fabricated to fit the length of the bottom of the cell to ensure an even dispersion of the carrier gas (Ar) which enters at the bottom of the vessel through the third opening (Figure 3.6a(3)) constructed in the middle of the vessel. The gas dispenser was designed with round indents on the sides to ensure that the Pt-$TiO_2$ suspension did not block the outlets (Figure 3.6c). Rubber o-rings were used to prevent any leakages.

a) 

b) 


**Figure 3.5: Specially designed reaction vessel used in the laser studies a) side view b) top view**

a) 


b) 

c) 

**Figure 3.6: a) Individual components of a specially designed reaction vessel b) Plastic rings used to keep the gas dispenser in place c) A side-front view to show the round indent of the gas dispenser**




**Figure 3.7: Gas sampling attachment used for $H_2$ sampling**

### *Experimental setup*

The laser measurements were conducted by using the third harmonic wavelength (355 nm) from an Nd:YAG pulsed laser (EKSPLA, NT 342B-SH-10-AW) with a pulse width (FWHM-Full Width at Half Maximum) of 3.6 ns and a pulse rate of 180µs. The laser power-fluence was kept at 22.1 MW/cm$^2$ and the laser beam width at 8 mm (Figure 3.8). Both the laser and the gas chromatograph (GC) were switched on an hour prior to a run was to be conducted. This enabled the laser to stabilize at 40 mJ (the set value) and the GC equipped with a TCD to stabilize at the chosen settings (Table 3.4). During this time the sample and reaction vessel were prepared for the run. 0.1 g of a chosen catalyst was weighed and suspended with an ultrasonic bath in 100 ml of solution (Table 3.3).

The reaction vessel was put together as shown in Figure 3.5 and the ultrasonic bath was filled with water. It was then placed in line with the laser (Figure 3.9e), 25cm from the laser, and 10 cm in front of the beam stopper (Figure 3.9b). The incident laser energy was 40mJ and the laser energy of the exiting beam at the back of the reaction cell, after penetrating through the catalysts solution, was 0.4mJ. Due to the use of an ultrasonic bath for keeping the catalyst in suspension, exposure of all the catalysts to the incident laser beam was ensured. The gas sampling attachment (Figure 3.9c) was connected to the reaction vessel and kept in place with a retort stand and clamp (Figure 3.9d).

Argon was then connected to the reaction vessel and flowed through the vessel at a constant flow rate of 2 NL/h for 10 min prior to irradiation and maintained for the duration of the experiment (60 min) with the ultrasonic bath set on a constant temperature of 25 °C. The catalyst sample (0.1 g photocatalyst suspended in a 1:1 aqueous methanol solution (100 mL)) was poured into the vessel after which the laser was focused on the vessel window. A gas sample was taken manually every 10 min with a 1ml gas-tight syringe and the amount of hydrogen present in the sample was measured with the gas chromatograph. An average of 3 repetitions was conducted to construct graphs for the determination of the amount of $H_2$ produced.

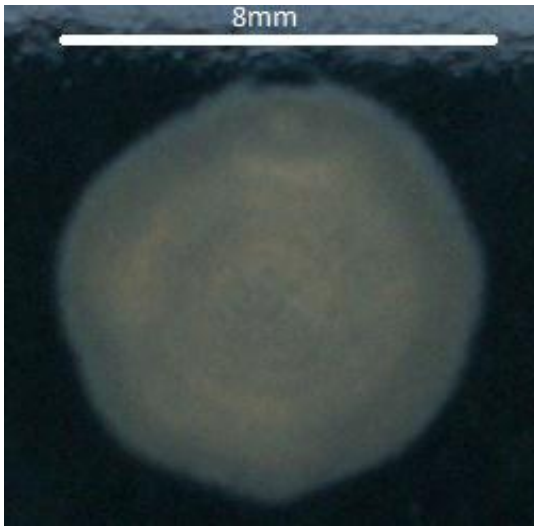



**Figure 3.8: Diameter of laser beam**

**Table 3.3: Experimental parameters**

| Catalyst | MilliQ water (min) | 50 ml methanol:50 ml MilliQ water (min) | |
|---|---|---|---|
| Pre-treated $TiO_2$ | 60 | 120 | 60 |
| 0.5wt % Pt-$TiO_2$ | 60 | 120 | 60 |
| 1.0wt% Pt-$TiO_2$ | 60 | 120 | 60 |
| 1.5wt% Pt-$TiO_2$ | 60 | 120 | 60 |
| 2.0wt% Pt-$TiO_2$ | 60 | 120 | 60 |
| None | 60 | 120 | 60 |

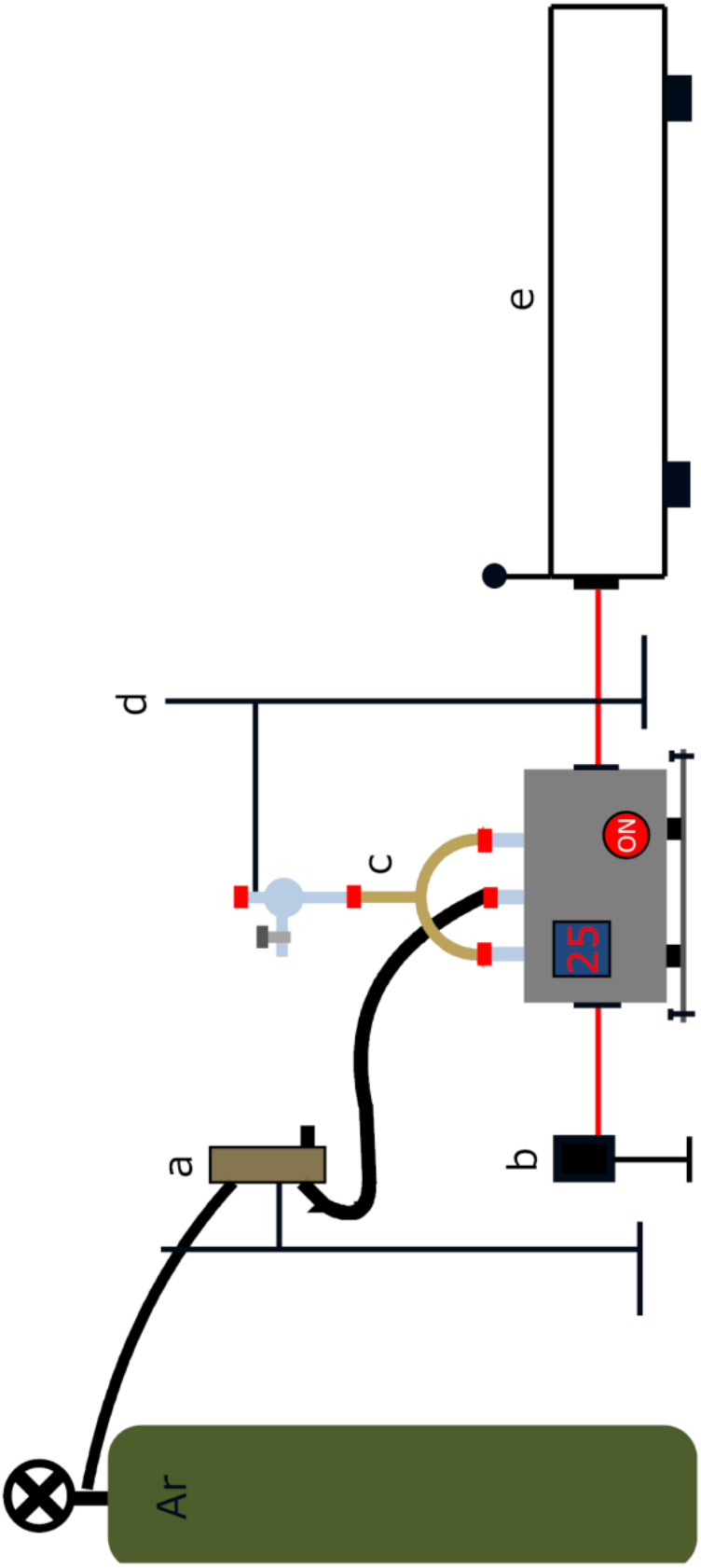



**Figure 3.9: Experimental setup for studying laser induced photocatalytic water splitting**

### *Gas chromatography*

A gas chromatograph (Clarus 500, Perkin Elmer) equipped with an 8 m, 0.53 mm inner diameter, molecular sieve 5A plot column, a TCD (Thermal Conductivity Detector) and the programme depicted in Table 3.4, was used to analyse the amount of hydrogen which evolved. A 1% hydrogen (balance nitrogen) gas, obtained from Supelco, (Scotty analysed gases), was used as standard to convert the amount of hydrogen being produced to ppm. Processing of the data was conducted with TotalChrom and SigmaPlot software.

**Table 3.4: Gas chromatography settings used for gas analyses**

| GC Parameters | Value |
|---|---|
| Injector | 90˚C |
| Oven | 75˚C |
| Carrier gas | Argon |
| Carrier control | Programmed velocity; set point 80 for 6min |
| Split control | 2:1 |
| TCD temperature | 200˚C |
| Range | 1 |
| Gases | Make up–10 ml/min<br>Reference gas–14 ml/min |

# CHAPTER 4: RESULTS AND DISCUSSION

## 4.1 Characterisation of the various photocatalysts

### *Optical characterisation using diffuse reflectance spectroscopy*

From the diffuse reflectance spectra of $TiO_2$ and the various Pt-$TiO_2$ photocatalysts (Figure 4.1) it is obvious that the untreated $TiO_2$ powder shows strong photo-absorption only at wavelengths up to 430nm, which is in good agreement with literature (Ohno *et al.*, 1999). On the other hand, the pre-treated $TiO_2$ shows photo-absorption in the visible region up to 460nm, which then gradually decreases with increasing wavelength. This may be due to defects that were generated within the $TiO_2$ as a result of prior exposure to light, thus altering the band gap. The reflectance spectra of the various Pt-$TiO_2$ photocatalysts show almost the same photo-absorption pattern as that of untreated $TiO_2$, just at lower percentage reflection and with different gradients. This is due to the change in absorption of light caused by the different amounts of loaded metal (Sakthivel *et al.*, 2004).

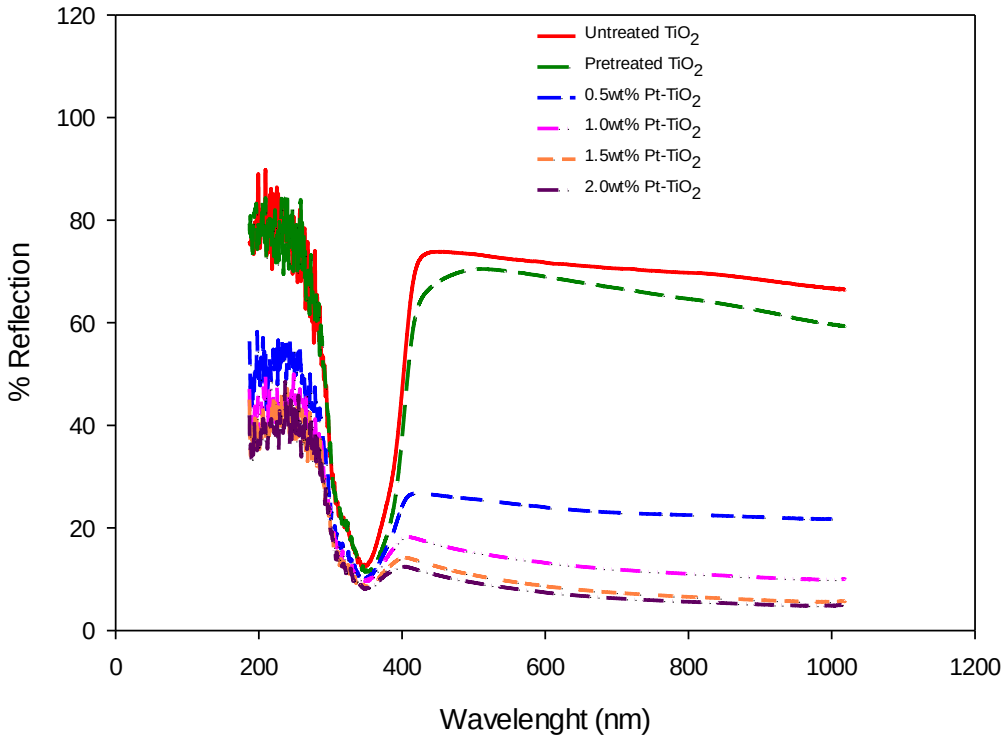



**Figure 4.1: Diffuse reflectance spectra of $TiO_2$ and the various Pt-$TiO_2$ photocatalyst**

Pt loaded onto $TiO_2$ in the powder form forms clusters (Linsebigler *et al.*, 1996). If the Pt clusters formed upon loading are roughly equal in size, constant absorption will be seen in the visible region (Sakthivel *et al.*, 2004). This is ascribed to the fact that Pt clusters give rise to localised energy levels (Sakthivel *et al.*, 2004) and capture the excited electrons in the $TiO_2$ conduction band produced by photo-absorption (Linsebigler *et al.*, 1996). According to various articles, the capture of electrons by the Pt clusters lessens electron-hole recombination and thereby facilitates transfer of holes and electrons to the reactants adsorbed on the $TiO_2$ surface (Ni *et al.*, 2007; Linsebigler *et al.*, 1996). The diffuse reflectance spectra were converted to Kubelka-Munk graphs by plotting $[F(R_\infty)hv]^2$ against $hv$(eV) in order to obtain values for the band gaps, so as to estimate where the individual photocatalysts photo-absorb. The band gaps can be obtained from the intersection between the linear fit and the photon energy axis (see Appendix a). Band gap values for Pt-$TiO_2$ photocatalysts synthesised by the photo-reduction loading method and calculated by the Kubelka-Munk method are extremely limited (Chen *et al.*, 2007; Sakthivel *et al.*, 2004; Li & Li, 2002; Sanchez & Lopez, 1995). The values of the band gaps are tabulated in Table 4.1.

**Table 4.1: Band gap values for the various photocatalysts**

| Loading (nm) | Band gap (eV) | Band gap ($x10^{-19}J \pm x10^{-21}$) | Wavelength (nm) |
|---|---|---|---|
| Untreated $TiO_2$ | 3.236 ± 0.0286 | 5.184 ± 4.588 | 383.210 ± 3.362 |
| Pre-treated $TiO_2$ | 3.201 ± 0.0101 | 5.128 ± 1.629 | 387.349 ± 1.228 |
| 0.5wt% Pt-$TiO_2$ | 3.196 ± 0.0236 | 5.120 ± 3.789 | 387.978 ± 2.878 |
| 1.0wt% Pt-$TiO_2$ | 3.165 ± 0.0280 | 5.071 ± 4.486 | 391.711 ± 3.481 |
| 1.5wt% Pt-$TiO_2$ | 3.131 ± 0.0303 | 5.016 ± 4.866 | 396.037 ± 3.856 |
| 2.0wt% Pt-$TiO_2$ | 3.100 ± 0.0279 | 4.966 ± 4.477 | 399.972 ± 3.621 |

The values obtained for both the pre-treated and untreated $TiO_2$ are in excellent agreement with the commonly accepted values of 3.2 eV and 3.22 eV published for $TiO_2$ (anatase), keeping in mind that the anatase:rutile relation and the preparation method have an influence on the value of the band gap (Chung-Chih *et al.*, 2011; Yasuro & Bessho, 2007; Banerjee *et al.*, 2006; Sreethawong & Yoshikawa, 2005; Sanchez & Lopez, 1995; Sclafani *et al.*, 1990). Due to this fact, few articles could be found which could be used to compare the band gap values obtained for the Pt-$TiO_2$ photocatalysts (Huang *et al.*, 2010). Therefore the band gap values obtained for the Pt-$TiO_2$ photocatalysts, subjected to the specific preparation conditions of this study, are unique. The different Pt-$TiO_2$ photocatalysts all exhibited a characteristic band gap which shifted slightly towards higher wavelengths as the amount of loaded metal increased. This is a clear indication that lower-energy transitions are possible as the band gap shifts towards the visible region. Thus for wavelengths (λ) shorter than 370nm, electrons ($e^-$) will be excited from the valence band (mainly from 2p oxygen orbitals hybridized with 3d Ti orbitals) to the conduction band (pure 3d $Ti^{4+}$ orbital) (Sakthivel *et al.*, 2004). Work conducted by Driessen and Grassian entails the deposition of Pt (0.1-, 0.5-, 1.0- and 2.0% onto the surface of $TiO_2$ (Degussa, P25) particles and predicting the absorption properties of photocatalysts by employing the Maxwell-Garnett theory. The UV-Vis spectrum was recorded for each photocatalyst and an increase in the absorption of Pt-$TiO_2$ at longer wavelengths compared to pure $TiO_2$ was observed and correlated with the predictions of the Maxwell-Garnett theory. A possibility for the absorption at longer wavelengths is due to the presence of new electronic states (as a result of added Pt) which lie in the band gap (Driessen & Grassian, 1998). Work conducted by Schierbaum *et al* also showed the presence of newly derived electronic states below the band gap due to the presence of Pt.

***Determination of crystal size by XRD***

The $TiO_2$ and Pt-$TiO_2$ samples were examined by XRD to determine their phase conditions (Figure 4.2). The XRD spectra of these samples showed the presence of three main peaks at $2\theta$ = 25.29, 38.59 and 48.08 respectively, regarded as an attributive indication of anatase (101). In addition to the characteristic peak of the 101 plane, diffraction peaks corresponding to rutile (110) also appeared on the spectra at $2\theta$ = 27.43, 36.98 and 41.28, respectively. No clear Pt peaks could, however, be observed.

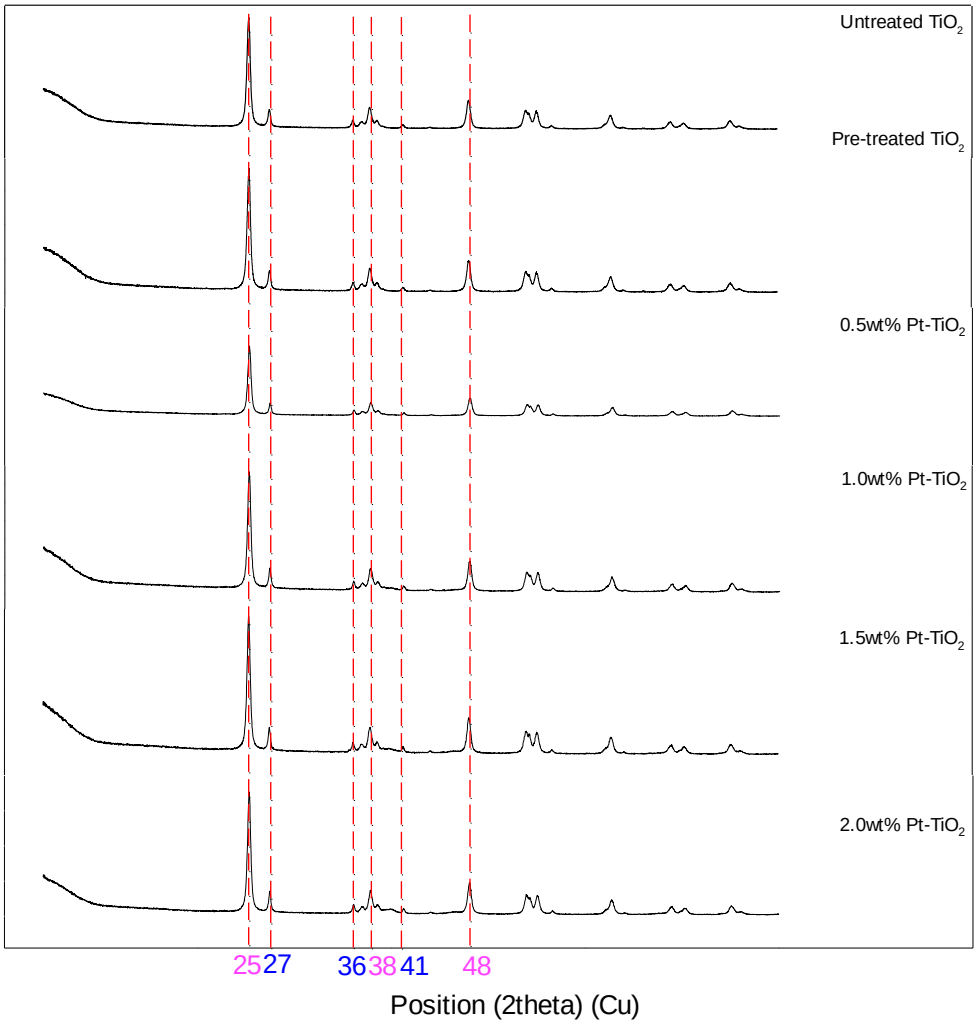



**Figure 4.2: XRD of $TiO_2$ and Pt loaded $TiO_2$ photocatalysts**

For this study the values of D (crystallite size) and $W_A$ (weight percentage anatase) were of interest (Table 4.2). The values obtained for D clearly indicated an increase which correlates with the increased amount of Pt that was loaded. However, the XRD pattern of $TiO_2$ did not change noticeably because the deposition of Pt mainly took place on the surface of $TiO_2$ (Jian-Wei *et al*, 2011). From the $W_A$ values it is clear that the predominant phase is anatase.

**Table 4.2: D and $W_A$ values obtained by XRD for the various photocatalysts**

| Catalyst | D(Å) | $W_A$(%) |
|---|---|---|
| **Pre-treated $TiO_2$** | 142.6 | 46.12 |
| **Untreated $TiO_2$** | 177.4 | 52.95 |
| **0.5wt% Pt-$TiO_2$** | 181.8 | 53.10 |
| **1.0wt% Pt-$TiO_2$** | 185.4 | 53.17 |
| **1.5wt% Pt-$TiO_2$** | 186.6 | 53.70 |
| **2.0wt% Pt-$TiO_2$** | 187.6 | 54.62 |

***Microstructure and morphology of Pt modified catalysts***

Transmission electron microscopy (TEM) analysis was conducted on the samples in order to find the grain size, structure and shape of the Pt-$TiO_2$ particles. The results obtained are shown in Figure 4.3. The small dark spots on the large $TiO_2$ particles are platinum particles/clusters (Linsebigler *et al.*, 1996). It was, however, difficult to find visible Pt particles for they are too small or too thin (Abe, R. *et al*, 2001). The $TiO_2$ particle size ranged from 40 to 130nm and the Pt particles/clusters were randomly dispersed on the $TiO_2$ crystal surface with a diameter of 11nm to 22 nm.

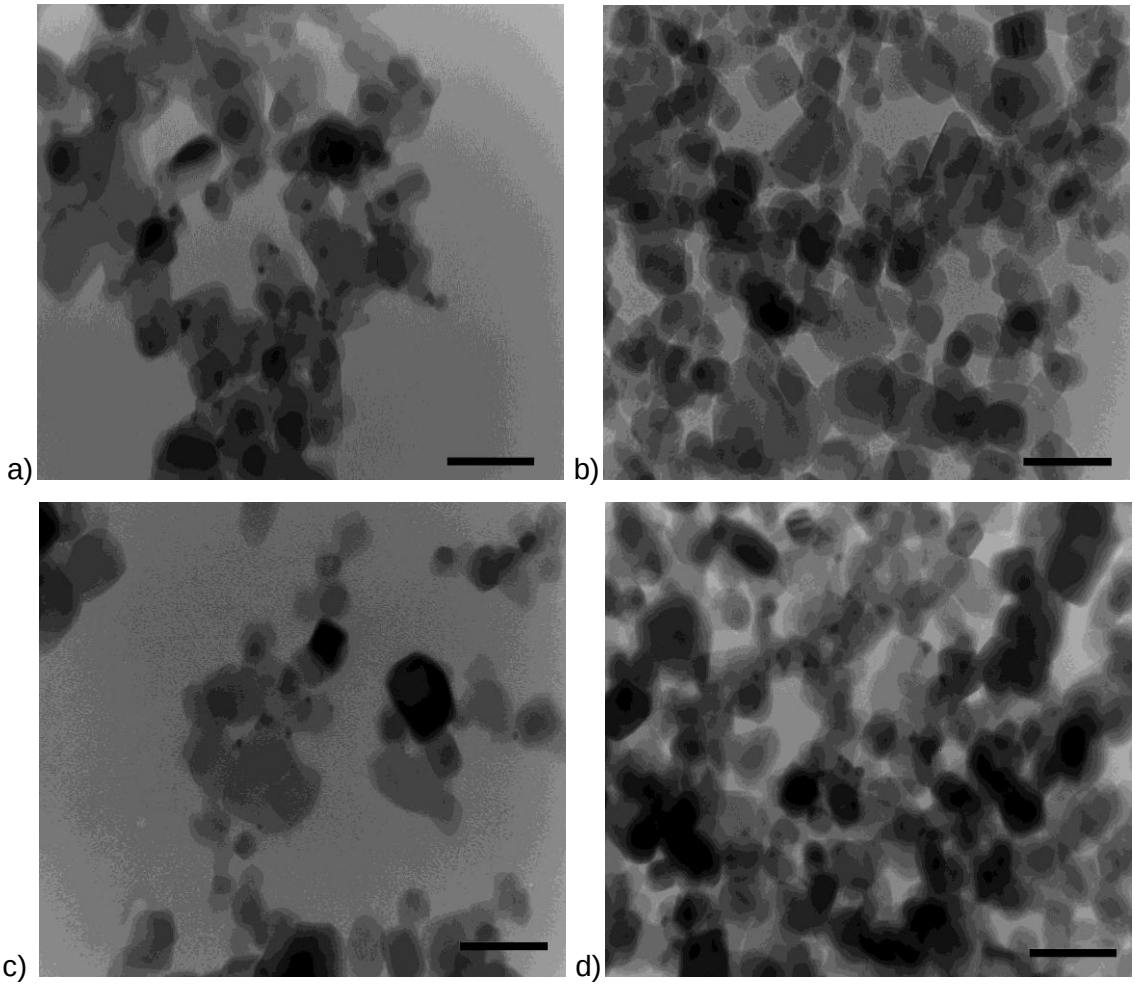



**Figure 4.3: TEM results for the a) 0.5wt%, b) 1.0wt%, c) 1.5wt% and d) 2.0wt% Pt loadings with a scale of 250 nm**

### *SEM and EDX*

Microphotographs of the untreated, pre-treated and various Pt-$TiO_2$ photocatalysts were obtained by scanning electron microscopy (Figure 4.4). All of the microphotographs were taken at the same magnification to compare the powder appearance of the various photocatalysts. It was found that the untreated $TiO_2$ differed from the other photocatalysts that were subjected to the photo-deposition method. This indicated that the photo-deposition method resulted in the development of aggregates of tiny crystals (Sakthivel *et al.*, 2004) and that repeatable results in respect of surface appearance were obtained.

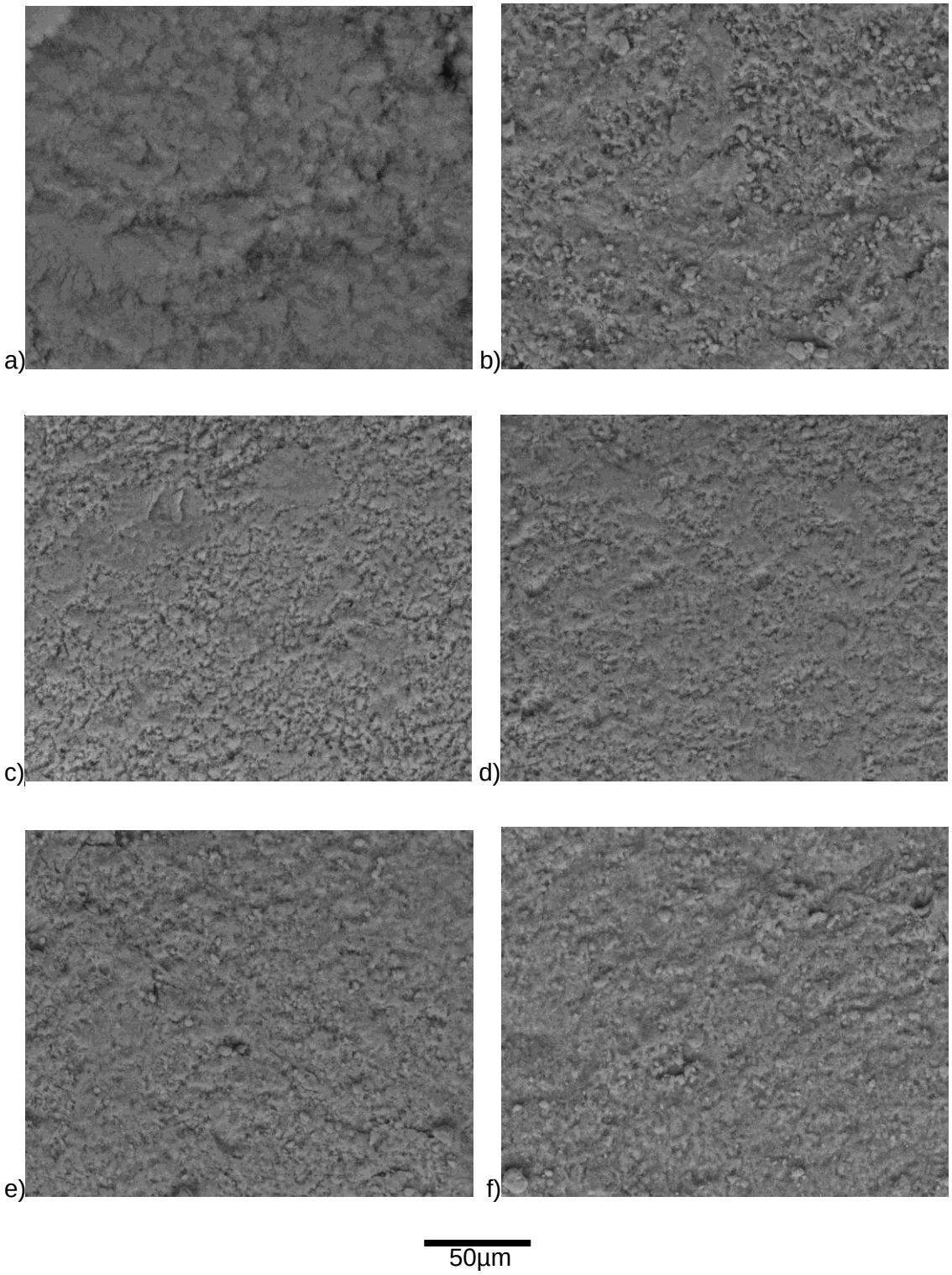



**Figure 4.4: SEM images a) untreated $TiO_2$, b) pre-treated $TiO_2$, c) 0.5wt% Pt-$TiO_2$, d) 1.0wt% Pt-$TiO_2$, e) 1.5wt% Pt-$TiO_2$ and f) 2.0wt% Pt-$TiO_2$**

The composition of the various photocatalysts was determined by energy-dispersive X-ray (EDX) analysis and the quantitative results are summarized in Table 4.3. The results obtained indicate that the actual weight percentage of Pt loaded onto the $TiO_2$ deviate slightly from the calculated amounts loaded. The greatest deviation was seen for the 1wt% Pt-$TiO_2$.

**Table 4.3: Composition of the photocatalysts as determined by EDX**

| Catalyst | Ti(wt%) | Pt(wt%) | O(wt%) |
|---|---|---|---|
| Untreated $TiO_2$ | 59.95 | | 40.05 |
| Pre-treated $TiO_2$ | 59.95 | | 40.05 |
| 0.5wt% Pt-$TiO_2$ | 59.55 | 0.57 | 39.88 |
| 1.0wt% Pt-$TiO_2$ | 59.36 | 0.84 | 39.79 |
| 1.5wt% Pt-$TiO_2$ | 58.94 | 1.45 | 39.61 |
| 2.0wt% Pt-$TiO_2$ | 58.55 | 2.01 | 39.44 |

## 4.2 Photocatalytic $H_2$ production

***Selection of laser energy (40mJ)***

From the available literature it is evident that lasers were employed as the irradiation source for the splitting of water by incorporating $TiO_2$ (rutile only) at 100mJ laser energy as a minimum. The reason for selecting this energy was that it showed to be optimum for other catalysts, i.e. $WO_3$, NiO, $Fe_2O_3$, in terms of $H_2$ production, but not specifically for $TiO_2$ (rutile). As part of this study the laser was operated at 40mJ, not because it is the optimum energy for $H_2$ production, but due to the following reasons.

1. There is no available literature where Pt-$TiO_2$ was studied by laser at any wavelength or laser energy. Higher laser energies result in higher amounts of

$H_2$ being produced according to literature (Gondal *et al.*, 2004a). By enhancing the photocatalytic properties of $TiO_2$ by depositing Pt on the surface, will hypothetically result in lower incident laser energy being required to achieve $H_2$ production.

2. Laser light and sunlight can`t be compared due to the special properties of laser light, therefore to work at the maximum energy of the laser (100mJ) will never be comparable to sunlight. It makes more sense to work at lower laser energy, even though it cannot be compared to sunlight but the knowledge obtained can possibly be applied to future work employing sunlight as the irradiation source (Gondal *et al.*, 2004a). Lower energy input is more economically viable than higher energy input.

3. As will be explained in the following paragraph, the higher the laser energy, the more rapidly conversion from the anatase phase to the rutile phase will occur, which is undesirable for it will change the properties of the photocatalyst too fast.

***The change in physical properties of $TiO_2$ following exposure to laser irradiation***

The pre-treated $TiO_2$ and the Pt-$TiO_2$ photocatalysts present in both the pure water and methanol:water solution changed colour from white and different shades of grey to a dark blue-grey colour (Figure 4.5) upon irradiation and is confirmed by literature (Zheng & Lim, 2004; Lee *et al.*, 2003). This colour change was observed as soon as the photocatalysts were irradiated with the laser light (40 mJ). At higher pulse powers the colour changes of the photocatalysts were more pronounced and turned darker much faster. Subsequent to irradiation and the resulting colour change, the pre-treated and Pt-$TiO_2$ photocatalysts were analysed by XRD.

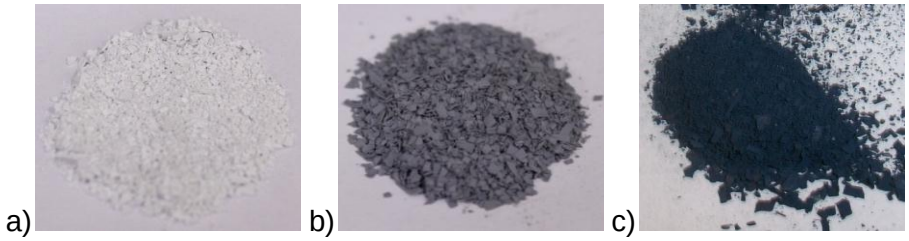



**Figure 4.5: a) Pre-treated $TiO_2$, b) Pt-$TiO_2$ photocatalyst c) blue-grey colour of the various photocatalysts after laser irradiation**

Table 4.4 summarises the effect of laser light on the rutile:anatase ratio for the various Pt-$TiO_2$ photocatalysts and a slight increase in the rutile:anatase ratio is evident. Work conducted by Exarhos also reported a similar change in the transition of anatase to rutile for $TiO_2$ (Exarhos, 1986). The rutile:anatase ratio shifted from 0.15 to 0.21 for untreated $TiO_2$ (Lee *et al.*, 2003).

**Table 4.4: Effect of laser light on the rutile:anatase ratio of the various Pt-$TiO_2$ photocatalysts**

| **Photocatalyst** | rutile:anatase ratio **before** laser irradiation | rutile:anatase ratio **after** laser irradiation |
|---|---|---|
| **0.5wt% Pt-$TiO_2$** | 0.1641 | 0.1820 |
| **1.0wt% Pt-$TiO_2$** | 0.1614 | 0.1682 |
| **1.5wt% Pt-$TiO_2$** | 0.1607 | 0.1723 |
| **2.0wt% Pt-$TiO_2$** | 0.1473 | 0.1560 |

A simple logical explanation for the colour changes is that the intense, linear focussing of laser light produces extreme localised energy centres (Ready, 1971), which generates temperatures within the crystal lattice structure of the powders that sufficient to convert anatase to rutile (Lee *et al.*, 2003). Several researchers (Le Mercier *et al.*, 1994; Honig & Zandt, 1975) attribute this colour change to the level of $Ti^{3+}$ species that increase. This may lead to non-stoichiometric forms of $TiO_2$, such as $Ti_2O_3$, $Ti_3O_5$ and $Ti_nO_{2n-1}$ (n = 4-60) (Magneli phases). They have a blue-black appearance and can be metallic. Regarding the band gap of the photocatalysts, it is expected that the band gap value will change due to more rutile phase being formed. According to Lee *et al.* (Lee *et al.*, 2003) it appears that the band gap energy of the $TiO_2$ is largely unaffected by the laser irradiation. Work done by Bilmes *et al.* proposed that the generation of Ti(III) sites creates energy levels in the band gap caused by the presence of oxygen vacancies associated with Ti(III) cations (Bilmes *et al.*, 2000). Le Mercier *et al.* also proposed this phenomenon of discrete energy levels forming in the band gap of $TiO_2$ (Le Mercier *et*

*al.*, 1994). Yet neither of these authors proposed that changes altering the overall band gap of $TiO_2$ took place and this is confirmed by work done by Lee *et al.* (2003).

***Effect of Pt on the photocatalytic activity of $TiO_2$***

During the photocatalytic process, $TiO_2$ absorbs a photon consisting of energy equal or larger than the band gap energy. This leads to the excitation of an electron ($e^-$) from the valence band to the conduction band, consequently generating a positive hole ($h^+$). Both the $e^-$ and the $h^+$ can migrate to the $TiO_2$ surface or they can undergo undesired electron-hole recombination. By loading the $TiO_2$ with Pt the electron-hole recombination process can be retarded. Many studies conducted on the enhancement of $TiO_2$ by loading Pt onto the surface report an enhancement in the photocatalytic activity of the reaction investigated when irradiated by conventional light sources (Moon *et al.*, 2003; Li & Li, 2002), although some report the reverse effect (Chen *et al.*, 2007).

The Pt acts as electron-accepting species by creating sinks for the electrons thus facilitating electron-hole separation and in this case promoting the formation of $H_2$ gas (Kandiel *et al.*, 2011; Wang *et al.*, 2004). However, at a higher Pt concentration the Pt clusters/particles act as recombination centres which cause the recombination rate between electrons and holes to increase exponentially with the increase of Pt concentration. This phenomenon is due to the fact that the average distance between trap sites decrease by increasing the number of Pt clusters (Li & Li, 2002). A speculated reaction mechanism was proposed by Sayama and Arakawa (Sayama & Arakawa, 1997) for the splitting of water over Pt-$TiO_2$ (Figure 4.6). Several side reactions can take place over Pt-$TiO_2$ as follows: 1) the formation of $H_2O$ through the back reaction of $H_2$ and $O_2$ over Pt, 2) photo-adsorption of $O_2$ and surface peroxide formation over $TiO_2$, and 3) $e^-$-$h^+$ recombination under irradiation. Although Pt-$TiO_2$ exhibits an intrinsic ability to split water into $H_2$ and $O_2$, the backward reaction taking place over Pt is thermodynamically favoured ($\Delta G < 0$) resulting in lower amounts of $H_2$ being produced during photocatalytic water splitting. $H_2$ is not affected by photo-absorption but $O_2$ is photo-absorbed onto the Pt-$TiO_2$ surface forming $O_2$ (a) and $O_2^{\cdot-}$(a) and some $O_2$ are altered to peroxide species and gradually accumulate on the photocatalyst surface. After an extended irradiation time $H_2$ evolution will stop because the pair reaction (A) becomes the major process (Kaneko & Okura, 2002; Mills & Porter, 1982b).

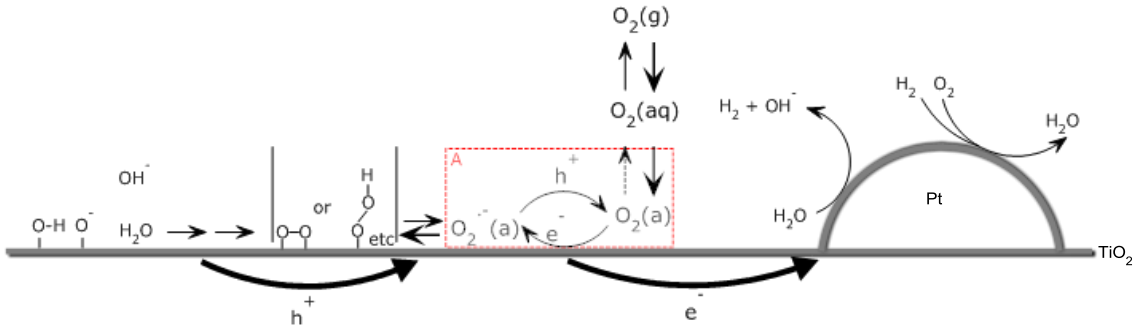



**Figure 4.6: Speculated reaction mechanism for water splitting over Pt-$TiO_2$ (Sayama & Arakawa, 1997)**

### *Photocatalytic production of $H_2$*

Photocatalytic hydrogen production from suspended photocatalysts in water and in an aqueous methanol solution was studied as part of this investigation. No literature is available where they investigated the effect of laser light on the production of $H_2$ from water and Pt-$TiO_2$ photocatalysts. Methanol is frequently used as a sacrificial agent to act as an electron donor for photocatalytic $H_2$ production, nonetheless only a few studies have been conducted where the mechanism involved was communicated (Galin'ska & Walendziewski, 2005; Chen *et al.*, 1999a; Chen *et al.*, 1999b). There is furthermore no available literature where the hydrogen is produced photocatalytically from aqueous methanol solutions, employing Pt-$TiO_2$ photocatalysts and a laser as energy source. There are three reasons why methanol was chosen as a sacrificial agent for this study.

1) According to literature methanol is the most reactive alcohol acting as a sacrificial agent for water splitting and can be produced from biomass, a renewable source (Yang *et al.*, 2006b; Cortright *et al.*, 2002; Sakata & Kawai, 1981)

2) Methanol can act as a direct source for $H_2$ production, but to what extent is not clear (Yang *et al.*, 2006a; Yang *et al.*, 2006b)

3) No literature is available on the irradiation of aqueous methanol solutions by laser although numerous articles were found where it was studied by employing UV lamps (Galin'ska & Walendziewski, 2005; Sreethawong & Yoshikawa, 2005).

Many studies conclude that the photocatalytic production of $H_2$ from aqueous methanol solutions is due to water splitting. Other studies describe it as the dehydrogenation of methanol to formaldehyde or reformation of methanol to generate carbon dioxide. According to Kandiel and other literature (Kandiel *et al.*, 2009; Wang *et al.*, 2004; Chen *et al.*, 1999b) methanol is photo-oxidized to carbon dioxide via the formation of stable intermediates, i.e. formaldehyde and formic acid (Figure 4.7):

$$CH_3OH \xrightarrow{h\upsilon, Pt-TiO_2} CH_2O + H_2$$

$$CH_2O + H_2O \rightarrow CH_2(OH)_2$$

$$CH_2(OH)_2 \xrightarrow{h\upsilon, Pt-TiO_2} HCOOH + H_2$$

$$HCOOH \xrightarrow{h\upsilon, Pt-TiO_2} CO_2 + H_2$$

---

$$CH_3OH + H_2O \xrightarrow{h\upsilon, Pt-TiO_2} CO_2 + 3H_2 \qquad (net\ reaction)$$

Upon irradiation, the following reaction pathways were suggested although no differentiation between these pathways can be made with certainty (Figure 4.7). The $e^-$-$h^+$ pairs migrate to the surface where redox reactions take place. The excited electron will be trapped at the Pt islands and will participate in the reduction of a proton from water and/or from methanol producing adsorbed $H^\bullet$ radicals. At the oxidative side three different pathways are possible for the positive holes: 1) they can react with surface Ti-OH groups, trapping the holes, 2) react with adsorbed water molecules producing adsorbed $OH^\bullet$ radicals and $H^+$ ions, or 3) they will be transferred directly to adsorbed methanol molecules (Kandiel *et al.*, 2011). Regardless of the reaction pathway, the only products formed by hydrogen abstraction are $^\bullet CH_2OH$ and $CH_3O^\bullet$ (Asmus *et al.*, 1973). Methoxy radicals can subsequently react with methanol to produce $^\bullet CH_2OH$ (Sonntag, 2006).

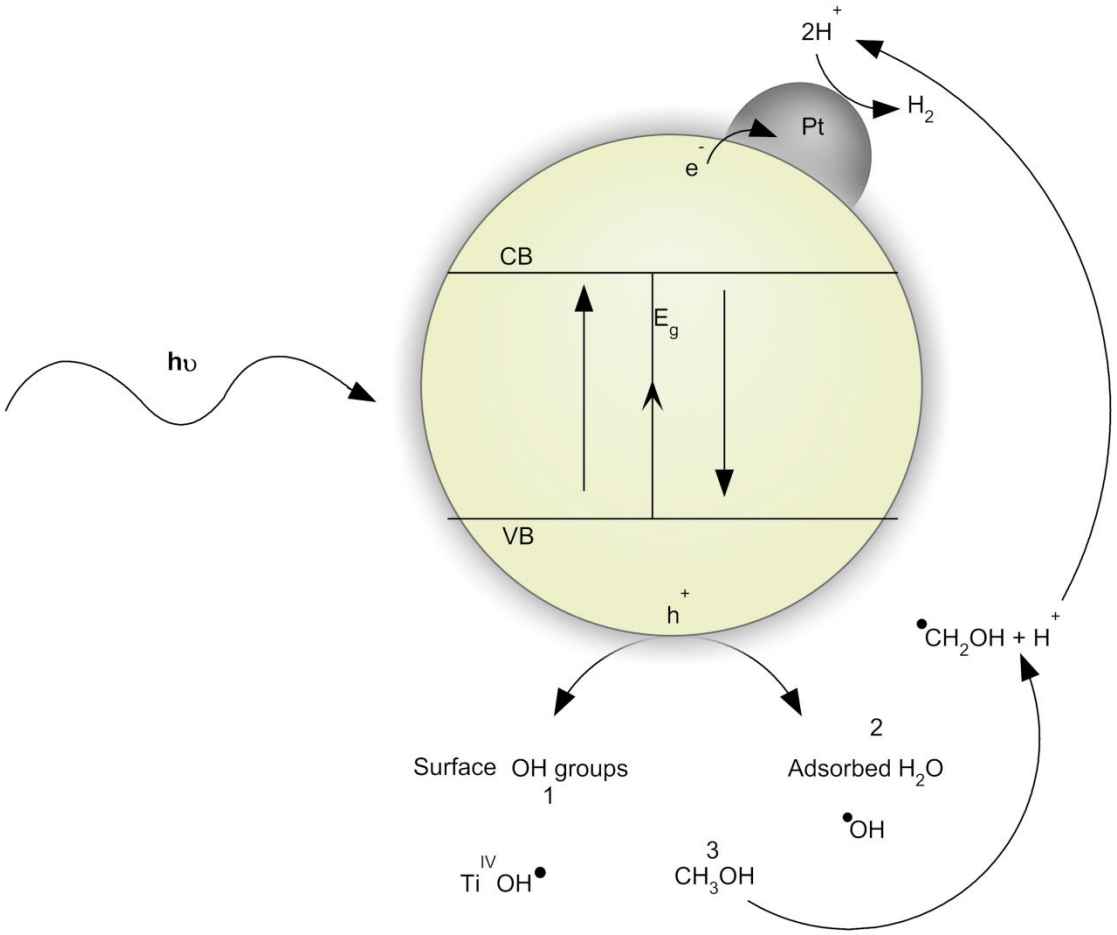



**Figure 4.7: Schematic representation of the proposed steps for the photocatalytic molecular hydrogen production from an aqueous methanol solution over Pt-$TiO_2$**

The aim of this study was not to investigate the mechanisms involved when irradiating aqueous methanol solutions incorporating various photocatalysts, but to monitor the amount of hydrogen evolved when the various Pt loaded $TiO_2$ photocatalysts were suspended in pure water and also in an aqueous methanol solution when irradiated with a laser.

No $H_2$ was detected when pure water or the aqueous methanol solution was irradiated in the absence of photocatalysts. There was also no $H_2$ detected for the various Pt-$TiO_2$ photocatalysts suspended in pure Milli-Q water (in good agreement with studies done with lamps (Kandiel *et al.*, 2011)), although the pre-treated $TiO_2$ showed a change in the base line of the gas-chromatograph where $H_2$ is expected but no definite peak was observed. This is an indication that the Pt present on the $TiO_2$ surface facilitates the

backward water forming reaction rather than the forward reaction and even eliminates the small change in the base line that was observed for pre-treated $TiO_2$.

Untreated $TiO_2$ was not investigated because it was not subjected to the same experimental conditions as the Pt-$TiO_2$ photocatalyst. A valuable comparison between the untreated $TiO_2$ and Pt-$TiO_2$ is therefore not possible.

Figure 4.8 shows the time dependence of the photocatalytic $H_2$ evolution from the aqueous methanol solution containing various Pt-$TiO_2$ photocatalysts by employing an Nd:YAG laser. Only trends observed for 60 min are shown in Figure 4.8. It was found unnecessary to do the runs for 120 min because no change in the plateau area was observed. From the graph it is obvious that the lowest concentration of $H_2$ produced was observed for the bare pre-treated $TiO_2$ suspended in the aqueous methanol solution. This can be ascribed to the recombination of the excited electrons with the positive holes and/or the interaction with intermediates present on the surface of the photocatalyst, instead of more excited electrons participating in oxidation and reduction reactions. Comparing this finding with literature it is concluded that more $H_2$ was evolved with the laser compared to studies done with a lamp where almost no $H_2$ was evolved (Kandiel *et al.*, 2011; Huang *et al.*, 2010). The concentration of $H_2$ produced for the various Pt-$TiO_2$ photocatalysts suspended in the 1:1 methanol:water solution was interpreted by dividing the graph into two areas. The first area is the first 20 minutes where a rapid increase in the amount of $H_2$ being produced was observed. The second area of the graph is where the plateaus are reached. Work conducted by Kandiel *et al.* (Kandiel *et al.*, 2011) investigated the effect of varying the light intensities of the lamp on the rate of $H_2$ being produced and they found that a plateau is quickly reached after turning on the light but why it happens is not clear. All of the Pt-$TiO_2$ photocatalysts exhibited a higher rate of $H_2$ production compared to that of $TiO_2$. This clearly indicates that the Pt present on the $TiO_2$ surface enhances the photocatalytic activity of the Pt-$TiO_2$ photocatalyst for this specific reaction being investigated.

The increase in the concentration of hydrogen being produced for the first 20 minutes is ascribed to the initial conditions of the experimental run and the plateaus due to physical changes taking place in the photocatalysts and are the following reasons put towards to elucidate the observation of an initial rise followed by a plateau after 20 minutes of irradiation:

- The water with methanol as the sacrificial agent is in excess due to the reaction only starting. This indicates that enough methanol is present to act as sacrificial agent and therefore hydrogen production will be efficient. According to literature, the amount of methanol present in the solution will decrease over time (Galin'ska & Walendziewski, 2005). This implies that the amount of hydrogen being produced will decrease due to either insufficient amounts of methanol acting as sacrificial agent, or as stated earlier insufficient amounts of methanol acting as the source of $H_2$ production. This phenomenon explains one possible reason for the plateau being reached after 20 minutes.

- The photocatalysts are still in their original state due to the small amount of time that they were subjected to laser irradiation. This implies that the photocatalyst still consist of their high photocatalytic activity. As stated earlier, the photocatalysts are subjected to physical change when irradiated by laser light forming more rutile phase in the photocatalysts. According to literature, rutile is less photocatalytically active, which will result in less $H_2$ being produced, which can also be a possible reason for the plateau being reached.

- From the methanol and water oxidation mechanisms discussed earlier, it is evident that other species form in solution. After the 20 min irradiation period many different species are present in solution and the excited $e^-$ and $h^+$ can be reacting with these adsorbed species instead of only participating in die $H_2$ production reactions which may be a reason for the plateau being reached.

For the individual Pt-$TiO_2$ photocatalysts it was found that the 0.5wt% Pt-$TiO_2$ produced $H_2$ at the steepest incline, the 2wt% the lowest concentration $H_2$ of all the Pt-$TiO_2$ photocatalysts and the 1- and 1.5wt% Pt-$TiO_2$ in between with almost equal inclines. The reason for the 2wt% Pt-$TiO_2$ producing the lowest concentration of $H_2$ is possibly due to the Pt blocking active sites on the $TiO_2$ because of the high amount which is loaded. According to the available literature, the optimum Pt loading lies in the 0.1-1wt% range for work done on lamps (Al-Mazroui *et al.*, 2007; Sreethawong & Yoshikawa, 2006; Pichat, 1987), which this study, conducted by utilising a laser, partially supports, for the 1.5wt% Pt-$TiO_2$ also resulted in $H_2$ concentrations close to this range. An explanation for this optimum Pt loading is a result of a decrease in $e^-$-$h^+$ recombination at the contact surface of $TiO_2$ and Pt competing with $e^-$-$h^+$ recombination taking place on the Pt (Rosseler *et al.*, 2010). In addition, loading the $TiO_2$ above a

certain metal wt% will 1) cover the light absorbing species ($TiO_2$) too such an extent that prevents sufficient light to reach the $TiO_2$ surface, and 2) result in Pt particles to touch and overlap which will decrease Pt contact with $TiO_2$ thus decreasing effective charge transfer (Rosseler *et al.*, 2010). This also explains why a decrease in the band gap can result in a decrease in the concentration of $H_2$ being produced. As just explained, the above-optimum increase in Pt loading results in increased $e^-$-$h^+$ recombination and with the band gap decreasing, recombination can occur more effortlessly due to the distance of separation of the $e^-$ and $h^+$ decreasing. For the first 10 min the increase in the amount of $H_2$ produced from the Pt-$TiO_2$ is in accordance with and increasing band gap. The explanation for the 1.5wt% Pt-$TiO_2$ reaching the highest plateau is not clear and more research on what happens at the plateau area has to be conducted. From Figure 4.9 it is evident that the pre-treated $TiO_2$ is the least photocatalytic active and that the Pt loaded onto $TiO_2$ enhances the photocatalytic significantly with the 0.5- and 1.5wt% Pt-$TiO_2$ giving the highest amounts. A clear trend between the Pt-$TiO_2$ photocatalysts cannot be observed but what is clear is that loading to much Pt (2wt% Pt-$TiO_2$) onto $TiO_2$, decreases the photocatalytic activity of the catalyst. Overall the amounts of $H_2$ produced for the various photocatalysts suspended in an aqueous methanol solution and irradiated by a laser is less than recently published literature on both lasers and lamps. This can be due to the sensitivity of these types of studies, for it must be emphasised that these $H_2$ production reactions are dependent on many factors such as, laser irradiation time, laser energy, laser type, temperature, whether the GC samples are taken manually or online, the way in which the photocatalyst are prepared will influence their photocatalytic activity, amount of photocatalyst (particle density) used, laser beam diameter, stirring rate, amount of solution used for potential $H_2$ production, pH of the solution and the type and amount of sacrificial agent used. A study done by Hameed and Gondal investigated the photocatalytic generation of hydrogen over NiO and $TiO_2$ where optimisation studies for NiO was done and compared to$TiO_2$. It was found that the optimum amount of catalyst is 0.3g and the optimum laser energy 100mJ. Comparing the small amounts of $H_2$ produced in this study with the amounts they obtained, it is clear that working under mild conditions (0.1g catalyst and 40mJ laser energy) influences the amounts of $H_2$ produced significantly (Hameed & Gondal, 2004).

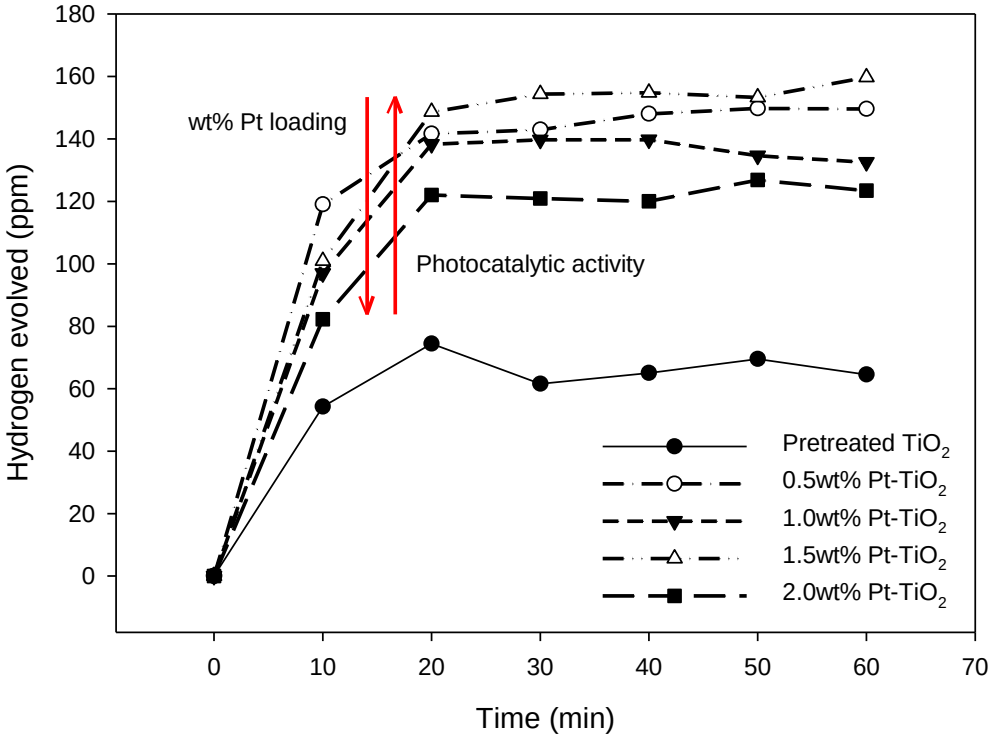



**Figure 4.8:** **Time course of the photocatalytic $H_2$ evolution over different photocatalysts. Conditions: 1g/L photocatalyst, water (50ml): methanol (50ml, 0.0125M), laser energy (40mJ), temperature 25°C (arrows indicating an increase)**

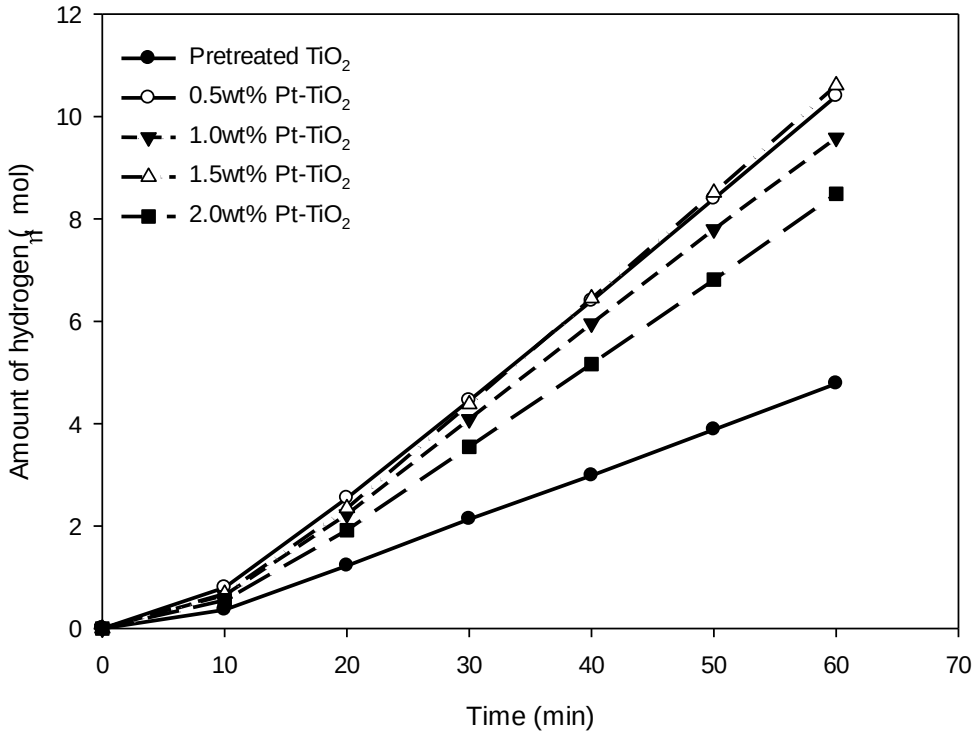



**Figure 4.9:** **Amount of $H_2$ produced over different photocatalysts**

# CHAPTER 5: CONCLUSION

## 5.1 Project evaluation

The success and shortcomings of this study will be discussed in accordance with the aims listed in CHAPTER 1. The points following below therefore correlate with the aims listed in Par 1.2:

- A wide-ranging literature study was conducted (CHAPTER 2). The situation of fossil fuels in the world today was discussed and the role of $H_2$ as a clean and viable alternative energy carrier was emphasised. The most studied photocatalyst in $H_2$ production studies is $TiO_2$ due to its high photocatalytic activity, great abundance and low cost. The wide employment of UV-lamps as well as the modification of $TiO_2$ with Pt together with the use of methanol as sacrificial agent, to enhance $H_2$ production, was accentuated. Employment of lasers as an alternative irradiation source for the potential production of $H_2$ was pointed out.

- The synthesis of various photocatalysts (0.5-, 1-, 1.5- and 2 wt% Pt-$TiO_2$) by means of a photo-reduction method was successful with regards to (i) the time it takes to synthesise the photocatalysts, (ii) the achievement of accurate loadings and (iii) the shifting of the band gap.

- Characterisation of the individual photocatalysts by XRD, TEM, ICP, SEM, and EDX gave insight into some properties of the various photocatalysts. XRD clearly indicated that the platinum was not present in the crystal structure of $TiO_2$, but was rather loaded onto the surface of $TiO_2$. TEM analysis confirmed the presence of Pt on the surface with a particle/cluster size between 11 nm and 22 nm. ICP and EDX indicated that the loading method was successful with only a slight deviation of the actual amount loaded from the calculated amount loaded. SEM showed that repeatable results in respect of surface appearance were obtained.

- Calculating the band gaps for the different photocatalysts by utilising diffuse reflectance spectroscopy (DRS) and Kubelka-Munk treatment resulted in an unambiguous calculation of the band gaps. A decrease in the band gap values

for the photocatalysts was obtained as the amount of Pt loaded increased. This is a clear indication that lower-energy transitions are possible as the band gap shifts towards the visible region.

- A successful laser setup was built for the production of $H_2$ and that allowed manual sampling and measurement with a GC. By building a glass cell into an ultrasonic bath, it ensured 1) that the photocatalysts stayed in suspension, 2) efficient mixing of the photocatalyst in such a way that all the catalysts were subjected to the 40 mJ incident laser light at different times during the run, and 3) that the ultrasonic action together with argon bubbling through the solution facilitated the release of produced $H_2$.

- The photocatalytic production of $H_2$ from pure water as well as from a water:methanol solution over Pt-$TiO_2$ photocatalysts was investigated by employing a laser as irradiation source. The difference in activity between the individual photocatalysts was discussed based on the following, e.g. initial conditions of the experiment, anatase:rutile composition and amount of Pt loaded. Upon irradiation the first observation was that the photocatalyst changed colour from white to dark blue grey. This is due to the incident intensity of the focused laser light transforming anatase to the rutile phase. No $H_2$ was detected from the suspended photocatalysts in pure water. From the aqueous methanol solution it was found that the 0.5wt% Pt-$TiO_2$ photocatalyst produced hydrogen at the highest rate where the 2wt% Pt-$TiO_2$ produced the least amount of hydrogen. By comparing the results obtained to those in literature where conventional lamps were employed, it was found that the laser produced sufficient amounts of $H_2$ in a much shorter period of time (minutes) compared with the amounts of $H_2$ produced over very long periods of time (hours, days).

## 5.2 Recommendations

Based on the literature and the results obtained, the following recommendations are made:

- From the literature survey it would seem that methanol is the most efficient sacrificial agent in facilitating $H_2$ production from water. From the results obtained it was indeed found that more $H_2$ was produced from the

photocatalysts suspended in the aqueous methanol solution compared with no hydrogen being detected from the photocatalysts suspended in pure water. Knowing that methanol can also act as a direct source of $H_2$, it was therefore ideal to employ it in $H_2$ studies by laser for the first time. It is, however, not clear how much of the $H_2$ detected was produced by the methanol itself and how much from methanol acting as a sacrificial agent in assisting water splitting. It is therefore recommended to investigate other sacrificial agents, e.g. NaI and $Na_2CO_3$, which do not dispose of the inhibiting property to produce $H_2$. By doing so $H_2$ is produced solely from water, which is the aim for future $H_2$ production, and the formation of $CO_2$ from methanol is eliminated.

- Work done by other researchers demonstrated that $H_2$ can be produced from suspended $TiO_2$ in water without sacrificial agents present at 100mJ laser energy. In this study no hydrogen was detected for any of the photocatalysts suspended in pure water at 40mJ. It is therefore proposed to do this study at higher laser energies for research purposes.

- In this study samples of the $H_2$ produced were measured by manually taking samples and injecting them into the GC consisting of a TCD detector. Doing it in this manner creates space for human error. It is therefore advisable to work with an online GC system incorporated with a PDHID (Pulsed Discharged Helium Ionization Detector) to eliminate human error and to increase the sensitivity of detecting $H_2$ by up to 500 times (Woo *et al.*, 1996) (Hunter *et al.*, 1998).

## 5.3 Final conclusion

Since this work was the first attempt at the North-West University, and according to available literature the first attempt in the scientific world, it does make a contribution to current work regarding the potential production of $H_2$ by employing different Pt-loaded $TiO_2$ photocatalysts and using methanol as a sacrificial agent with the emphasis on the use of a laser as the irradiation source. It also facilitated the identification of the scope of potential future studies, which could contribute positively to the future of $H_2$ as an alternative energy carrier.

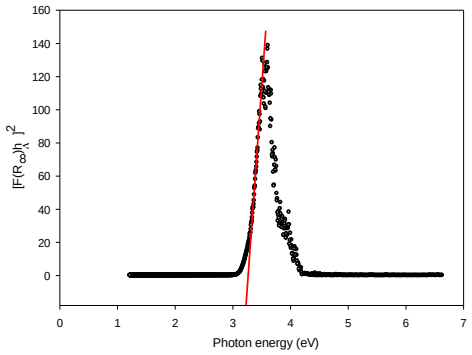
# Appendix

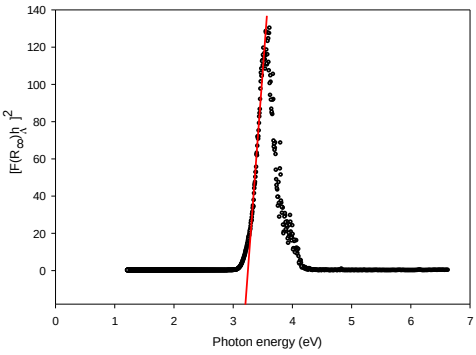
## a) Band gaps

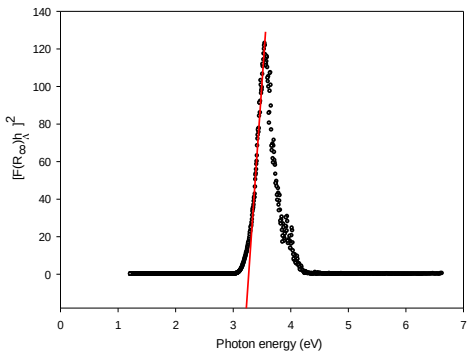
### Determination of the band gaps

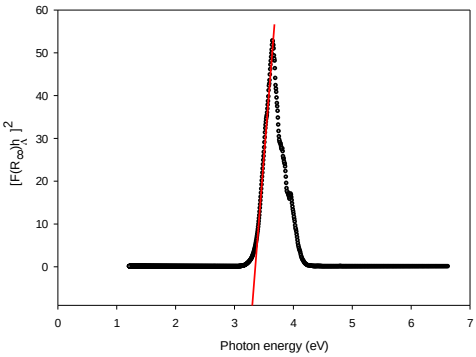
An average of six values was taken as the final band gap value for the individual photocatalysts.

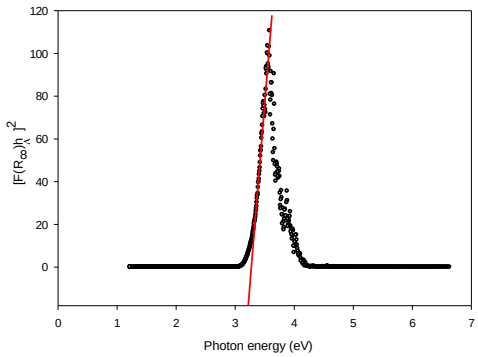
Untreated $TiO_2$

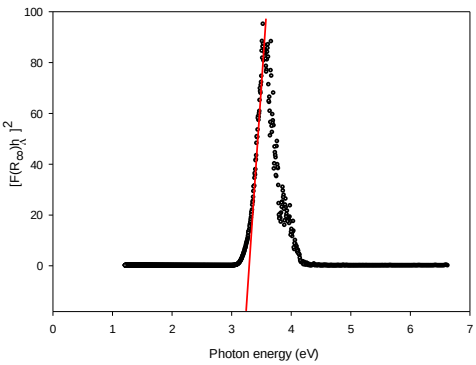


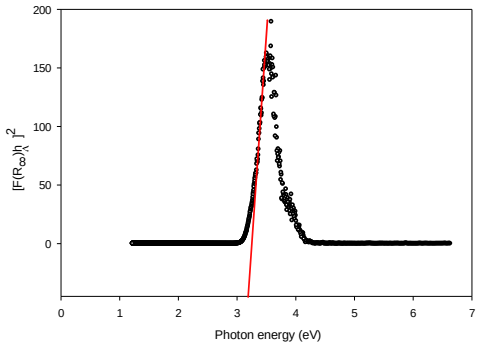



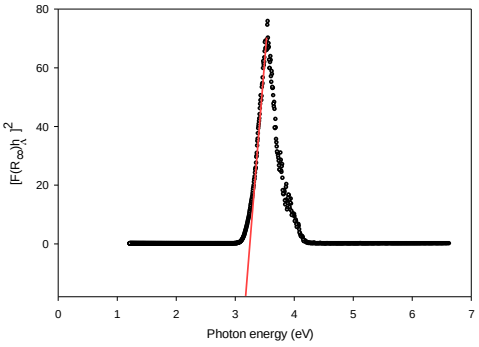



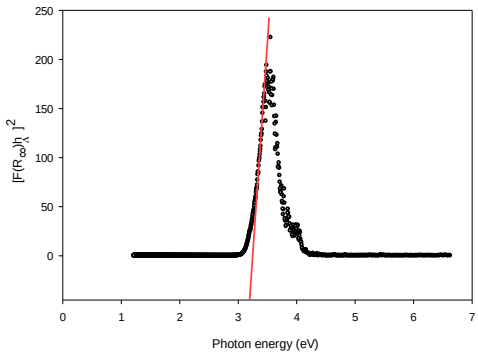



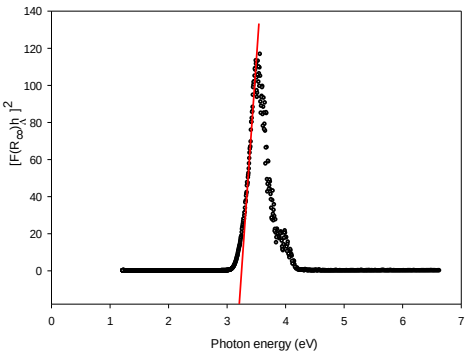



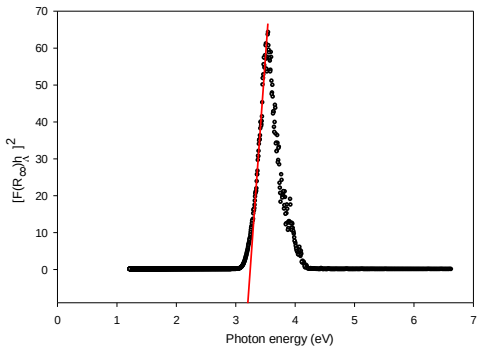
Pre-treated $TiO_2$

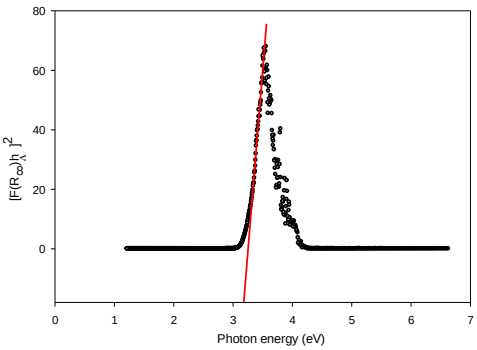


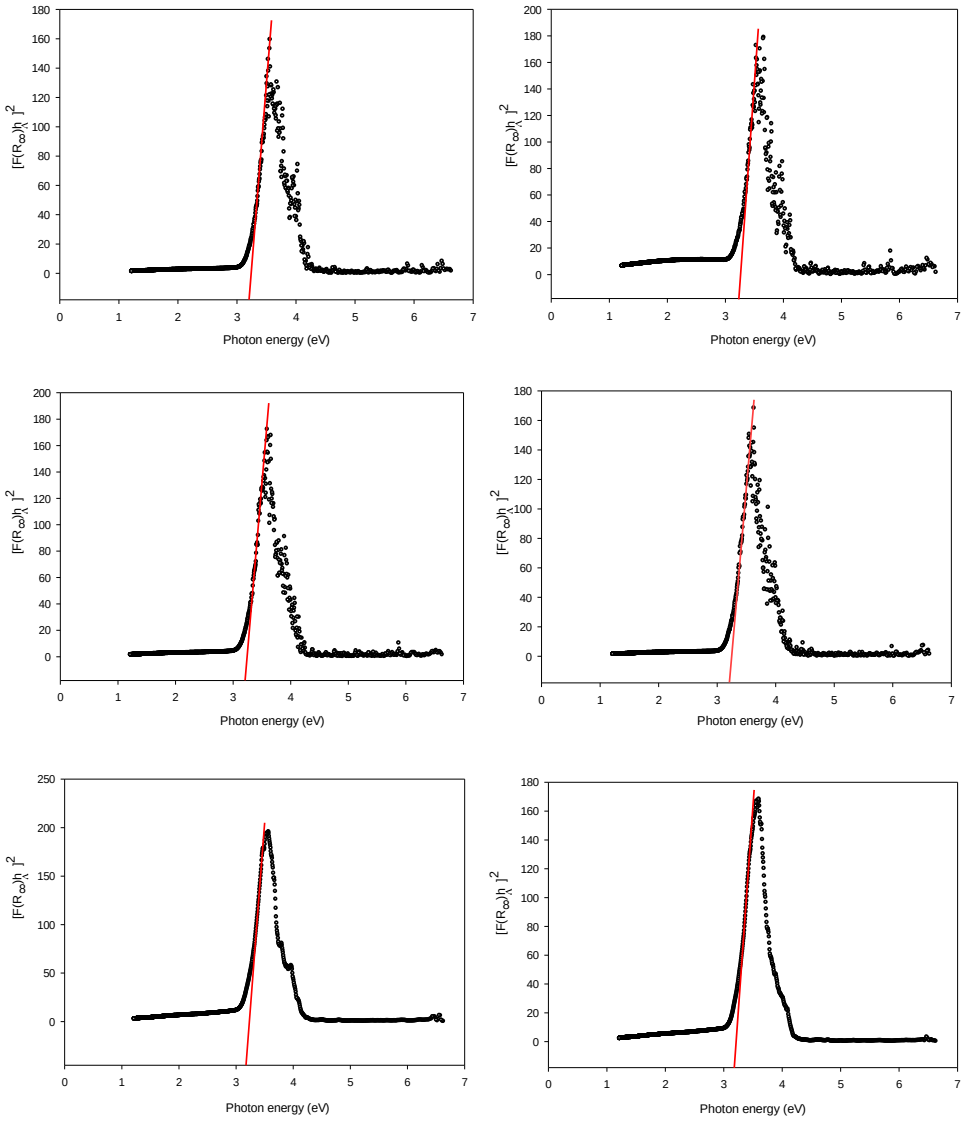



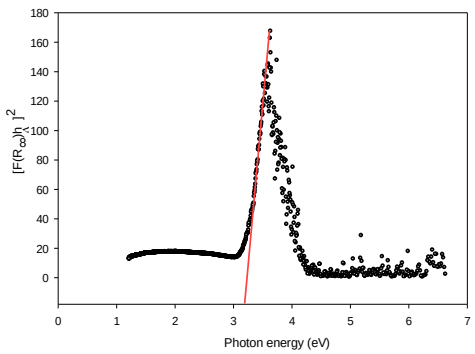



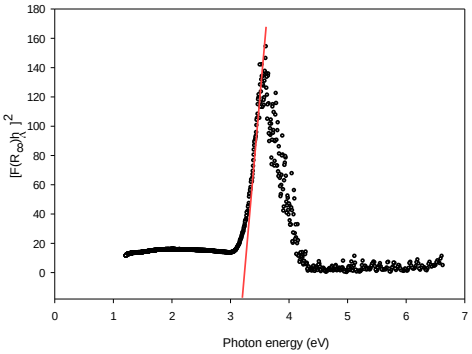



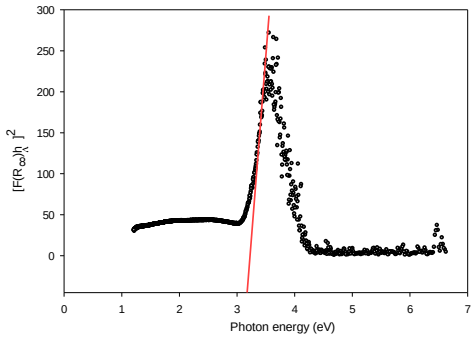
0.5wt% Pt-$TiO_2$

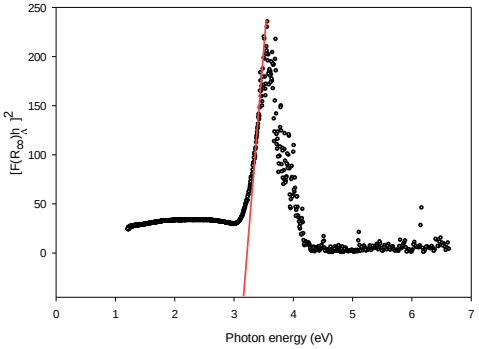


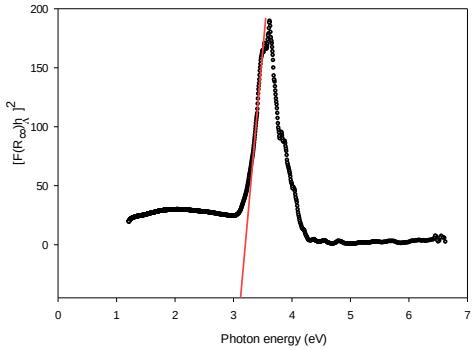
1.0wt% Pt-$TiO_2$

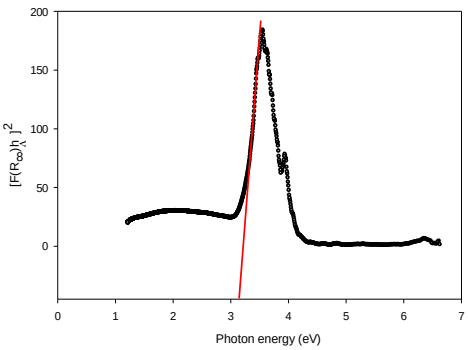

[F(R∞)hν ]^2
Photon energy (eV)


[F(R∞)hν ]^2
Photon energy (eV)

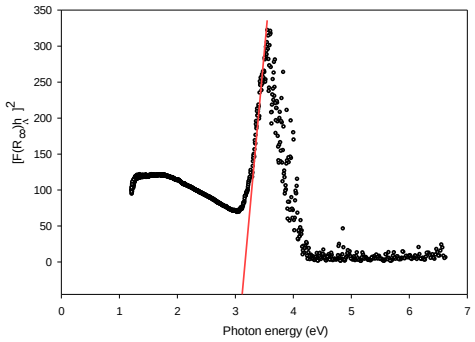

[F(R∞)hν ]^2
Photon energy (eV)

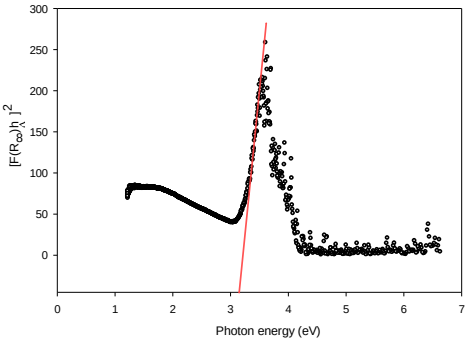

[F(R∞)hν ]^2
Photon energy (eV)

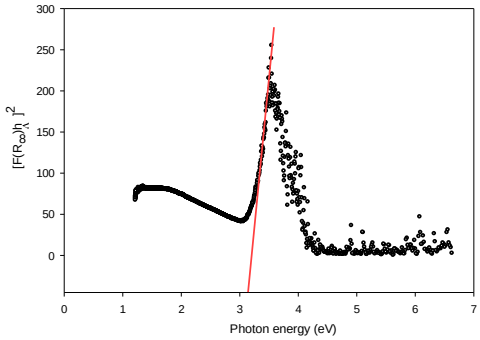

[F(R∞)hν ]^2
Photon energy (eV)

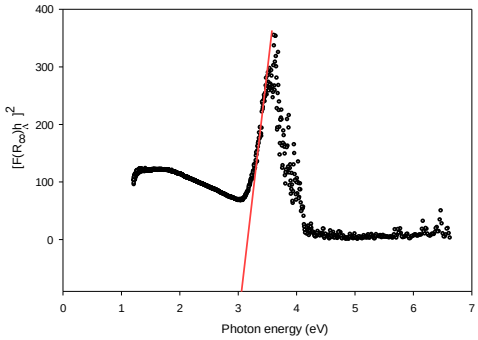

[F(R∞)hν ]^2
Photon energy (eV)

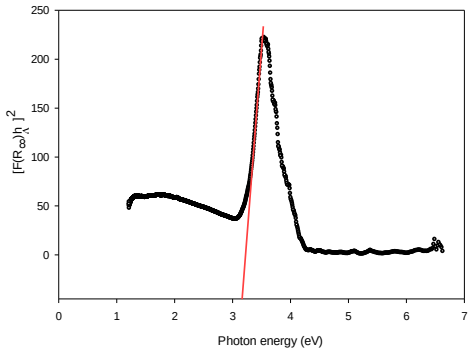
1.5wt% Pt-$TiO_2$

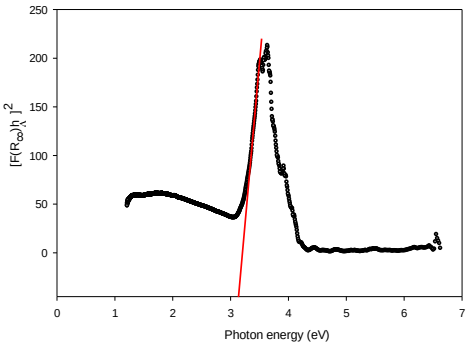

[F(R∞)hν ]^2
Photon energy (eV)


[F(R∞)hν ]^2
Photon energy (eV)

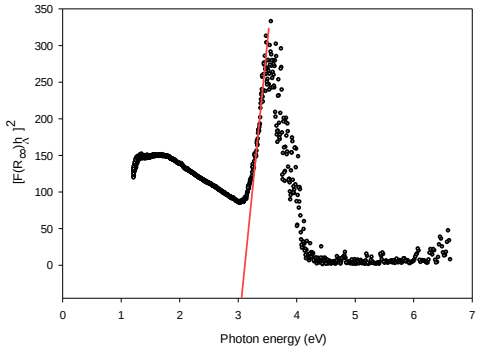

[F(R∞)hν ]^2
Photon energy (eV)

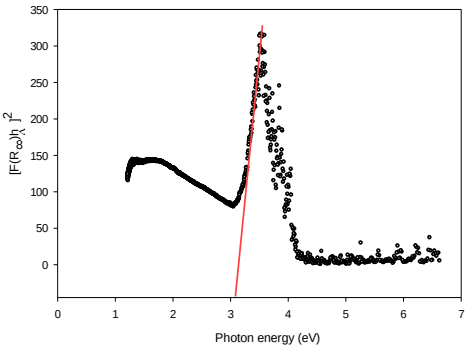

[F(R∞)hν ]^2
Photon energy (eV)

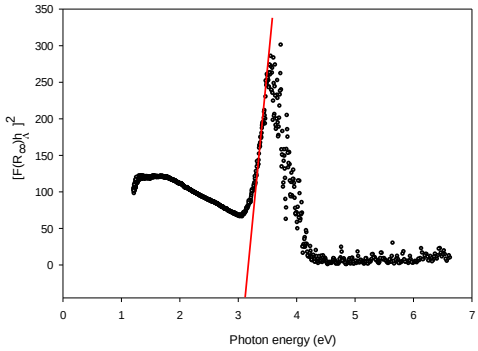

[F(R∞)hν ]^2
Photon energy (eV)

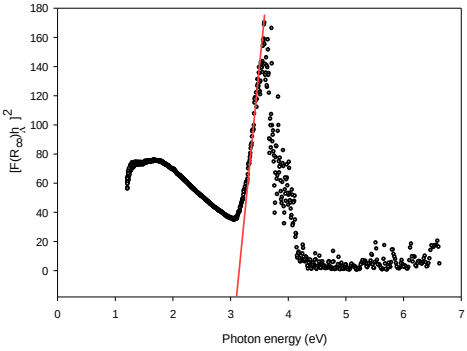

[F(R∞)hν ]^2
Photon energy (eV)

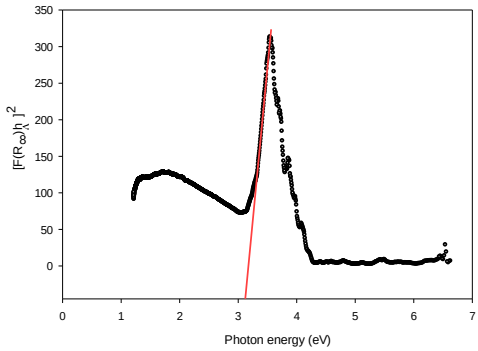
2.0wt% Pt-$TiO_2$

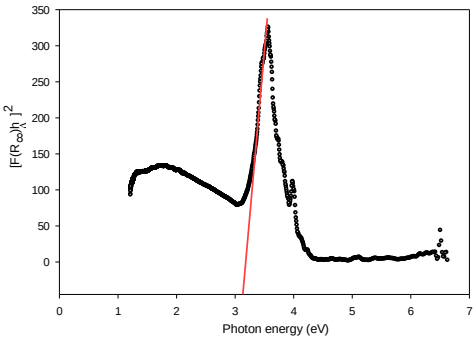

[F(R∞)h ν ]^2
Photon energy (eV)


[F(R∞)h ν ]^2
Photon energy (eV)

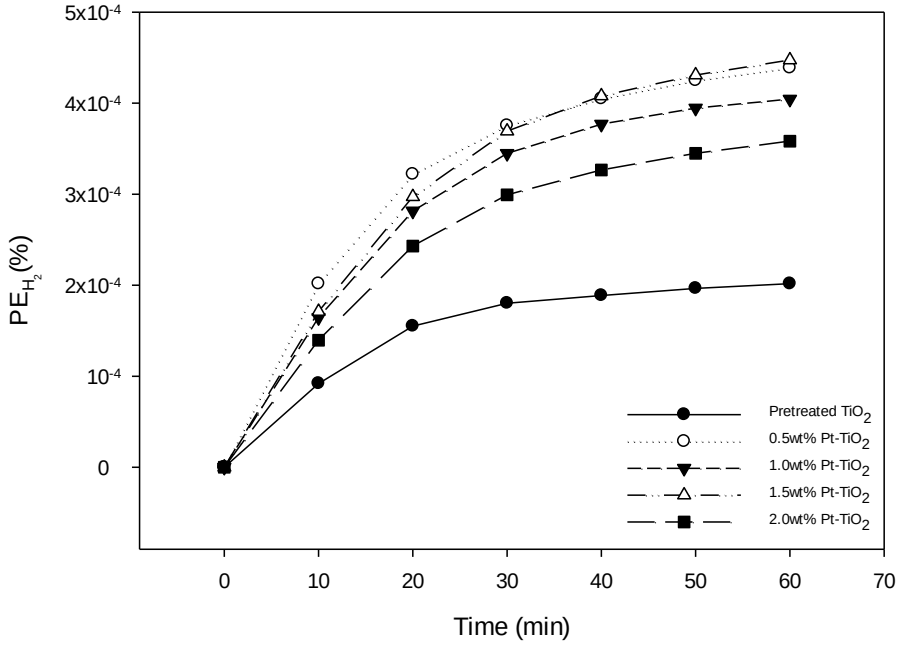

[F(R∞)h ν ]^2
Photon energy (eV)


[F(R∞)h ν ]^2
Photon energy (eV)


[F(R∞)h ν ]^2
Photon energy (eV)


[F(R∞)h ν ]^2
Photon energy (eV)

**b) Photonic efficiency**



# BIBLIOGRAPHY


ABE, R., SAYAMA, K. & ARAKAWA, H. 2003. Significant effect of iodide addition on water splitting into $H_2$ and $O_2$ over Pt-loaded $TiO_2$ photocatalyst: suppresion of backward reaction. *Chemical physics letters*, 371:360-364.

ABE, R., SAYAMA, K., DOMEN, K. & ARAKAWA, H. 2001. A new type of water splitting system composed of two different TiO2 photocatalysts (anatase, rutile) and a IO3-/I- shuttle redox mediator. *Chemical physical letters*, 344:339-344.

AL-MAZROUI, L.S., BOWKER, M., DAVIES, P., DICKINSON, A., GREAVES, J., JAMES, D. & MILJARD, L. 2007. The photocatalytic reforming of methanol. *Catalysis today*, 122(1-2):46.

AMEMIYA, S. 2004. Titanium-oxide photocatalyst. Date of access: 2011. <http://www.threebond.co.uk/Portals/0/tech62.pdf>

ANASTAS, P. 2009. Handbook of green chemistry. Weinheim: WILEY-VCH.

ANON. 1991. Chemistry of platinum group metals. Amsterdam, Oxford, New York, Tokyo: Elsevier.

ANON. 2007. Laser-based research and development at the CSIR. Date of access: 2011. <http://www.csir.co.za/lasers/basics_of_lasers.html#>

ANPO, M. & TAKEUCHI, M. 2002. The design and development of highly reactive titanium oxide photocatalyst operating under visible light irradiation. *Journal of catalysis*, 216:505-516.

ASHOKKUMAR, M. 1998. An overview on semiconductor particulate systems for photoproduction of hydrogen. *International journal of hydrogen energy.*, 23:427-438.

ASMUS, K.D., MOCKEL, H. & HENGLEIN, A. 1973. Pulse radiolytic study of the site of hydroxyl radical attack on aliphatic alcohols in aqueous solution. *Journal of physical chemistry*, 77:1218.

ATKINS, P.W. 1998. Atkin`s physical chemistry 6th. Oxford: Oxford: Unversity press.

ATKINS, P. & DE PAULA, J. 2006. Atkin`s physical chemistry 8th. Oxford: Oxford:University press.

ATKINS, P., OVERTON, T., JONATHAN, R., WELLER, M. & AMSTRONG, F. 2006. Inorganic chemistry 4th. Oxford: University press.

BAK, T., NOWOTNY, J., REKAS, M. & SORRELL, C.C. 2003. Defect chemistry and semiconducting properties of titanium dioxide. I. Defect diagrams. *Journal of physics and chemistry of solids.*, 64:1043-1056.

BAMWENDA, G.R. & ARAKAWA, H. 2001. The photoinduced evolution of suspension $O_2$ and $H_2$ from $WO_3$ aquaous suspension in the presence of $Ce_4^+/Ce_3^+$. *Solar energy materials and solar cells*, 70:1-14.

BAMWENDA, G.R., TSUBOTA, S., NAKAMURA, T. & HARUTA, M. 1995. Photoassisted hydrogen production from a water-ethanol solution: a comparison of activities of Au-$TiO_2$ and Pt-$TiO_2$. *Journal of photochemistry and photobiology A: Chemistry*, 89(2):177-189.

BANERJEE, S., GOPAL, J., MURALEEDHARAN, R., TYAGI, A.K. & RAJ, B. 2006. Physics and chemistry of photo catalytic titanium dioxide: Visualize of bacterial activity using atomic force microscopy. *Current science*, 90:1378.

BARBIR, F., VEZIROGLU, T.N. & PLASS, H.J. 1990. Environmental damage due to fossil fuel use. *International journal of hydrogen energy*, 15:739-749.

BILMES, S.A., MANDELBAUM, P., ALVAREZ, F. & VICTORIA, N.M. 2000. Surface and Electronic Structure of Titanium Dioxide Photocatalysts. *Journal of physical chemistry B*, 104(42):9851.

BI, Z. & TIEN, H.T. 1984. Photoproduction of hydrogen by dye-sensitized systems. *International journal of hydrogen energy.*, 9(8):717-722.

BOLTON, J.R. 1987. Solar fuels. The production of energy-rich compounds by the photochemical conversion and storage of solar energy. *Science*, 202(4369):705-710.

BOLTON, J.R., STRICKLER, J.S. & CONNOLLY, J.S. 1985. Limiting and realizable efficiencies of solar photolysis of water. *Nature*, 316:495-500.

BUSH, K., VON FREYMANN, G., LINDEN, S.F., MINGALEV, S.f., TKESHELASHVILI, L. & WEGENER, M. 2007. Periodic nanostructure for photonics. *Physics reports*, 444(3-6):101-202.

CARP, O., HUISMAN, C.L. & RELLER, A. 2004. Photoinduced reactivity of titanium dioxide. *Progress in solid state chemistry*, 32:33-177.

CARP, O., HUISMAN, C.L. & RELLER, A. 2004. Photoinduced reactivity of titanium dioxide. *Progress in solid state chemistry.*, 32:33-177.

CHEN, H., KU, Y. & KUO, Y. 2007. Effect of Pt/TiO2 characteristics on temporal behavior of o-cresol decomposition by visible light-induced photocatalysis. *Water research*, 41:2069-2078.

CHEN, J., OLLIS, D.F., RULKENS, W.H. & BRUNING, H. 1999a. Kinetic processes of photocatalytic mineralization of alcohols on metallized titanium dioxide. *Water research*, 33:661.

CHEN, J., OLLIS, D.F., RULKENS, W.H. & BRUNING, H. 1999b. Photocatalyzed oxidation of alcohols and organochlorides in the presence of native $TiO_2$ and metallized $TiO_2$ suspensions. Part (II): Photocatalytic mechanisms. *Water research*, 33:669.

CHOI, W.Y., TERMIN, A. & HOFFMANN, M.R. 1994. The role of metal ion dopants in quantum-sized $TiO_2$: correlation between photoreactivity and charge carrier recombination dynamics. *Journal of physical chemistry*, 84:13669-13679.

CHUNG-CHIH, Y., DA-YUNG, W., LI-SHIN, C. & HAN C, S. 2011. Characterization and photocatalytic activity of Fe- and N-co-deposited TiO2 and first principles study for electronic structure. *Journal of solid state chemistry*, 184(8):2053-2060.

CLARK, M.J., REISFELD, R. & JORGENSEN, C.K. 1982. Structure and bonding solar energy materials. Berlin Heidelberg New York: Springer-Verlag.

CORTRIGHT, R.D., DAVDA, R.R. & DUMESIC, J.A. 2002. Hydrogen from catalytic reforming of biomass-derived hydrocarbons in liquid water. *Nature*, 418:964.

DRIESSEN, M.D. & GRASSIAN, V.H. 1998. Photooxidation of Trichloroethylene on $Pt/TiO_2$. *Journal of physical chemistry B*, 102:1418-1423.

DUONGHONG, D., BORGARELLO, E. & GRATZEL, M. 1981. Dyanmics of light-induced water cleavage in colloidal systems. *Journal of the american chemical society*, 103:4685-4690.

ESCOBEDO MORALES, A., SANCHEZ MORA, E. & PAL, U. 2006. Use of diffuse reflectance spectroscopy for optical characterization of unsupported nanostructures. *Revista mexicana de fisica.*, 53(5):18-22.

EXARHOS, G.J. 1986. Raman determination of molecular structure and physical properties of dielectric coatings. *Journal of vacuum science and technology A4*, 4(6):2962.

FUJISHIMA, A., HASHIMOTO, K. & WATANABE, T. 1999. Photocatalysis. Fundamentals and applications. *Tokyo: BKC*:14-176.

FUJISHIMA, A. & HONDA, K. 1972. Electrochemical photolysis of water at a semiconductor electrode. *Nature*, 238:37-38.

FUJISHMA, A., RAO, T.N. & TRYK, D.A. 2000. Titanium dioxide photocatalysis. *Journal of photochemistry and photobiology C: Photochemistry review*, 1:1-21.

GALIN'SKA, A. & WALENDZIEWSKI, J. 2005. Photocatalytic Water Splitting over Pt-$TiO_2$ in the Presence of Sacrificial Reagents. *Energy & Fuels*, 19:1143-1147.

GAL, D., MASTAI, Y. & HODES, G. 1999. Band gap determination of semiconductor powders via surface photovoltage spectroscopy. *Journal of applied physics.*, 86(10):5573-5577.

GONDAL, M.A., HAMEED, A. & SUWAIYAN, A. 2002. Photo-catalytic conversion of methane into methanol using visible laser. *Applied catalysis A general*, 243:165-174.

GONDAL, M.A., HAMEED, A., YAMANI, Z.H. & SUWAIYAN, A. 2004a. Laser induced photocatalytic/splitting of water over alfa-$Fe_2O_3$, $TiO_2$ and NiO catalyst: activity comparison. *Chemical phyics letters*, 385:111-115.

GONDAL, M.A., HAMEED, A., YAMANI, Z.H. & SUWAIYAN, A. 2004b. Production of hydrogen and oxygen by water splitting using laser induced photo-catalysis over Fe2O3. *Applied catalysis A general*, 268(1-2):159-167.

HALLIDAY, D., RESNICK, R. & WALKER, J. 2001. Fundamentals of physics, 6th ed. New York: John Wiley & Sons, Inc.

HAMEED, A. & GONDAL, M.A. 2004. Laser induced photocatalytic generation of hydrogen and oxygen over NiO and $TiO_2$. *Journal of molecular catalysis A: Chemical*, 219:109-119.

HAMEED, A., GONDAL, M.A. & YAMANI, Z.H. 2004a. Effect of transition metal doping on photocatalytic activity of $WO_3$ for water-splitting under laser illumination: role of 3d-orbital. *Catalysis communications*, 5:715-719.

HAMEED, A., GONDAL, M.A., YAMANI, Z.H. & ZAHYA, A.H. 2004b. Significanca of pH measurements in photocatalytic splitting of water using 355nm UV laser. *Journal of molecular catalysis A*, 227:241-246.

HASHIMOTO, K., HABAZAKI, H., YAMASAKI, M., MEGURO, S., SASAKI, T., KATAGIRI, H., MATSUI, T., FUJIMURA, K., IZUMIYA, K., KUMAGAI, N. & AKIYAMA, E. 2001. Advanced materials for global carbon dioxide recycling. *Materials science and engineering A*, 304-306:88-96.

HONIG, J.M. & ZANDT, L.L.V. 1975. The metal-insulator transition in selected oxides. *Annual review of materials science*, 5:225-278.

HUANG, B., CHANG, F. & WEY, M. 2010. Photocatalytic properties of redox-treated $Pt/TiO_2$ photocatalysts for $H_2$ production from an aqueous methanol solution. *International journal of hydrogen energy*, 35:7699-7705.

HUNTER, M.C., BARTLE, K.D., LEWIS, A.C., MCQUAID, J.B., MYERS, P., SEAKINS, P.W. & VAN TILBURG, C. 1998. The Use of the Helium Ionization Detector for Gas Chromatographic Monitoring of Trace Atmospheric Components. *Journal of high resolution chromatography*, 21(2):75.

IKUMA, Y. & BESSHO, H. 2007. Effect of Pt concentration on the production of hydrogen by a $TiO_2$ photocatalyst. *International journal of hydrogen energy*, 32:2689-2692.

IMS. 2011. Atomistic scalensimulations using computational packages. http://www.ims.demokritos.gr/ims_topic.php?lang=en&ergo=G107&topic=7

1&PHPSESSID=7ee1d51c73cc34aa26286daf000f9a0f Date of access: 2 November 2011.

JANA, A.K. 2000. Solar cells based on dyes. *Journal of photochemistry and photobiology A: Chemistry*, 132:1-17.

KANDIEL, T.A., DILLERT, R. & BAHNEMANN, D.W. 2009. Enhanced photocatalytic production of molecular hydrogen on $TiO_2$ modified with Pt–polypyrrole nanocomposites. *Photochemistry and photobiology science*, 8:683.

KANDIEL, T.A., DILLERT, R., ROBBEN, , L. & BAHNEMANN, D.W. 2011. Photonic efficiency and mechanism of photocatalytic molecular hydrogen production over platinized titanium dioxide from aqueous methanol solutions. *Catalysis today*, 161:196-201.

KANEKO, M. & OKURA, I. 2002. Photocatalysis: science and technology. Japan: Springer: New York.

KIWI, J. 1986. Quantative determination of titanium(3+) formation in semiconductor dispersions induced under light irradiation. *Journal of physical chemistry*, 90:1493.

KOCA, A. & SAHIM, M. 2002. Photocatalytic hydrogen production by direct sun light from sulpide/sulphide solution. *International journal of hydrogen energy*, 27:363-367.

KOTZ, J.C., TREICHEL, P.M. & WEAVER, G.C. 2006. Chemistry & chemical reactivity 6th. Belmont, USA: Thomson Brooks/Cole.

KRIEK, R.J. 1994. Separation of Pt, Pd and Rh by differential photocatalytic reduction. Potchefstroom: NWU. (Dissertation-MSc).

LE MERCIER, T., QUARTOM, M., FONTAINE, M.F., HAUGE, C.F. & MARIOT, J. 1994. Near-surface defects created by 355 nm laser irradiation of rutile. *Journal of applied physics*, 76:3341.

LEE, S., ROBERTSON, p.K.J., MILLS, A., MCSTAY, D., ELLIOTT, N. & MCPHAIL, D. 2003. The altertion of the structural properties and photocatalytic activity of $TiO_2$ following exposure to non-linear irradiation sources. *Applied Catalysis B:Environmental*, 44:173-184.

LI, F.B. & LI, X.Z. 2002. The enhancement of photodegradation efficiency using Pt-$TiO_2$ catalyst. *Chemoshere*, 48:1103-1111..

LINSEBIGLER, A., RUSU, C. & J.T. YATES, Jr. 1996. Absence of platinum enhancement of a photoreaction on $TiO_2$-CO photooxidation on Pt/TiO2(110). *The journal of the american chemical society*, 118:5284-5289.

MARUTHAMUTHU, P., ASHOKKUMAR, M., GURUNATHAN, E., SUBRAMANIAN, E. & SHASTRI, M.V.C. 1989. Hydrogen evolution from water with visible radiation in presence of Cu(ll)/$WO_3$ and electron relay. *International journal of hydrogen energy*, 14(8):525-528.

MATSUOKA, M., KITANO, M., TAKEUCHI, M., TSUJIMARU, K., ANPO, M. & THOMAS, J.M. 2007. Photocatalysis for new energy production.Recent advances in photocatalytic water splitting reactions for hydrogen productions. *Catalysis today.*, 122:51-61.

MECERRIL, M., SILVA-LOPEZ, H. & ZELAYA-ANGEL, O. 2004. Band gap energy in Zn-rich Zn1iXCDXTE thin films grown by R.F. sputtering. *Revista mexicana de fisica*, 50:588.

MIDILI, A. & DINCER, I. 2008. Hydrogen as a renewable and sustainable solution in reducing global fossil fuel consumption. *Internationl journal of hydrogen energy*, 33:4209-4222.

MIESSLER, G.L. & DONALD, A.T. 2004. Inorganic chemistry 3ed. New Jersey, USA: Pearson prentice hall.

MILLS, A. & PORTER, G. 1982a. Photoreduction of carbonic acid by mercury coated n-titanium dioxide. *Journal of the chemical society, Faraday transactions*, 78:3659.

MILLS, A. & PORTER, J. 1982b. Photosensitised dissociation of water using dispersed suspensions of n-type semiconductors. *Journal of the chemical society, Faraday Transactions, 1*, 78:3659.

MOON, J., YUN, C.Y., CHUNG, K.W., KANG, M.S. & YI, J. 2003. Photocatalytic activation of $TiO_2$ under visible light using Acid Red 44. *Catalysis today*, 87(1-4):77-86.

MURPHY, A.B. 2007. Band gap determination from diffuse reflectance measurements of semiconductor films and applications to photoelectrochemical water-splitting. *Solar energy materials & Solar cells.*, 91:1326-1337.

NADA, A.A., BARAKAT, M.H., HAMED, H.A., MOHAMED, N.R. & VEZIROGLU, T.N. 2005. Studies on the photocatalytic hydrogen production using suspended modified $TiO_2$ photocatalysts. *International journal of hydrogen energy*, 30(7):687-691.

NAITO, H. & ARASHI, H. 1995. Hydrogen production from direct watersplitting at high temperatures using a $ZrO_2$ - $TiO_2$ - $Y_2O_3$ membrane. *Solid state ionics*, 79:366-370.

NI, M., LEUNG, M.K.H., LEUNG, D.Y.C. & SUMATHY, K. 2007. A review and recent developments in photocatalytic water splitting using $TiO_2$ for hydrogen production. *Renewable and sustainable energy reviews*, 11:401-425.

NI, M., LEUNG, M.K.H., SUMATHY, K. & LEUNG, D.Y.C. 2004. Water electrolysis - a bridge between renewable resources and hydrogen. (*In* Proceedings of the International Hydrogen Energy forum. Beijing: PRC. p. 475-480.)

NOWOTNY, J., BAK, T., NOWOTNY, M.K. & SHEPPARD, L.R. 2006. Titanium dioxide for solar hyrogen I. Functional properties. *International journal of hydrogen energy*, 32:2609-2629.

NOWOTNY, J., SORRELL, C.C., SHEPPARD, L.R. & BAK, T. 2005. Solar hydrogen: environmental safe fuel for the future. *International jounal for hydrogen energy.*, 30:521-544.

OHNO, T., HAGA, D., FUJIHARA, K., KAIZAKI, K. & MATSUMURA, M. 1998. Photocatalitic oxidation of water in $TiO_2$-coated $WO_3$ particles by visible light using Iron(lll) ions as electron acceptor. *Journal of Photochemistry and Photobiology A: Chemistry*, 118:41-44.

OHNO, T., TANIGAWA, F., FUJIHARA, K., IZUMI, S. & MATSUMURA, M. 1999. Photocatalytic oxidation of water by visible light using ruthenium-doped titanium dioxide powder. *Journal of photochemistry and photobiology A: Chemistry*, 127:107-110.

OUDENHOVEN, J.F.M., SCHEIJEN, F.J.E. & WOLFFS, M. 2004. Fundamentals of photocatalytic water splitting by visible light. *Technishe universiteit eindhoven*:4-16.

PASCHOTTA, R. 2008. Encyclopedia of laser physics and technology. Germany: Wiley-VCH.

PICHAT, P. 1987. Surface properties, activity and selectivity of bifunctional powder photocatalysts. *New journal of chemistry*, 11:135.

RAYALU, S.S., DUBEY, N., LABHSETWAR, N.K., KAGNE, S. & DEVOTTA, S. 2007. UV and visibly active photocatalyts for water splitting reaction. *International journal of hydrogen energy.*, 32:2776-2783.

READY, J.F. 1971. Effects of high power laser radiation. New York: Academic Press.

RECORD, F.A., BUBENICK, D.V. & KINDYA, R.J. 1982. Acid rain-Information book. Noyes Dtata Corp., Park Ridge.

ROSSELER, O., SHANKAR, M.S., KARKMAZ-LE DU, M. & SCHMIDLIN, L. 2010. Solar light photocatalytic hydrogen production from water over Pt and Au/$TiO_2$(anatase/rutile) photocatalysts: Influence of noble metal and porogen promotion. *Journal of catalysis*, 269(1):179-190.

SAKATA, T. & KAWAI, T. 1981. Heterogeneous photocatalytic production of hydrogen and methane from ethanol and water. *Chemical physics letters*, 80:341-344.

SAKTHIVEL, S., SHANKAR, M.V., PALANICHAMY, M., ARABINDOO, B., BAHNEMANN, D.W. & MURUGESAN, V. 2004. Enhancement of photocatalytic activity by metal deposition: characterisation and photonic efficiency of Pt, Au and Pd deposited on $TiO_2$ catalyst. *Water Research*, 38:3001-3008.

SANCHEZ, E. & LOPEZ, T. 1995. Effect of the preparation method on the band gap of titania and platinum-titania sol-gel materials. *Materials Letters*, 25:271-275.

SAYAMA, K. & ARAKAWA, H. 1992. Significant effect of carbonate addition on stoichiometric photodecomposition of liquid water into hydrogen and oxygen from platinum-titanium(IV)oxide suspension. *Journal of the chemical society, chemical communications*, 2:150-152.

SAYAMA, K. & ARAKAWA, H. 1996. Effect of carbonate addition on the photocatalytic decomposition of liqiud water over a ZrO2 catalyst. *Journal of photochemistry and photobiology A: Chemistry*, 94:67-76.

SAYAMA, K. & ARAKAWA, H. 1997. Effect of carbonate salt addition on the photocatalytic decomposition of liquid water over Pt-$TiO_2$ catalysts. *Journal of the Chemical Society, Faraday Transactions*, 93:1653.

SCLAFANI, A., PALMISANO, L. & SCHIAVELLO, M. 1990. Influence of the preparation methods of titanium dioxide on the photocatalytic degradation of phenol in aqueous dispersion. *Journal of physical chemistry*, 94(2):829-832.

SERRANO, E., RUS, G. & GARCIA-MARTINEZ, J. 2009. Nanotechnology for sustainable energy. *Renewable and sustainable energy Reviews*, 13:2373-2384.

SHAFIEE, S. & TOPAL, E. 2008. When will fossil fuel reserves be diminished? *Energy policy*, 37:181-189.

SILFVAST, W.T. 2004. Laser fundamentals. Cambridge: Cambridge university press.

SONNTAG, C.V. 2006. Free-radical-induced DNA damage and its repair. A chemical perspective. Berlin, New York, Heidelberg: Springer-Verlag.

SREETHAWONG, T. & YOSHIKAWA, S. 2005. Comparative investigation on photocatalytic hydrogen evolution over Cu-, Pd-, and Au-loaded mesoporous $TiO_2$ photocatalysts. *Catalysis Communications*, 6:661–668.

SREETHAWONG, T. & YOSHIKAWA, S. 2006. Enhanced photocatalytic hydrogen evolution over Pt supported on mesoporous $TiO_2$ prepared by single-step so-gel process with surfactant template. *International journal of hydrogen energy*, 31(6):786-796.

THOMAS, C.E., JAMES JR, B.D. & LOMAX, F.D. 1998. Market penetration scenarios for fuel cell vehicles. *International journal of hydrogen energy*, 23:949-966.

U.S. DEPARTMENT OF ENERGY. 2011. Hydrogen Production. USA. Date of access: 25 June 2011. <http://www1.eere.energy.gov>

VARIN, A., CZUJKO, T. & WRONSKI, Z.S. 2009. Nanomaterials for solid state hydrogen storage. Springer.

WANG, C.Y., PAGEL, R., BAHNEMANN, D.W. & DOHRMANN, J.K. 2004. Quantum yield of formaldehyde formation in the presence of colloidal $TiO_2$-based photocatalysts:

Effect of intermittent illumination, platinization, and deoxygenation. *Journal of physical chemistry B*, 108:14082.

WOO, J.C., MOON, K.D. & KAWAGUCHI, H. 1996. Design and Characterization of a Helium-Discharge Ionization Detector for Gas Chromatography. *Analitical science*, 12(2):195.

YANG, Y.Z., CHANG, C.H. & IDRISS, H. 2006b. Photo-catalytic production of hydrogen form ethanol over M/$TiO_2$ catalysts (M = Pd, Pt or Rh). *Applied Catalysis B: Environmental*, 67:217–222.

YANG, H., GUO, L., YAN, W. & LUI, H. 2006a. A novel composite photocatalyst for water splitting hydrogen production. *Journal of power sources*, 159(2):1305-1309.

YASURO, I. & BESSHO, H. 2007. Effect of Pt concentration on the production of hydrogen by a $TiO_2$ photocatalyst. *International journal of hydrogen energy*, 32:2689-2692.

ZHENG, H. & LIM, G.C. 2004. Laser-effected darkening in TPEs with $TiO_2$ additives. *Optics and lasers in Engineering*, 41(5):791.